QUANTIFYING SOYBEAN PHENOTYPES USING UAV IMAGERY AND MACHINE LEARNING, DEEP LEARNING METHODS

A Thesis presented to

the Faculty of the Graduate School

at the University of Missouri-Columbia

In Partial Fulfillment

of the Requirements for the Degree

Master of Science

by

SHAGOR SARKAR

Dr. Jianfeng Zhou, Thesis Supervisor

JULY 2023

The undersigned, appointed by the dean of the Graduate School, have examined the dissertation entitled

QUANTIFYING SOYBEAN PHENOTYPES USING UAV IMAGERY AND MACHINE LEARNING, DEEP LEARNING METHODS

presented by Shagor Sarkar,

a candidate for the degree of Master of Science in Food and Hospitality Systems, and hereby certify that, in their opinion, it is worthy of acceptance.

Professor Jianfeng Zhou

Professor Teng Teeh Lim

Professor Andrew Scaboo

Professor Noel Aloysius

DEDICATION

In the hopes that this study may contribute as a tool for the soybean breeders and associated researchers for identifying advanced genotypes, this is dedicated to all the members who supported and encouraged throughout my career.

ACKNOWLEDGEMENT

First and foremost, I am immensely grateful to my academic advisor and committee chair Dr. Jianfeng Zhou, whose expertise, patience, and unwavering dedication have been instrumental in shaping this research. His insightful feedback, constructive criticism, and constant encouragement have motivated me to strive for excellence. He provided me with an exceptional opportunity to study and work in the Mizzou Precision and Automated Agriculture Lab (PAAL), enabling me to acquire extensive research experience in tackling agricultural challenges and enhancing agricultural productivity through engineering methods and techniques. Moreover, his continuous support and willingness to connect me with other research groups greatly contributed to the successful completion of my dissertation projects and facilitated the expansion of my professional network. I am grateful for his guidance and assistance, as these projects would not have been achievable without his supervision and support.

I extend my heartfelt thanks to the members of my thesis committee, Dr. Teng Teeh Lim, Dr. Andrew Scaboo, and Dr. Noel Aloysius for their valuable insights and constructive suggestions that have enhanced the quality of this work. Their expertise and thoughtful inputs have broadened my understanding of the subject matter and have been invaluable in refining my research.

I would like to express my cordial thanks to all of my past and present co-workers, especially, Dr. Jing Zhou, Dr. Chin Nee Vong, Dr. Xiteng Zu, Tian Fengkai, Sazzad Rifat, Abdul Ghani for their helpful and generous assistance in data collection, data analysis, and manuscript preparation. Throughout my master's program, they have consistently been my unwavering pillars of support, mentors, and dear friends. Working alongside them has been an absolute pleasure and privilege. Their encouragement has played an indispensable role in helping me successfully navigate and complete my master's journey.

Finally, I would like to show my gratitude and immense respect to my family members for their unconditional love and support throughout the study period. I am incredibly grateful to my wife for her unwavering love, understanding, and support throughout the entire process of completing this thesis. Her constant encouragement, patience, and belief in my abilities have been a driving force behind my perseverance. Her sacrifices and willingness to lend a helping hand, providing emotional support, or simply offering a listening ear, have been invaluable. I am truly fortunate to have her by my side, and I am forever indebted to her for being my rock and my source of inspiration.

To all those mentioned above and to anyone else who has directly or indirectly contributed to this thesis, I extend my heartfelt thanks. Your support and guidance have been instrumental in shaping this work, and I am truly grateful for your invaluable contributions.

TABLE OF CONTENTS

LIST OF ILLUSTRATIONS

LIST OF TABLES

LIST OF ABBREVIATIONS

US	United States
UAV	Unmanned Aerial Vehicle
MAV	Manned Aerial Vehicle
RGB	Red-Green-Blue
XGBoost	Extreme Gradient Boosting
RF	Random Forest
KNN	K-Nearest Neighbor
ANN	Artificial Neural Network
SMOTE	Synthetic Minority Oversampling Technique
ENN	Edited Nearest Neighbor
NC	Nominal Continuous
ADASYN	Adaptive Synthetic
OA	Overall Accuracy
DNA	Deoxyribonucleic Acid
HTP	High-throughput Phenotyping
GNSS	Global Navigation System
GCP	Ground Control Point
RADAR	Radio Detection and Ranging
LiDAR	Light Detection and Ranging
EMS	Electromagnetic Spectrum
ML	Machine Learning
DL	Deep Learning
SVM	Support Vector Machine
PLSR	Partial Least Square Regression
PCA	Principle Component Analysis
NN	Neural Network
PH	Plant Height
CSM	Crop Surface Model
CNN	Convolutional Neural Network
PPC	Plant Projective Cover

USDA	United States Department of Agriculture
R3	Reproductive growth Stage 3
R5	Reproductive growth Stage 5
R6	Reproductive growth Stage 6
GLCM	Gray-Level Co-occurrence Matrix
NDVI	Normalized Difference Vegetation Index
NL	Non-lodging
ML	Medium lodging
HL	High lodging
SL	Severe lodging
RTK	Real-Time Kinematic
RFE	Recursive Feature Elimination
ROI	Region of Interest
TPE	Tree-Structured Parzen Estimator
CV	Cross-validation
TP	True Positive
FP	False Positive
TN	True Negative
FN	False Negative
ROC	Receiver Operating Characteristics
AUC	Area Under the Curve
PR	Precision-Recall
AP	Average Precision
MLC	Maximum Likelihood Classification
NASS	National Agricultural Statistics Survey
PT	Progeny Trial
PYT	Preliminary Yield Trial
AYT	Advanced Yield Trial
LBP	Local Binary Pattern
HOG	Histogram of Oriented Gradients
SIFT	Scale Invariant Feature Transform

T	Tawny
G	Gray
S	Segregating
ResNet	Residual Network

QUANTIFYING SOYBEAN PHENOTYPES USING UAV IMAGERY AND MACHINE LEARNING, DEEP LEARNING METHODS

Shagor Sarkar

Dr. Jianfeng Zhou, Thesis Supervisor

ABSTRACT

Crop breeding programs aim to introduce new cultivars to the world with improved traits to solve the food crisis. Food production should need to be twice of current growth rate to feed the increasing number of people by 2050. Soybean is one the major grain in the world and only US contributes around 35% of world soybean production. To increase soybean production, breeders still rely on conventional breeding strategy, which is mainly a 'trial and error' process. These constraints limit the expected progress of the crop breeding program. The goal was to quantify the soybean phenotypes of plant lodging and pubescence color using UAV-based imagery and advanced machine learning. Plant lodging and soybean pubescence color are two of the most important phenotypes for soybean breeding programs. Soybean lodging and pubescence color is conventionally evaluated visually by breeders, which is time-consuming and subjective to human errors. The goal of this study was to investigate the potential of unmanned aerial vehicle (UAV)-based imagery and machine learning in the assessment of lodging conditions and deep learning in the assessment pubescence color of soybean breeding lines. A UAV imaging system equipped with an RGB (red-green-blue) camera was used to collect the imagery data of 1,266 four-row plots in a soybean breeding field at the reproductive stage. Soybean lodging scores and pubescence scores were visually assessed by experienced breeders. Lodging scores were grouped into four classes, i.e., non-lodging, moderate lodging, high lodging, and severe lodging. In contrast, pubescence color scores were grouped into three classes, i.e., gray, tawny, and segregation.

UAV images were stitched to build orthomosaics, and soybean plots were segmented using a grid method. Twelve image features were extracted from the collected images to assess the lodging scores of each breeding line. Four models, i.e., extreme gradient boosting (XGBoost), random forest (RF), K-nearest neighbor (KNN), and artificial neural network (ANN), were evaluated to classify soybean lodging classes. Five data pre-processing methods were used to treat the imbalanced dataset to improve the classification accuracy. Results indicate that the pre-processing method SMOTE-ENN consistently performs well for all four (XGBoost, RF, KNN, and ANN) classifiers, achieving the highest overall accuracy (OA), lowest misclassification, higher F1-score, and higher Kappa coefficient. This suggests that Synthetic Minority Over-sampling-Edited Nearest Neighbor (SMOTE-ENN) may be an excellent pre-processing method for using unbalanced datasets and classification tasks.

Furthermore, an overall accuracy of 96% was obtained using the SMOTE-ENN dataset and ANN classifier. On the other hand, to classify the soybean pubescence color, seven pre-trained deep learning models, i.e., DenseNet121, DenseNet169, DenseNet201, ResNet50, InceptionResNet-V2, Inception-V3, and EfficientNet were used, and images of each plot were fed into the model. Data was enhanced using two rotational and two scaling factors to increase the datasets. Among the seven pre-trained deep learning models, ResNet50 and DenseNet121 classifiers showed a higher overall accuracy of 88%, along with higher precision, recall, and F1-score for all three classes of pubescence color. In conclusion, the developed UAV-based high-throughput phenotyping system can gather image features to estimate soybean crucial phenotypes and classify the phenotypes, which will help the breeders in phenotypic variations in breeding trials. Also, the RGB imagery-based classification could be a cost-effective choice for breeders and associated researchers for plant breeding programs in identifying superior genotypes.

CHAPTER ONE

INTRODUCTION

1.1 Background

The most pressing challenge in the 21st century is to increase food production for the growing population and increasing demand for fuel and clothing. Developing highly productive cultivars through the breeding program and providing them to the farmers is the most sustainable solution to address these demands (Hickey et al., 2019). By definition, crop breeding is both the art and science which modifies the traits of crops to achieve the desired characteristics (BATS Center, 1995). The traits include the improvement of yield and other agronomic aspects such as height, biotic and abiotic tolerance. The conventional breeding program relies on the trial-and-error process, which involves multiple phases of crossing, selection, and testing, encompasses a long process to develop new plant varieties, and can take one or two decades to produce a new cultivar (Ahmar et al., 2020). The soybean breeding program takes approximately seven to eight years to develop a new soybean variety (Kruger, 2019). Once a key problem is identified in a program, breeders choose parent lines from the existing populations that possess the necessary traits to solve the problem. These chosen parent lines are then crossed to produce new progeny that may concurrently inherit the desired features from both parents. The future generations of each cross are progressed to produce a suitable number of seeds for planting progeny lines, and each cross is planted and harvested individually. A combination of desired traits consider while evaluating and choosing the progeny lines, and those who inherit undesirable traits from their parents are eliminated. The chosen progeny lines are kept in order to undergo multi-location yield experiments for additional evaluation. Breeders evaluate the performance of the lines in these trials across diverse geographic contexts to ensure adaptability and appropriateness. Furthermore, breeders

continue choosing lines that show broad adaptability across diverse locations or that are specifically adapted to selected regions, depending on the precise aims of the breeding program. Until superior lines with the desired combination of traits are found and designated as new crop types for commercial production or additional breeding efforts, this iterative process of selection, evaluation, and progress continues.

Crop's genetic improvement process has become significantly faster with the revolution of biotech, which helps researchers to analyze the large population of genetical variations and markers targeting the genome sequence of large number of crops in the breeding program (Thomson et al., 2014; Mir et al., 2019). Genetic analysis has its highest value with the association of phenotypic traits from the target crops, enabling the need for high-throughput accurate acquisition and multidimensional phenotypes on a comprehensive scale throughout the crop development (Yang et al., 2020). Despite the exponential growth of analyzing DNA and genome sequences, the advancement in phenotypic study has not reached in a benchmark due to the phenotypic data acquisition issues in crop breeding and functional genomic studies (Furbank and Tester, 2011; Hu et al., 2020) and validating the high-throughput phenotyping (HTP) is still a bottleneck (Reynolds et al., 2020; Yang et al., 2020). Conventional phenotypic method is very laborious, time consuming, subjected to human error, and frequently plant destructive (Chen et al., 2014; Langre et al., 2019). In the breeding program, modern-day breeders still rely on each plot's visual evaluations and ratings to estimate the crucial agronomic traits. Breeders evaluate tens of thousands of plots by visually assessing, which is very challenging, and the actual data notes and subjective criterium by human ratings might generate the inaccuracies on the phenotypic data collection (Haghighattalab et al., 2016; Zhao et al., 2019). However, in recent years the advancement of technologies with the widespread adaption opens a new window for the

researchers by using different sensors, machine vision, telemetry, robotics, and automation in the agro-food industry and precision agriculture to enhance the efficiency. The integration of these technologies and applications helps scientists to identify the phenotypic traits, to develop bioinformatic tools, and crop quality assessment (Zhao et al., 2019).

The application of HTP approaches enables significant advancements in phenotyping standards for agronomic traits, which enhance the understanding of genetic basis and diversity of the traits, as well as the environmental influences throughout the crop development period (Reynolds et al., 2020). Thus, the high dimensional marker information and high dimensional phenotyping information can be used to characterize the genotypes comprehensively (Jarquin et al., 2018). In recent days, HTP became the emerging technology and considered as a key component in the crop breeding program, adopting the non-destructive and non-invasive sensors to efficiently screen a large amount of crop lines with reduced time and effort (Araus, Kefauver, Zaman-Allah, Olsen, & Cairns, 2018). Despite the advancement in the HTP which is capable of estimating various phenotypic traits with the advancement of different sensors and hardware platforms, the wide adoption of HTP into routine breeding procedures faces several limitations and challenges (Araus et al., 2018). Thus, it's very important to address these hurdles to ensure the actual application of the HTP in the breeding program to achieve the increased genetic gain.

1.2 Literature Review

1.2.1 High-throughput phenotyping platforms

Several remote sensing-based platforms have recently been designed for HTP and data collection. Among those, ground base platforms and aerial base platforms are most common. Ground base platforms includes pole/tower-based equipment's, gantry-based, ground mobile, and cable suspended systems (Andrade-Sanchez et al., 2014; Ge, Bai, Stoerger, & Schnable, 2016; White et

al., 2012). These systems offer higher spatial and temporal resolution than the aerial platforms and can be used with multiple devices. However, one noticeable drawback is ground-based platform have lower efficiency in terms of field coverage (Li et al., 2021). Aerial based HTP platforms (Chapman et al., 2014; Eitel, Long, Gessler, & Hunt, 2008; Geipel, Link, Wirwahn, & Claupein, 2016; Kefauver et al., 2017a)) are mainly three types based on the imaging distance: unmanned aerial vehicles (UAVs), manned aerial vehicles (MAVs), and satellite platforms. With the increasing of imaging distance, these platforms exhibit decreased image pixel resolutions. However, aerial based HTP platforms possess the advantage of covering large-scale fields, ranging from a few to hundred acres of lands within a short period of time. The data collection using UAVs and MAVs require two individuals and devices to provide the information from the global navigation system (GNSS) and ground control points (GCPs). On the other hand, satellite platforms such as Landsat series and WorldView series (C. Zhang et al., 2020) provides meter-level resolution data with several spectral bands and radio detection and ranging (RADAR) data (Jin et al., 2021).

1.2.2 Sensors

Sensors attached to the above-described platforms include but are not limited to red-green-blue (RGB), multispectral, hyperspectral, thermal, spectrometer, stereo cameras, and light detection and ranging (LiDAR) devices. Figure 1 shows the different wavelengths corresponding correspondent to different sensors. There are overlaps in the wavelengths, but these sensors differ in bandwidth, image resolution, quality, and price.

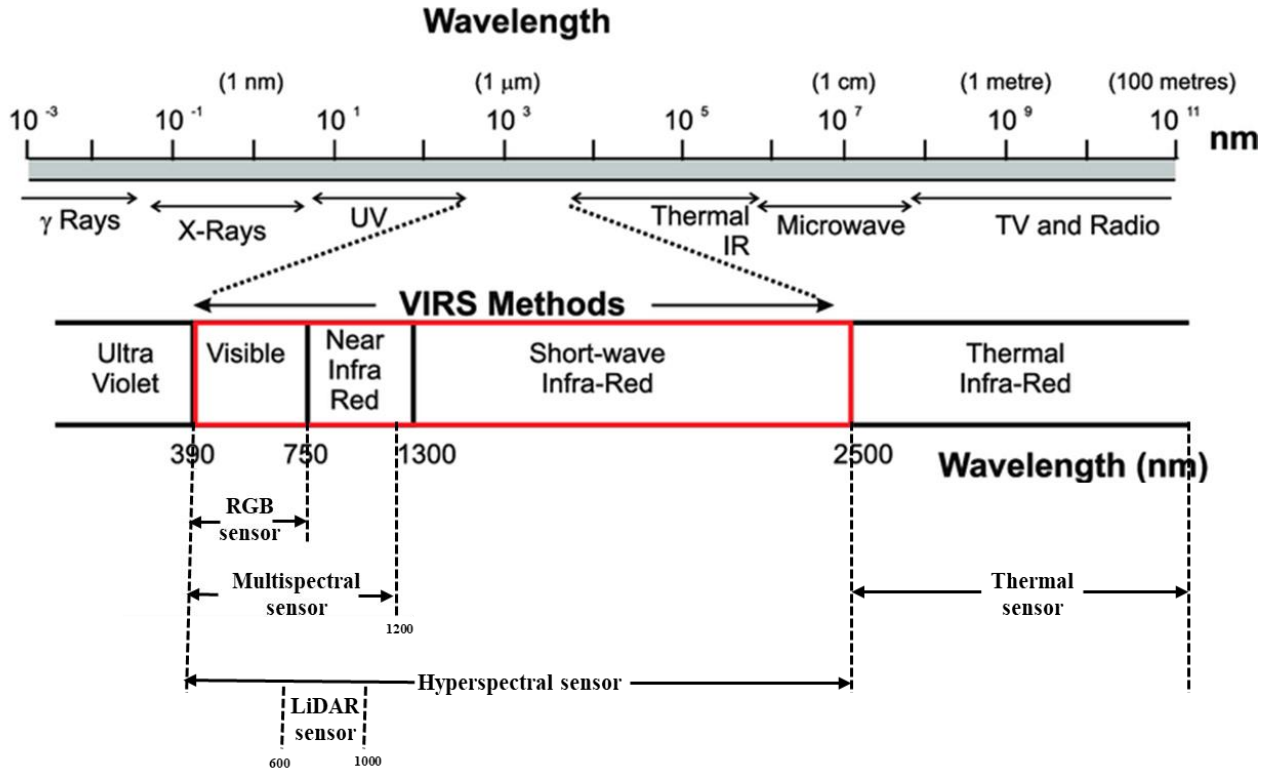

Figure 1-1. The electromagnetic spectrum (EMS) showing the regions of different sensors corresponding to different wavelengths. Image modified from (Kerr et al.,2011).

These sensors can contribute to estimate different phenotypic traits such as height, temperature, maturity which help researchers to explain genetic traits and justify the potentiality to facilitate the crop breeding process. Furthermore, because of their similarity of the electromagnetic spectrum over which the human eye operates, RGB-bases imagery technology has been used by numerous researchers for the automation of phenotyping that are traditionally human performed. Different morphological traits have been quantified by different researchers. Such as, UAV-based RGB imagery technology was used to quantify the Sorghum plant height and its application to genomic prediction (Watanabe et al., 2017; Wang et al., 2018). Poppy crop height and capsule volume were estimated by Iqbal et al., (2017). Canopy area, tree height, and crown volume, which provide important information about plant status and crop production, were monitored using RGB imagery

and UAV technology by Sanchez et al., (2015). Other research such as, digital maize count, wheat biomass estimation, wheat emergence and plant density, plant height, tomato detection, grassland monitoring, assessing olive tree crown, weed classification, leaf angle estimation, and so on using RGB based imagery (Gnädinger and Schmidhalter, 2017; Schirrmann et al., 2016; Jin et al., 2017; Madec et al., 2017; Senthilnath et al., 2016; Chang et al., 2017; Lussem et al., 2017; Han et al., 2018; Hu et al., 2018; Holamn et al., 2016; Diaz-Varela et al., 2015; Lottes et al., 2017; Ribera et al., 2018; McNeil et al., 2016; Iersel et al., 2018).

Images at small numbers, usually between 3 to 10 of wavebands of the electromagnetic spectrum are known as multispectral cameras (Guo et al., 2021). In crop science mainly, red, green, blue, red-edge, and near-infrared bands are mostly used. It's because the reflectance of chloroplast has a peak in the near-infrared band and changes rapidly at the red-edge band (Guo et al., 2021). Using these two bands, various vegetation indices can be measured (Jones et al., 2010; Seager et al., 2005) and can use to quantify crop traits. Researchers have used multispectral sensor in quantifying different traits and qualities of crop such as crop yield, biomass, leaf area index (LAI), nitrogen, water status, soybean variety selection, and so on (Vega et al., 2015; Swain et al., 2010; Potgieter et al., 2017; Hunt et al., 2010; Ballester et al., 2017, Baluja et al., 2012; Kumar et al., 2012; Zhou et al., 2022; Fukano et al.,2021).

Imaging across a variety of electromagnetic spectrum wavebands is possible using hyperspectral cameras. The two scales at which these cameras have usually been employed are (a) over entire fields and (b) at the level of individual plants. Hyperspectral cameras have a variety of benefits over other imaging modalities since they can cover a greater range of the electromagnetic spectrum. Hyperspectral cameras can now offer useful information on the biophysical and biochemical characteristics of several crop species due to their expanded spectral coverage.

Additionally, they are efficient at identifying biotic and abiotic stresses, providing information on the physiological characteristics of crops and their reactions to environmental factors (Nagasubramanian et al., 2019; Krause et al., 2019).

Thermal imagery is a system to capture infrared portion of the electromagnetic spectrum emitted by an object. For crops, thermal imaging physiologically significant because healthy plant emit radiation in the infrared range. This infrared emission of the plant canopy can provide the valuable insights into various biotic and abiotic stresses (Guo et al., 2021). Therefore, researchers used thermal imagery as a high-throughput approach to evaluate the plant physiological state. Crop water status to improve the understanding of crop growth, health, vigour, and yield was monitored by (Deery et al., 2016; Ludovisi et al., 2017; Sagan et al., 2019; Lacerda et al., 2022).

1.2.3 Analytical methods and models

Different HTP platforms and sensor produces a wealth of multi-dimensional data which encompass hundreds or thousands of breeding lines for the characterization of crop phenotypic traits at spatial and temporal scales. However, to efficiently use these data for different research purposes, it is essential to apply dedicated methods that can eliminate irrelevant features from the data to obtain the expected outcomes. From past few years, machine learning (ML) and deep learning (DL) methods have become more popular than the conventional regression-based models to analyze different sensor-based data in crop breeding program and related research. Different supervised and unsupervised ML models, such as random forest (RF), support vector machine (SVM), partial least square regression (PLSR), naïve bayes, K-means clustering, K-nearest neighbor (KNN), decision tree, principal component analysis (PCA) have been used by scientist and researchers for the crop trait quantification and detection. Such as, maize yield was predicted using random forest ML method, Bayesian optimizer and SVM method was used for the crop drought mapping using

UAV remote sensing RGB imagery, wheat nitrogen status estimation using PLSR, vegetation patch identification from a sugar beet field with a high diffusion of weeds using logistic regression, KNN, RF, decision tree, neural network (NN), and SVM (Ramos et al., 2020; Su et al., 2019; Fu et al., 2020; Fargassa et al., 2023). DL is one of the most important branches of ML which allows hierarchical data learning. Numerous research is spotted on from last few years using UAV imagery and deep learning methods such as cotton and rice yield estimation (Ashapure et al., 2020; Yang et al., 2019), water stress monitoring (Gao et al., 2020), crop monitoring (Theau et al., 2020; Wu et al., 2021), pesticide and fertilizer spraying (Hasan et al., 2019), and wheat lodging (Zhang et al., 2020).

1.2.4 Application of HTP in crop breeding

In crop breeding program, HTP platform equipped with different sensors have been used by many researchers due to the efficiency, flexibility, shorter time required, and easy operation compared to other methods. This section of literature review consists of UAV-based HTP used in obtaining the crop traits and phenotypes for breeding purposes.

Plant height (PH) is an important trait in the crop breeding program. Volpato et al., (2021) used UAV based HTP system to estimate the PH from wheat breeding lines. The study involves using temporal and high-spatial resolution images collected from a fixed-wing multi-rotor UAV platform from two wheat populations. The crop surface models (CSMs) were generated from the dense point clouds to estimate the PH. The CSMs shows a high correlation range from 0.35-0.88 and root mean square error varying from 0.39 to 4.02 cm while comparing with the ground-based PH. The study reflects the feasibility of using UAV based RGB imagery for the estimation of wheat plant height for a breeding program, which enables the efficient and scalable applications in wheat breeding lines.

Yield is one of the primary traits to select the superior genotypes and evaluate the breeding efficiency of a breeding program. Soybean yield was estimated using UAV based HTP system by Zhou et al., (2021) using convolutional neural network CNN). The study focused on evaluating 972 soybean breeding lines from three maturity groups under the rainfed conditions for testing the drought tolerance. Image features were derived from the images related to the plant height, canopy color, canopy texture to estimate the yield. A mixed CNN model was developed and tested which achieved 78% explanation of the measured yield, with root mean square error of 391.0 $kgha^{-1}$, equivalent to 33.8% of the average yield. From this result, it justifies the potentiality of using UAV based HTP system for the measurement of yield and selecting superior genotypes.

Salinity stress resistive genotype selection is another important task for the breeders. Johansen et al., (2019) used UAV-based radiometric data for assessment of salt tolerance in tomato plants for the breeding program. The study involves 600 control plants and 600 salt treatment plants of 199 accessions of the wild tomato species. Image was used to extract the relevant information of plant area, growth rates, condition, and Plant Projective Cover (PPC). These traits were used for the identification of best accession based on the yield and salt tolerance. An object-based image analysis was done, and the result showed 99% accuracy in automatically detecting tomato plants during most campaigns. The study encompasses the most yielding accession using muti-temporal UAV based phenotyping system.

Flooding stress can have detrimental effect on soybean which resulted in poor seed quality and significant yield reduction, hence the flooding stress genotypes selection is another challenge for the soybean breeders. Zhou et al., (2021) used UAV-based HTP system to estimate flood-induced soybean injuries. A total of 724 soybean breeding lines were visually assessed by the breeders where there is a clear flood induced injury occurs. Multispectral and thermal imagery was obtained

from three different height of 20m, 50m, and 80m using UAV platform. Image features were extracted related to the canopy temperature, vegetation index, canopy area, width, and length. DL method was employed to classify the five classes of flooding injury scores and find out that accuracy of 90% can be achieved using 20m height UAV data. This study demonstrates the promise of using HTP system to estimate flood-induced soybean injuries in a soybean breeding program.

A few research has been discussed here in this section using UAV-based HTP system for the breeding program, but the method are not limited here only. Though there are advancement in breeding program using these HTP system, still there is limitations which bottlenecking the crop breeding from genotyping to phenotyping. Data acquisition, integration, processing, management, analyzing, interpreting, and modeling are the core of HTP to obtain the accurate measurements of plant traits (D. Li et al., 2021), which requires manual input and interactions from the skilled personnel. Such as, UAVs operating skill, programming, and statistical knowledge are required to work with these setups. Though there is several software have been developed recently to work with HTP system and data analyzing, still it's very challenging for the breeders to use those software's and tune them properly (Zhou et al., 2021). So, there is a gap between breeders and phenotyping researchers that need to be considered and come up with a more-breeders friendly solution to use these HTP systems.

1.2.5 Goal and objectives

In the soybean breeding program, UAV-based HTP systems have been used previously to quantify the primary and secondary traits mostly, such as, yield, maturity date, biotic and abiotic stress, plant height. Rather than these primary and secondary traits there are still some crucial traits phenotypes such as lodging and pubescence color that the breeders look from every breeding

population. Insufficient attention has been paid to these soybean phenotypes to quantify using UAV-based HTP systems and advanced machine learning methods.

This study's goal was to quantify the soybean phenotypes of plant lodging and pubescence color using UAV-based imagery and advanced machine learning methods. To achieve this goal, this study includes following objectives: (1) to develop a lodging classification model using machine learning and the imbalanced dataset to fast assess plant lodging, (2) to classify the soybean pubescence color using UAV imagery and deep learning methods.

Reference

Ahmar, S., Gill, R. A., Jung, K.-H., Faheem, A., Qasim, M. U., Mubeen, M., et al. (2020). Conventional and molecular techniques from simple breeding to speed breeding in crop plants: recent advances and future outlook. International Journal of Molecular Sciences, 21(7), 2590. 10.3390/ijms21072590

Andrade-Sanchez, P., Gore, M. A., Heun, J. T., Thorp, K. R., Carmo-Silva, A. E., French, A., White, J. W. (2014). Development and evaluation of a field-based, high-throughput phenotyping platform. Functional Plant Biology, 41(1), 68–79. 10.1071/FP13126.

Ballester, C., Hornbuckle, J., Brinkhoff, J., Smith, J., Quayle, W. (2017). Assessment of in-season cotton nitrogen status and lint yield prediction from unmanned aerial system imagery. Remote Sensing, 9(11), 1149. 10.3390/rs9111149.

BATS Center, B. a. S. (1995). Methods of Plant Breeding. Retrieved from https://www.bats.ch/bats/publikationen/1995-1_TA/2-methods.php

Caturegli, L., Corniglia, M., Gaetani, M., Grossi, N., Magni, S., Migliazzi, M., Angelini, L., Mazzoncini, M., Silvestri, N., Fontanelli, M., Raffaelli, M., Peruzzi, A., Volterrani, M.

(2016). Unmanned aerial vehicle to estimate nitrogen status of turfgrasses. PLOS ONE, 11(6), e0158268. 10.1371/journal.pone.0158268.

Chang, A., Jung, J., Maeda, M. M., Landivar, J. (2017). Crop height monitoring with digital imagery from unmanned aerial system (UAS). Computers and Electronics in Agriculture, 141, 232–237. 10.1016/j.compag.2017.07.008.

Chapman, S., Merz, T., Chan, A., Jackway, P., Hrabar, S., Dreccer, M., et al. (2014). Pheno-Copter: A low-altitude, autonomous remote-sensing robotic helicopter for high-throughput field-based phenotyping. Agronomy, 4(2), 279–301. 10.3390/agronomy4020279

David M. D., Greg J. R., Jose A. J. B., Richard A. J., Anthony G. C., William D. B., Paul, H., Jamie, S., Robert, D., Robert T. F. (2016). Methodology for high-throughput field phenotyping of canopy temperature using airborne thermography. Frontiers in Plant Science, 7, 2016. 10.3389/fpls.2016.01808.

Díaz-Varela, R. A., De la Rosa, R., León, L. Zarco-Tejada, P. J. (2015). High-resolution airborne UAV imagery to assess olive tree crown parameters using 3D photo reconstruction: application in breeding trials. Remote Sensing, 7(4), 4213–4232. 10.3390/rs70404213.

Eitel, J. U. H., Long, D. S., Gessler, P. E., Hunt, E. R. (2008). Combined spectral index to improve ground-based estimates of nitrogen status in dryland wheat. Agronomy Journal, 100(6), 1694–1702. 10.2134/agronj2007.0362.

Fragassa, C., Vitali, G., Emmi, L., Arru, M. (2023). A new procedure for combining UAV-based imagery and machine learning in precision agriculture. Sustainability, 15(2), 998. 10.3390/su15020998.

Fu, Y., Yang, G., Li, Z., Song, X., Li, Z., Xu, X., Wang, P., Zhao, C. (2020). Winter wheat nitrogen status estimation using UAV-based RGB imagery and gaussian processes regression. Remote Sensing, 12(22), 3778. 10.3390/rs12223778.

Fukano, Y., Guo, W., Aoki, N., Ootsuka, S., Noshita K., Uchida K., Kato Y., Sasaki K., Kamikawa S., Kubota H. (2021). GIS-based analysis for UAV-supported field experiments reveals soybean traits associated with rotational benefit. Frontiers in Plant Science, 12. 10.3389/fpls.2021.637694.

Furbank, R. T., & Tester, M. (2011). Phenomics - technologies to relieve the phenotyping bottleneck. Trends in Plant Science, 16(12), 635–644. 10.1016/j.tplants.2011.09.005.

Ge, Y., Bai, G., Stoerger, V., Schnable, J. C. (2016). Temporal dynamics of maize plant growth, water use, and leaf water content using automated high throughput RGB and hyperspectral imaging. Computers and Electronics in Agriculture, 127, 625–632. 10.1016/j.compag.2016.07.028.

Geipel, J., Link, J., Wirwahn, J., Claupein, W. (2016). A programmable aerial multispectral camera system for in-season crops biomass and nitrogen content estimation. Agriculture, 6(1), 4. 10.3390/agriculture6010004.

Gnädinger, F., & Schmidhalter, U. (2017). Digital counts of maize plants by unmanned aerial vehicles (UAVs). Remote Sensing, 9(6), 544. 10.3390/rs9060544.

Han, X., Thomasson, J. A., Bagnall, G. C. et al. (2018). Measurement and calibration of plant-height from fixed-wing UAV images. Sensors, 18(12), 4092. 10.3390/s18124092.

Herrero-Huerta, M., Rodriguez-Gonzalvez, P., Rainey, K. M. (2020). Yield prediction by machine learning from UAS-based multi-sensor data fusion in soybean. Plant Methods. 16(78), 1–20. 10.1016/j.tplants.2018.11.007.

Hickey, L. T., N. Hafeez, A., Robinson, H., Jackson, S. A., Leal-Bertioli, S. C. M., Tester, M., et al. (2019). Breeding crops to feed 10 billion. Nature Biotechnology, 37, 744-754. 10.1038/s41587-019-0152-9.

Holman, F. H., Riche, A. B., Michalski, A., Castle, M., Wooster, M. J., Hawkesford, M. J. (2016). High throughput field phenotyping of wheat plant height and growth rate infield plot trials using UAV based remote sensing. Remote Sensing, 8(12), 1031. 10.3390/rs8121031.

Hu, P., Chapman, S. C., Wang, X. et al. (2018). Estimation of plant height using a high throughput phenotyping platform based on unmanned aerial vehicle and self-calibration: example for sorghum breeding. European Journal of Agronomy, 95, 24–32. 10.1016/j.eja.2018.02.004.

Iqbal, F., Lucieer, A., Barry, K., Wells, R. (2017). Poppy crop height and capsule volume estimation from a single UAS flight. Remote Sensing, 9(7), 647. 10.3390/rs9070647.

Jin, X., Liu, S., Baret, F., Hemerlé, M., Comar, A. (2017). Estimates of plant density of wheat crops at emergence from very low altitude UAV imagery. Remote Sensing of Environment, 198, pp. 105–114. 10.1016/j.rse.2017.06.007.

Jin, X., Zarco-Tejada, P. J., Schmidhalter, U., Reynolds, M. P., Hawkesford, M. J., Varshney, R. K., et al. (2021). High-throughput estimation of crop traits: a review of ground and aerial phenotyping platforms. IEEE Geoscience and Remote Sensing Magazine, 9(1), 200-231. 10.1109/MGRS.2020.2998816.

Jing Z., Jianfeng Z., Heng Y., Ali, M. L., Chen, P., Henry T. N. (2021). Yield estimation of soybean breeding lines under drought stress using unmanned aerial vehicle-based imagery and convolutional neural network. Biosystems Engineering, 204, 90-103. 10.1016/j.biosystemseng.2021.01.017.

Jing, Z., Eduardo, B., Caio Canella, V., Dennis, Y., Jianfeng, Z., Andrew, S., Pengyin, C. (2022). Improve soybean variety selection accuracy using UAV-based high-throughput phenotyping technology. Frontiers in Plant Science. 12. 10.3389/fpls.2021.768742.

Jing, Z., Huawei, M., Jianfeng, Z., Liakat, A. M., Heng, Y., Pengyin, C., Henry T. N. (2021). Qualification of soybean responses to flooding stress using UAV-based imagery and deep learning. Plant Phenomics. 2021, 9892570. 10.34133/2021/9892570.

Jones, H. G. & Vaughan, R. A. (2010). Remote sensing of vegetation: principles, techniques, and applications, Oxford University Press, 2010, https://market.android.com/details?id=book-sTmcAQAAQBAJ.

Kasper, J., Mitchell J. L. M., Yoann M. M., Bruno, A., Samir K. A. M., Matteo G. Z. et al. (2019). Unmanned aerial vehicle-based phenotyping using morphometric and spectral analysis can quantify responses of wild tomato plants to salinity stress. Frontiers in Plant Science, 10, 370. 10.3389/fpls.2019.00370.

Kefauver, S. C., Vicente, R., Vergara-Díaz, O., Fernandez-Gallego, J. A., Kerfal, S., Lopez, A., Araus, J. L. (2017a). Comparative UAV and field phenotyping to assess yield and nitrogen use efficiency in hybrid and conventional barley. Frontiers in Plant Science, 8, 1–15. 10.3389/fpls.2017.01733.

Kerr, A., Rafuse, H., Sparkes, G., Hinchey, J., Sandeman, H. (2011). Visible/infrared spectroscopy (VIRS) as a research tool in economic geology: background and pilot studies from Newfoundland and Labrador. Current Research of Newfoundland and Labrador Department of Natural Resources Geological Survey, Report 11-1

Krause, M. R., González-Pérez, L., Crossa, J., Pérez-Rodríguez, P., Montesinos-López, O., Singh, R. P., Dreisigacker, S., Poland, J., Rutkoski, J. Sorrells, M., Gore, M. A., Mondal, S. (2019). Hyperspectral reflectance-derived relationship matrices for genomic prediction of grain yield in wheat. G3: Genes, Genomes, Genetics, 9(4), 1231–1247. 10.1534/g3.118.200856.

Krueger, S. (2019). How Breeders Develop New Soybean Varieties. Retrieved from https://emergence.fbn.com/inputs/how-breeders-develop-new-soybean-varieties

Leonardo, V., Francisco, P., González-Pérez L., Gilberto, T. I., Aluízio, B. et al. (2021). High throughput field phenotyping for plant height using UAV-based RGB imagery in wheat breeding lines: feasibility and validation. Frontiers in Plant Science. 12, 591587. 10.3389/fpls.2021.591587.

Li, D., Quan, C., Song, Z., Li, X., Yu, G., Li, C., et al. (2021). High-throughput plant phenotyping platform (ht3p) as a novel tool for estimating agronomic traits from the lab to the field. Frontiers in Bioengineering and Biotechnology, 8(1533), 1-24. 10.3389/fbioe.2020.623705.

Lorena N. L., John L., Snider, Yafit C., Vasileios L., Stefano G., George V. (2021). Using UAV-based thermal imagery to detect crop water status variability in cotton. Smart Agricultural Technology, 2, 100029. 10.1016/j.atech.2021.100029.

Lottes, P., Khanna, R., Pfeifer, J., Siegwart, R., Stachniss, C. (2017). UAV-based crop and weed classification for smart farming. Paper presented at the Proceedings of IEEE International Conference on Robotics and Automation (ICRA), Singapore, 3024–3031.

Lussem, U., Hollberg, J., Menne, J., Schellberg, J., Bareth, G. (2017). Using calibrated RGB imagery from low-cost UAVs for grassland monitoring: case study at the Rengen Grassland Experiment (RGE), Germany. The International Archives of Photogrammetry, Remote Sensing and Spatial Information Sciences, XLII-2(W6), 229-233. 10.5194/isprs-archives-XLII-2-W6-229-2017.

Madec, S., Baret, F., de Solan, B., et al. (2017). High-throughput phenotyping of plant height: comparing unmanned aerial vehicles and ground LiDAR estimates. Frontiers in Plant Science, 8, 2002. 10.3389/fpls.2017.02002.

McNeil, B. E., Pisek, J., Lepisk, H., Flamenco, E. A. (2016). Measuring leaf angle distribution in broadleaf canopies using UAVs. Agricultural and Forest Meteorology, 218(219), 204-208. 10.1016/j.agrformet.2015.12.058.

Mir, R. R., Reynolds, M., Pinto, F., Khan, M. A., and Bhat, M. A. (2019). High-throughput phenotyping for crop improvement in the genomics era. Plant Science, 282, 60–72. 10.1016/j.plantsci.2019.01.007.

Nagasubramanian, K., Jones, S., Singh, A. K., Sarkar, S., Singh, A., Ganapathysubramanian, B. (2019). Plant disease identification using explainable 3D deep learning on hyperspectral images. Plant Methods, 21(15), 98. 10.1186/s13007-019-0479-8. eCollection 2019.

Potgieter, A. B., George-Jaeggli, B., Chapman, S. C., Laws, K., Suárez Cadavid, L. A., Wixted, J., Watson, J., Eldridge, M., Jordan, D. R., Hammer, G. L. (2017). Multi-spectral imaging

from an unmanned aerial vehicle enables the assessment of seasonal leaf area dynamics of sorghum breeding lines. Frontiers in Plant Science, 8, 1532. 10.3389/fpls.2017.01532.

Ramos, A. P. M., Osco, L. P., Furuya, D. E. G., Gonçalves, W. N., Santana, D. C., Teodoro, L. P. R., Antonio da Silva Junior, C., Capristo-Silva, G. F., Li, J., et al. (2020). A random forest ranking approach to predict yield in maize with UAV-based vegetation spectral indices. Computers and Electronics in Agriculture, 178, 105791. 10.1016/j.compag.2020.105791.

Reynolds, M., Chapman, S., Crespo-Herrera, L., Molero, G., Mondal, S., Pequeno, D. N. L., et al. (2020). Breeder Friendly Phenotyping. Plant Science, 295, 110396. 10.1016/j.plantsci.2019.110396.

Ribera, J., He, F., Chen, Y., Habib, A. F. Delp, E. J. (2018). Estimating phenotypic traits from UAV based RGB imagery. Computer Vision and Pattern recognition, arxiv.org/abs/1807.00498.

Riccardo, L., Flavia, T., Riccardo, S., Sacha, K., Giuseppe, M. S., Antoine, H. (2017). UAV-based thermal imaging for high-throughput field phenotyping of black poplar response to drought. Frontiers in Plant Science, 8, 1681. 10.3389/fpls.2017.01681.

Sagan, V., Maimaitijiang, M., Sidike, P., Eblimit, K., Peterson, K. T., Hartling, S., Esposito, F., Khanal, K., Newcomb, M., Pauli, D. et al. (2019). UAV-based high resolution thermal imaging for vegetation monitoring, and plant phenotyping using ICI 8640 P, FLIR Vue Pro R 640, and thermos Map Cameras. Remote Sensing, 11(3), 330. 10.3390/rs11030330.

Schirrmann, M., Hamdorf, A., Garz, A., Ustyuzhanin, A., Dammer, K. H. (2016). Estimating wheat biomass by combining image clustering with crop height. Computers and Electronics in Agriculture, 121, 374–384. 10.1016/j.compag.2016.01.007.

Seager, S., Turner, E. L., Schafer, J., Ford, E. B. (2005). Vegetation's red edge: a possible spectroscopic biosignature of extraterrestrial plants. Astrobiology, 5(3), 372–390. 10.1089/ast.2005.5.372.

Senthilnath, J., Dokania, A., Kandukuri, M., Ramesh, K. N., Anand, G., Omkar, S. N. (2016). Detection of tomatoes using spectral-spatial methods in remotely sensed RGB images captured by UAV. Biosystems Engineering, 146, 16–32. 10.3389/fpls.2017.02002.

Su, J., Coombes, M., Liu, C., Zhu, Y., Song, Y. et al. (2019). Machine learning based crop drought mapping system by UAV remote sensing RGB imagery. Unmanned Systems, 8(1), 71–83. 10.1142/S2301385020500053.

Sumesh K. C., Sarawut, N., Jaturong, S. (2021). Integration of RGB-based vegetation index, crop surface model and object-based image analysis approach for sugarcane yield estimation using unmanned aerial vehicle. Computers and Electronics in Agriculture, 180, 105903. 10.1016/j.compag.2020.105903.

Swain, K. C., Thomson, S. J., Jayasuriya, H. P. W. (2010). Adoption of an unmanned helicopter for low-altitude remote sensing to estimate yield and total biomass of a rice crop. Transaction of ASABE, 53(1), 21-27. 10.13031/2013.29493.

Thomson, M. J. (2014). High-Throughput SNP genotyping to accelerate crop improvement. Plant Breeding Biotechnology. 2(3), 195–212. 10.9787/pbb.2014.2.3.195.

Torres-Sánchez, J., López-Granados, F., Serrano, N., Arquero, O., Peña, J. M. (2015). High-throughput 3-D monitoring of agricultural-tree plantations with unmanned aerial vehicle (UAV) technology. PLOS One, 10(6), 10.1371/journal.pone.0130479.

van Iersel, W., Straatsma, M., Addink, E., Middelkoop, H. (2018). Monitoring height and greenness of non-woody flood plain vegetation with UAV time series. ISPRS Journal of Photogrammetry and Remote Sensing, 141, 112–123. 10.1016/j.isprsjprs.2018.04.011.

Vega, F. A., Ramírez, F. C., Saiz, M. P., Rosúa, F. O. (2015). Multi-temporal imaging using an unmanned aerial vehicle for monitoring a sunflower crop. Biosystems Engineering, 132, 19-27. 10.1016/j.biosystemseng.2015.01.008.

Vega, F. A., Ramírez, F. C., Saiz, M. P., Rosúa, F. O. (2015). Multi-temporal imaging using an unmanned aerial vehicle for monitoring a sunflower crop. Biosystems Engineering, 132, 19-27. 10.1016/j.biosystemseng.2015.01.008.

Wang, X., Singh, D., Marla, S., Morris, G., Poland, J. (2018). Field-based high-throughput phenotyping of plant height in Sorghum using different sensing technologies. Plant Methods, 14, 53. 10.1186/s13007-018-0324-5.

Watanabe, K., Guo, W., Arai, K. et al. (2017). High-throughput phenotyping of Sorghum plant height using an unmanned aerial vehicle and its application to genomic prediction modeling. Frontiers in Plant Science, 8, 1-11. 10.3389/fpls.2017.00421.

Wei, G., Matthew, C. E., Arti, S., Tyson L. S., Nirav, M., Soumik, S., Asheesh K. S., Baskar, G. (2021). UAS-based plant phenotyping for research and breeding applications. Plant Phenomics 2021:9840192, 10.34133/2021/9840192.

White, J. W., Andrade-Sanchez, P., Gore, M. A., Bronson, K. F., Coffelt, T. A., Conley, M. M., Wang, G. (2012). Field-based phenomics for plant genetics research. Field Crops Research, 133, 101–112. 10.1016/j.fcr.2012.04.003.

Yang, W., Feng, H., Zhang, X., Zhang, J., Doonan, J. H., Batchelor, W. D., et al. (2020). Crop phenomics and high-throughput phenotyping: past decades, current challenges, and future perspectives. Molecular Plant, 13(2), 187–214. 10.1016/j.molp.2020.01.008.

Yang, W., Feng, H., Zhang, X., Zhang, J., Doonan, J. H., Batchelor, W. D., et al. (2020). Crop phenomics and high-throughput phenotyping: past decades, current challenges, and future perspectives. Molecular Plant, 13(2), 187–214. 10.1016/j.molp.2020.01.008.

Zhang, C., Marzougui, A., Sankaran, S. (2020). High-resolution satellite imagery applications in crop phenotyping: An overview. Computers and Electronics in Agriculture, 175, 105584. 10.1016/j.compag.2020.105584.

CHAPTER TWO

ASSESSMENT OF SOYBEAN LODGING USING UAV IMAGERY AND MACHINE LEARNING

2.1 Abstract

Plant lodging is one of the most important phenotypes for soybean breeding programs. Soybean lodging is conventionally evaluated visually by breeders, which is time-consuming and subjective to human errors. The goal of this study was to investigate the potential of unmanned aerial vehicle (UAV)-based imagery and machine learning in assessment of lodging conditions of soybean breeding lines. An UAV imaging system equipped with an RGB (red-green-blue) camera was used to collect the imagery data of 1,266 four-row plots in a soybean breeding field at the reproductive stage. Soybean lodging scores were visually assessed by experienced breeders, and the scores were grouped into four classes, i.e., non-lodging, moderate lodging, high lodging, and severe lodging. UAV images were stitched to build orthomosaics, and soybean plots were segmented using a grid method. Twelve image features were extracted from the collected images to assess the lodging scores of each breeding line. Four models, i.e., extreme gradient boosting (XGBoost), random forest (RF), K-nearest neighbor (KNN), and artificial neural network (ANN), were evaluated to classify soybean lodging classes. Five data pre-processing methods were used to treat the imbalanced dataset to improve the classification accuracy. Results indicate that the pre-processing method SMOTE-ENN consistently performs well for all four (XGBoost, RF, KNN, and ANN) classifiers, achieving the highest overall accuracy (OA), lowest misclassification, higher F1-score, and higher Kappa coefficient. This suggests that Synthetic Minority Oversampling-Edited Nearest Neighbor (SMOTE-ENN) may be a good pre-processing method for using unbalanced datasets and classificationon tasks. Furthermore, the overall accuracy of 96% was obtained using the SMOTE-ENN dataset and ANN classifier. The study indicated that an imagery-based classification

model could be implemented in a breeding program to effectively differentiate phenotyping of soybean lodging and classify soybean lodging.

2.2 Introduction

Soybean is one of the major grain productions in the USA, and a total of 87.6 million acres of land were planted in 2021 with the average soybean yield of 3.45 metric tons per hectare, according to the report the of United States Department of Agriculture (USDA), National Agriculture Statistics Service (Barrett, 2021). However, soybean yield may be significantly affected by environmental conditions (Veas et al., 2021). Breeding programs aim to develop new crop varieties with improved traits, such as improved yield, resistance to biotic and abiotic stresses, desired maturity stage and no lodging. Lodging occurs when the plant stems break or bend over, and the plants completely displaced from its original position. Lodging is a morphological trait and lodged soybean plants can significantly reduce yield. Lodging in different growing stages, such as at R5 stage (Fehr et al., 1971) yield can be reduced by 18-32%, at stages of R3 and in R6 (Fehr et al., 1971) yield can be reduced by 12-18% and 13-15%, respectively (Woods and Swearingin, 1977). Furthermore, complete lodging at the stage of full maturity can cause more than 30% yield reduction (Saito et al., 2012). Therefore, developing soybean cultivars with lodging tolerance is important to enhance the productivity and improve yield stability (Kitabatake et al., 2019).

Improvement of lodging resistance cultivars not only improve yield by increased solar radiation interception but also improve mechanical harvesting efficiency (Kato et al., 2020). Lodging tolerant soybean cultivars selection is one of soybean breeders' efforts in developing high yielding soybean cultivars. Soybean lodging can be caused by environmental factors, such as moist and fertile soil, densely populated lines, soybean stem borer (Lodging of soybean, 2021), and meteorological conditions (Vann et al., 2018). Lodging can also be caused by external forces, wind,

rain, hail (Wu and Ma, 2016) and morphological parameters of the cultivars. Numerous studies have been conducted on rice, maize, oats, barley, and canola lodging to determine the impact on crop yield and development (Tian et al., 2021; Sun et al., 2019; Zhang et al., 2014; Vlachopoulos et al., 2021). It is very important to develop lodging resistant cultivars. Conventional breeding programs quantify lodging tolerance traits based on visual observation and score them into the ranges from 1 to 5. Visual observation and scoring are subjected to human errors and biases that may hinder the breeding efficiency and to identify the right genotypes (Zhou et al., 2020; Bagherzadi, 2017). Meanwhile, manual measurement and visual observation are also very time consuming, laborious, and costly (Berry et al., 2002). Therefore, it's a prime concern to develop a high throughput selection approach for quantifying soybean lodging score using remote sensing technologies. For example, unmanned aerial vehicle (UAV)-based imagery sensors such as digital and multispectral cameras have been used previously to select breeding lines using image derived features of breeding rows within abbreviated time (Yang et al., 2017). UAV image derived features have been used by numerous researchers to quantify crop responses to biotic and abiotic stress (Al-Tamimi et al., 2022), such as, drought stress (Duan et al., 2018), salt (Zhou et al., 2018), flooding stress (Cao et al., 2019). Furthermore, image features show active correlation with soybean traits such as maturity, plant height, yield, flowering time, wilting and canopy size (Zhou et al., 2020; Teodoro et al., 2021; Díaz-Varela et al., 2015; Zhou et al., 2019; Duan et al., 2017; Bai and Purcell, 2018), which are particularly important in breeding program.

Studies have been conducted to identify lodging resistant genotypes of different crops in general and breeding purpose such as rice, maize, oats, barley and canola (Tian et al., 2021; Bagherzadi, 2017; Zhang et al., 2014; Vlachopoulos et al., 2021) using remote sensing technologies. Image features have been used for lodging detection, such as textural features and Gray-Level Co-

occurrence Matrix (GLCM) were used for wheat and canola lodging detection (Rajapaksa et al., 2018; Mardanisamani et al., 2019). In addition, Gabor filtering was used by Mausda (Mausda et al., 2012) to detect the degree and direction of rice lodging. (Liu et al., 2005; Chauhan et al., 2019) investigated and found that canopy spectral reflectance increased and Normalized Difference Vegetation Index (NDVI) decreased with the high severity of lodging. (Liu et al., 2014) also used textural features adopting an airborne for the improvement of wheat lodging classification accuracy. (Yang et al., 2017) combines spectral features with textural features for the rice lodging classification.

Many machine learning and deep learning models have been used to identify the crop lodging, such as decision tree (Yang et al., 2017), logistic regression (Han et al., 2018), support vector machine (Chauhan et al., 2020), deep learning (Zhang et al., 2020) were used for rice, maize and canola lodging detection. However, within a breeding field, the number of lodged plots is much lower than the number of non-lodged plots under natural conditions, which makes the dataset imbalanced in the analysis process. Imbalanced data may cause increased errors and decreased robustness of developed models. To improve the accuracy, imbalanced datasets are usually pre-processed using Synthetic Minority Oversampling Technique (SMOTE) and Edited Nearest Neighbors under-sampling algorithm (SMOTE-ENN) (Batista et al., 2004).

Though several research has been conducted using machine learning and deep learning methods to detect crop lodging, to the best of our knowledge there is no re-search conducted on crop lodging detection for soybean breeding using UAV imagery technique. Hence, the goal of this study was to investigate the potential of quantifying lodging scores of soybean breeding lines using UAV-based imagery and machine learning methods. The textural image features provide supplementary information about the object properties which can help the heterogenous crop fields assessment

(Zhou et al., 2022). The specific objectives were: (1) to develop an RGB image texture feature-based lodging classification models using machine learning algorithms, (2) to assess the classification accuracies among different classification models. The current research makes the following contributions:

i. Imbalanced dataset processing: This study has contributed by outlining the methods used for texture feature extraction, preprocessing of imbalanced datasets, including image feature extraction, feature selection, and applying various resampling techniques such as SMOTE-Tomek Link, SMOTE-ENN, Borderline-SMOTE, SMOTE-NC, and ADASYN to address the class imbalance issue in the lodging dataset.

ii. Efficient lodging assessment for soybean breeding: For the first time we evaluated the potential and methods to assess lodging score of soybean breeding lines in field conditions using UAV-based imagery and machine learning.

2.3 Materials and methods

2.3.1 Field experiment and ground data collection

The field experiment was conducted in 2019 at the Bay Farm Research Facility (38°54'08.3"N, 92°12'29.8"W), Columbia, Missouri, United States. The field is in a humid subtropical climate region (Köppen climate classification code: Cfa) (Rubel et al., 2017). A thousand and seven hundred seventy-three (1,773) soybean genotypes were planted in four-row plots with a row length of 3.6 m and row spacing of 0.8 m on June 3, 2019 (without replicates). Weather conditions during all over the growing season showed in Figure 1 which includes daily average temperature and cumulative precipitation. The weather data was acquired from the nearby weather station which is a part of Missouri Mesonet – Weather Station Network.

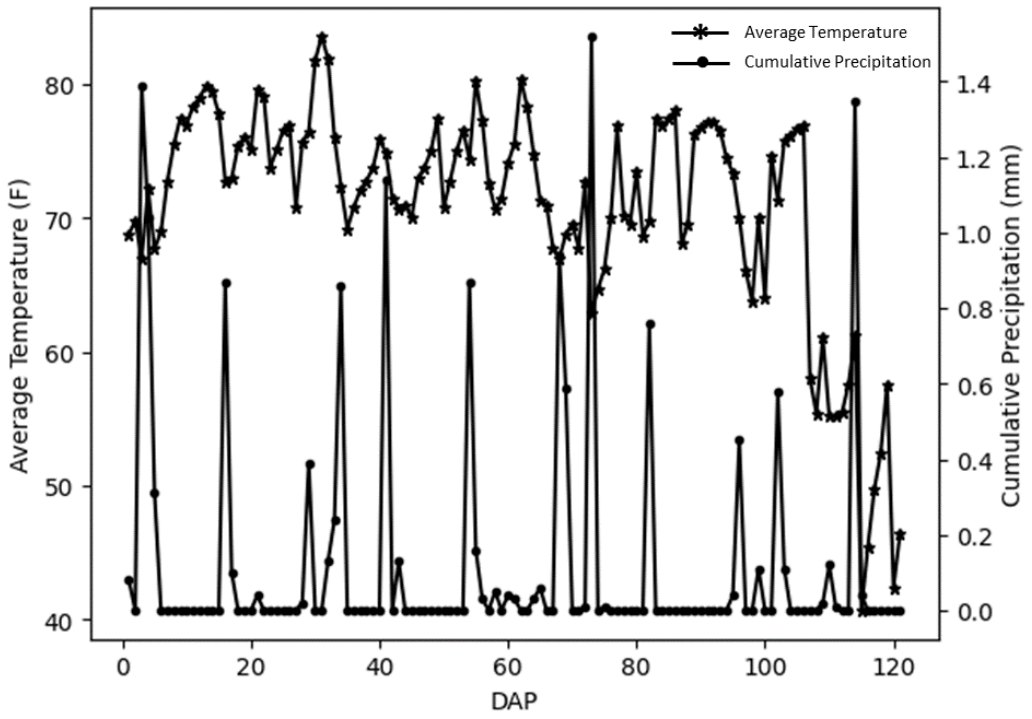

Figure 2-1. Daily average temperature and daily precipitation during the growing season in the experimental field. The asterisk and round marks are the day of data collection.

Lodging was rated on a 1 to 5 scale with 0.5 increments by the experienced breeders at the maturity stage R8. A rating of 1 showed that all plants and branches were erect, 2 showed that all plants leaning slightly or a few plants down, 3 showed that plants leaning moderately (45 degree), or 25% to 50% of the plants down, 4 showed that all plants leaning considerably, or 50% to 80% of the plants down and 5 showed that all plants are down. All plots were then assigned into four classes based on their scores, namely no lodging (NL, score 1.0, 1.5), medium lodging (ML, score 2.0, 2.5), high lodging (HL, score 3.0, 3.5) and severe lodging (SL, scores 4.0, 4.5 & 5.0). Some examples of plots with different lodging scores are shown in Figure 2. A total of 1,773 plots were processed, among which 1,266 plots were used for the image feature calculation and rest of the

plots were filler and were discarded. In this study, the number of plots of each lodging class NL, ML, HL, and SL are non-lodging, medium lodging, high lodging, and severe lodging, respectively.

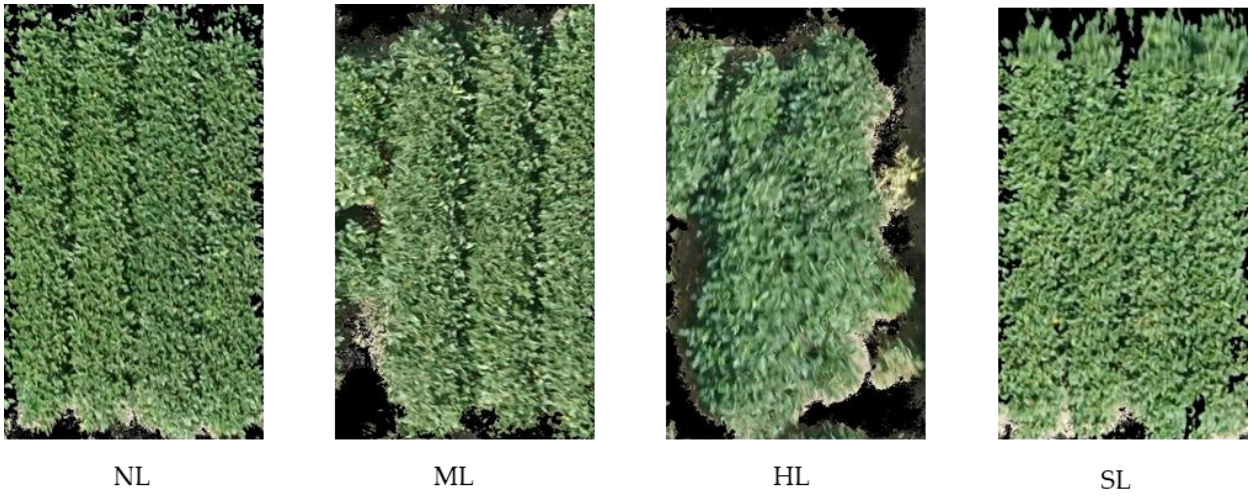

Figure 2-2. Ground-based classification scale of filed plots of soybean lodging with four classes, i.e., non-lodging (NL), moderate lodging (ML), high lodging (HL), and severe lodging (SL).

2.3.2 UAV imagery data collection

The aerial images were collected at the full seed development stage of R6 on 29th August 2019 using an UAV platform (DJI Matrice 600 Pro, DJI, Shenzhen, China) equipped with a Sony A6300 (Sony Corporation, Tokyo, Japan) camera. Images were taken at 0.5 frames per second (fps) with the resolution (number of pixels) of 6000×4000 pixels at a flight height of 30 m above the ground level with an overlap of 80% for both sides of the image. During the image acquisition, the camera was set to shutter 1/1000 s, ISO 100-200, F-stop auto and daylight mode. A Real-Time Kinematic (RTK) GNSS positioning system (Reach RS+, Emlid, St. Petersburg, Russia) was used to obtain the GNSS coordinates of the GCPs. To ensure sufficient satellite reception, the base station was mounted on a tribrach that was fixed in an open area in the fields. The base position was obtained in the initial setting by accumulating its GNSS coordinates for 30 minutes. The base station was

placed at the same location of each data collection. The rover receiver was placed vertically in the holes on a monopod after the GCPs were pulled out, and the GNSS coordinate of each GCP was recorded after accumulating for 10 seconds using ReachView (Emlid, St. Petersburg, Russia). The geo-referencing in-formation of each image was recorded in a separate .csv file. Images were stitched using Agisoft PhotoScan Pro (v1.3.4, St. Petersburg, Russia) for further processing.

2.3.3 Image processing

Figure 3 illustrates image processing and data analysis pipelines used in this study. First, texture feature was extracted from RGB orthomosaic after a few pre-processing steps. Then optimal features were selected using Random Forest-Recursive Feature Elimination (RF-RFE) method. Five resampling methods, namely Synthetic Minority Oversampling (SMOTE)-Tomek Links, SMOTE-Edited Nearest Neighbor (ENN), Adaptive Synthetic Oversampling (ADASYN), Borderline-SMOTE and SMOTE-Nominal Continuous (NC) method was compared for treating the data imbalance. At last, the performance of four machine learning models in the lodging classification were compared.

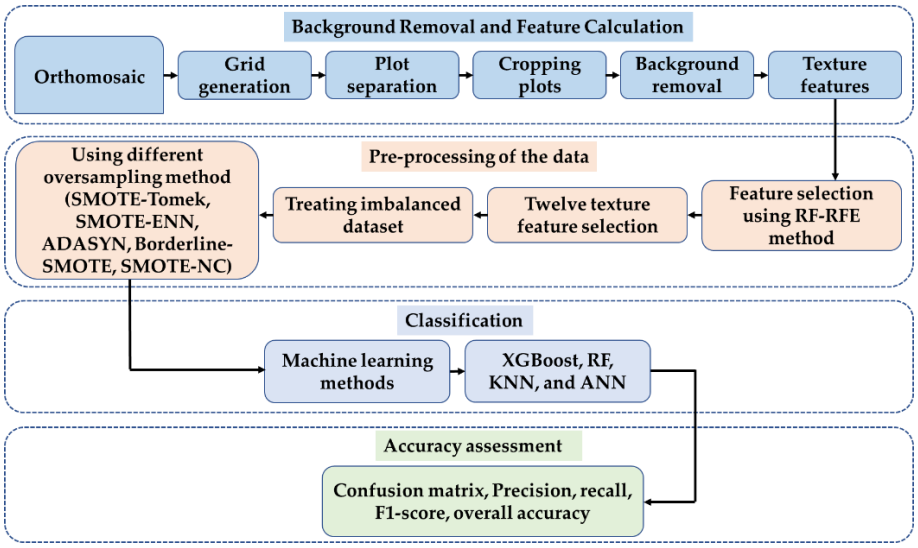

Figure 2-3. The flowchart of the soybean lodging classification.

An orthomosaic image was generated using Agisoft PhotoScan Pro. following the procedures described by (Zhou et al., 2018). The orthomosaic image was exported as .tif image and were processed using the Matlab Image Processing Toolbox and Computer Vision System Toolbox (ver. 2021b, The MathWorks, Natick, MA, USA). Individual soybean plots were separated from orthomosaic image by manually cropping a rectangle region of interest (ROI) around each plot. Size of each plot varied due to the planting error, hence the size of ROI also varied to cover each soybean plot according to its width and length. The background of each image (e.g., soil, leaf shadow and plant residue) was removed by detecting the projected canopy contours using the "activecontour" function (Whitaker, 1998) with the "Chan-Vese" method (Chan and Vese, 2001). The foreground, which is soybean plants are the pixels within a full contour and the outside of the contours are the background. Contours with extremely small regions were detected as noises using the "regionprops" function and then removed from the foreground.

2.3.4 Texture feature extraction and selection

A variety of image features could be used in machine learning for the accurate classification of lodging and non-lodging plots. Color image features which show variation in leaves or stem color of the plant and doesn't represent the lodging or non-lodging condition of the plots. On the other hand, lodging plots most likely have non-uniform and heterogenous patterns and non-lodging plots have uniform and homogenous patterns (Zhang et al., 2020). Considering these factors, textural features were extracted from the selected plots. Texture is one of the most important features for digital image processing and has been vastly used by numerous researchers for processing remote sensing data such as, object detection, image classification, crop trait classification, image evaluations, lodging detection (Hall-Beyer, 2017; Gao et al., 2010; Kwak et al., 2019; Mardanisamani et al., 2019). Furthermore, to reduce the noise in isolated pixels in classification,

texture information is one of the prime features for classification (Kwak et al., 2019). Gray Level Co-occurrence Matrix (GLCM) was first developed by (Haralick, 1973) and the GLCM considers pairs of pixels that are separated by a certain distance and orient-ed at a specific angle within the image. It calculates the frequency of occurrence of these pixel pairs with different combinations of grey levels (Singh et al., 2017). To calculate the texture feature, the original image is first converted to gray-scale image. Then the features of the gray-scale images are extracted using the relationship of brightness values be-tween the center pixel and its neighborhood pixel within the predefined kernel. The GLCM can produce different texture information according to its gray scale level, kernel size and direction by using the relationship. The selected texture features used in this study is listed in Table 1. Those features were angular second moment, contrast, correlation, variance, inverse difference moment, sum average, sum variance, sum entropy, entropy, difference variance, difference entropy, information measures of correlation I, information measures of correlation II, and maximum correlation coefficient.

Table 2-1. Texture features equation and uses by researchers.

Texture features	Equation	Reference
Angular second moment	$\sum_{i}\sum_{j} p(i,j)^2$	Wheat, soybean, rice and maize classification (Iqbal et al., 2021)
Contrast	$\sum_{k=0}^{N_g-1} k^2\, p_{x-y}(k)$	Crop disease and different crop classification (Pinto et al., 2016; Iqbal et al., 2021)
Correlation	$\frac{\sum_{i=1}^{N_g}\sum_{j=1}^{N_g}(ij)p(ij) - \mu_x\mu_y}{\sigma_x\sigma_y}$	Weed classification, crop disease and different crop classification (Mekhalfa

		and Yacef, 2021; Pinto et al., 2016; Iqbal et al., 2021)
Variance	$\sum_{i=1}^{N_g}\sum_{j=1}^{N_g}(i-u)^2 p(i,j)$	Olive, potato, wheat and sugar beet classification, weed classification, crop disease and different crop classification, crop type mapping (Akhtar et al., 2012; Mekhalfa and Yacef, 2021; Pinto et al., 2016; Iqbal et al., 2021; Moumni and Lahrouni, 2021)
Inverse difference moment	$\sum_{i=1}^{N_g}\sum_{j=1}^{N_g}\frac{1}{1+(i-j)^2}p(i,j)$	Land cover classification (Lu et al., 2010)
Sum average	$\sum_{i=2}^{2N_g} ip_{x+y}(i)$	Poultry carcass identification (Park and Chen, 2010)
Sum variance	$\sum_{i=2}^{2N_g}(i-f_s)^2 p_{x+y}(i)$	Poultry carcass identification (Park and Chen, 2010)
Sum entropy	$\sum_{i=2}^{2N_g} p_{x+y}(i)log(p_{x+y}(i))$	Crop discrimination (Soares et al., 1997)
Entropy	$-\sum_{i=1}^{N_g}\sum_{j=1}^{N_g} p(i,j)log(p(i,j))$	Crop classification using UAV multispectral imagery (Yang et al., 2021)
Difference variance	$Variance\ of\ p_{x-y}$	Poultry carcass identification (Park and Chen, 2010)

Difference entropy	$-\sum_{i=0}^{N_g} p_{x-y}(i) log(p_{x-y}(i))$	Poultry carcass identification (Park and Chen, 2010)
Information measures of correlation I	$\frac{Entropy - HXY1}{\max(HX, HY)}$	Plant identification (Shearer, 1990)
Information measures of correlation II	$[1 - \exp(-2(HXY2 - Entropy))]^{1/2}$	Plant identification (Shearer, 1990)
Maximal correlation coefficient	($Second\ largest\ eigenvalue\ of$ where, $Q(i,j) = \sum_k \frac{p(i,k)p(j,k)}{p_x(i)p_y(k)}$	Crop classification (Zhou et al., 2019)

Where, N_g denotes the gray-scale level, and P(i,j) is the normalized gray-scale value at the position i and j within the kernel and its sum is 1. μ_x, μ_y, σ_x and σ_y are the means and standard deviations of p_x and p_y. Also, HX and HY are the entropies of p_x and p_y.

The feature selection step eliminates the less important feature at each iteration. The random forest recursive feature elimination (RF-RFE) method (Genuer et al., 2015) was used to select the optimal texture features which is basically a recursive process that make the ranking of features according to the feature importance given by the RF. Through iterative loops, the texture feature set was continuously reduced to select the required features. The 10-fold cross validation strategy was used to select the best basis function for the feature selection.

2.3.5 Pre-process imbalanced data

In this study, sample number of each lodging class was imbalance with only few high and severe lodging plots. Data balancing or resampling are commonly used methods to tackle the issue of

class imbalance in machine learning models, by isolating it from the classification algorithms. Five pre-processing methods (i.e., SMOTE-Tomek Links, SMOTE-ENN, Borderline-SMOTE, SMOTE-NC and ADASYN) were compared to identify the suitable models for the imbalanced data in this study.

Synthetic Minority Oversampling Technique (SMOTE) algorithm is a resampling method based on random oversampling algorithm that generates synthetic samples by the difference between adjacent minority samples (Amiruddin et al., 2022). The process includes the selection of an example of x minority class and the nearest minority class neighbors. The synthetic data is created by choosing one of the k nearest neighbors y at random, then connecting x and y to from a line segment in space characteristics. Then the synthetic dataset is produced as a combination of two selected samples x and y (He and Garcia, 2009). SMOTE can increase the number of minority classes of the dataset (Skryjomski and Krawczyk, 2017; Fernández et al., 2018). Several over-sampling methods has been derived using the SMOTE as a basis (Zeng et al., 2016) which includes SMOTE-Tomek Links, SMOTE-ENN, Borderline SMOTE, SMOTE-NC, in this study.

The SMOTE-Tomek Links method involves the integration of SMOTE oversampling and Tomek Links undersampling techniques (Ai-Jun and Peng, 2020). It generates synthetic data for the minority class using SMOTE, and simultaneously, removes data that are identified as Tomek Links from the majority class. The SMOTE-ENN is a com-bination of SMOTE and Edited Nearest Neighbor (ENN), which is an undersampling method. SMOTE-ENN enhance the accuracy of classifying minority classes by eliminating observations from the majority classes that are near the class boundary of dis-tinct classes calculated through the nearest neighbor algorithm (Shi et al., 2020). One of the main characteristics of SMOTE-ENN method is that the processed data does not have the same number of instances in different classes. Instead of having equal numbers of in-

stances in each category, the resampled majority class will still be larger than the minority class, but the size difference between the categories will be reduced. In addition, Borderline-SMOTE is another technique used for oversampling in datasets that are not balanced. The Borderline SMOTE technique enhances the distribution of samples with-in a dataset by generating new samples based on a small number of samples that are located at the boundary (Gao et al., 2020). Lastly, SMOTE-NC is an extension of SMOTE that takes into account several factors, such as the nearest neighbors of the minority instances, the median of the standard deviation of both nominal and continuous variables, the Euclidean distance between the minority instance and its k-nearest neighbors, and the desired ratio of the minority class over the majority class (Rashu et al., 2014; Chawla et al., 2002).

On the other hand, Adaptive Synthetic (ADASYN) sampling approach was also tested in this study. Similar to SMOTE method, ADASYN generates more synthetic samples for the minority classes along the linear function by weighting distance (Taghizadeh-Mehrjardi et al., 2020) and according to the level of difficulty in learning (He and Garcia, 2009). ADASYN utilizes a weighted distribution for diverse minority classes as a basis to determine the quantity of artificial samples that must be produced for each minority category (He et al., 2008).

2.3.6 Machine learning models for soybean lodging classification

Extreme gradient boosting (XGBoost) method is one of widely used decision tree method for classification. XGBoost controls the overfitting by using the regularized model formalization, which resulted in better performance compared to the previous boosted algorithms (Cisty and Soldanova, 2018). XGBoost consists of a few hyperparameters such as nrounds (the number of trees), eta, learning rate and depth (the depth of the tree) (Georganos et al., 2018) that can be optimized to improve the performance. To optimize the XGBoost model performance, a nested

cross-validation approach was applied to find the optimal hyper-parameter factors to produce the best models. Hyper-parameter was tuned for each of the pre-processed dataset and are included in the Table 2 and 3. The study uses Tree-Structured Parzen Estimator (TPE) method to tune the hyper-parameters, which involves defining the hyper-parameter spaces and distributions. The aim was to develop a model with high precision and re-call for the soybean lodging classification.

An ensemble classification algorithm, random forest (RF) model was used to classify soybean lodging based on image feature. RF is a group of tree-based classifiers and uses bootstrapping to improve the diversification of classification trees. Random Forest takes advantage of the high speed and accuracy of decision tree algorithm for classification problems by generating multiple decision tree models. Each decision tree is in-dependent, and the errors are minimized in a collaborative way, resulting in more ac-curate and reliable classification results (Zhu et al., 2022). To optimize the RF model performance, grid search method was used with 5-fold cross-validation to find the optimal hyper-parameters. Six hyper-parameters were tuned using the grid search method for each of the treated dataset including original dataset. Best values of hyper-parameters are included in the Table 4 and 5. RF was used to develop soybean lodging classification model using these best hyper-parameter values.

The K-nearest neighbor (KNN) is a non-parametric supervised machine learning algorithm which is one of the popular algorithms for data processing and modeling (Uddin et al., 2022). The KNN algorithm was used to classify the soybean lodging genotypes selection, where the primary parameter “n_neighbor” = 3 was set for the analysis.

Artificial neural networks (ANNs) have been extensively used for the classification of crops and crop traits (Murthy et al., 2003; Wang et al., 2009; Vieira et al., 2022). ANN contains an input layer, multiple hidden layers, and one output layer. Each hidden layer contains multiple numbers

of neurons and quantifies the related mathematical equations to identify the complex relationship be-tween the data and the input layer and the data in the output layer. An artificial neural network can be constructed with the tuning of two hyperparameters such as the number of nodes in the hidden layer and the number of control iterations (Beck et al., 2018).

Table 2-2. Description of the hyperparameters used for the analysis using XGBoost Classifier.

Hyper-parameters	Description
n_estimators	The number of boosting rounds or decision tree to be built.
max_depth	The maximum depth of each decision tree.
learning_rate	The step size shrinkage used in updating weights during each boosting round. A lower learning rate can help prevent overfitting but may require a higher number of boosting rounds.
gamma	The minimum loss reduction required to split a node. A higher value can lead to fewer and more conservative splits, while a lower value can lead to more splits and potentially overfitting.
subsample	The fraction of observations to be randomly sampled for each tree. A lower value can lead to a more conservative model, while a higher value can lead to overfitting.
colsample_bytree	The fraction of columns to be randomly sampled for each tree. A lower value can lead to a more conservative model, while a higher value can lead to overfitting.
min_child_weight	The minimum sum of instance weight needed in a child. A higher value can lead to a more conservative model, while a lower value can lead to overfitting.

Table 2-3. XGBoost hyper-parameter best values using TPE method for the analysis of original dataset and treated dataset (SMOTE-Tomek Links, SMOTE-ENN, Borderline-SMOTE, SMOTE-NC and ADASYN) for balancing.

Hyper-parameter	Search Space	Best Values					
		Original dataset	Dataset Treated by SMOTE-Tomek Link	Dataset Treated by SMOTE-ENN	Dataset Treated by Borderline-SMOTE	Dataset Treated by SMOTE-NC	Dataset Treated by ADASYN
n_estimators	100, 1000	348	593	337	664	944	652

max_depth	3, 10	6	8	10	10	8	9
learning_rate	0.01, 1	0.01	0.08	0.08	0.03	0.06	0.09
gamma	0, 1	0.56	0.20	0.03	0.003	0.19	0.13
subsample	0.5, 1	0.99	0.62	0.8	0.80	0.8	0.71
colsample_bytree	0.5, 1	0.79	0.90	0.98	0.83	0.9	0.76
min_child_weight	1, 5	2	1	2	2	1	1

Table 2-4. Description of the hyperparameters used for the analysis using RF Classifier.

Hyper-parameters	**Description**
n_estimators	Determines the number of decision trees to be built in the random forest.
max_features	Identifies the maximum number of features needed when splitting a node in each decision tree. It controls the randomness in feature selection.
min_samples_split	This hyperparameter determines the minimum number of samples needed to split an internal node in a decision tree.
min_samples_leaf	Identifies the minimum number of samples required to be at a leaf node in a decision tree.
Max_depth	Identifies the number of maximum depths of a decision tree which mainly limits the number of levels in the tree, prevents overcomplexity, and reduce the overfitting.
bootstrap	Determines the bootstrap samples were used or not to build each decision tree in the random forest.

Table 2-5. RF hyper-parameter best values using grid search method for the analysis of original dataset and treated dataset (SMOTE-Tomek Links, SMOTE-ENN, Borderline-SMOTE, SMOTE-NC and ADASYN) for balancing.

Hyper-parameter	Search Space	Best Values					
		Original dataset	Dataset Treated by SMOTE-Tomek Link	Dataset Treated by SMOTE-ENN	Dataset Treated by Borderline-SMOTE	Dataset Treated by SMOTE-NC	Dataset Treated by ADASYN
n_estimators	50, 100, 200	50	50	100	100	100	50

max_features	sqrt, log2	sqrt	sqrt	sqrt	sqrt	sqrt	sqrt
min_samples_split	1, 2, 4	1	2	1	1	1	1
min_samples_leaf	1, 10	5	5	5	10	5	5
Max_depth	1, 10, 50	10	10	10	10	10	10
bootstrap	True, False	True	True	True	True	True	True

2.3.7 Data analysis and accuracy assessment

All the analysis and modeling were performed in Google Colaboratory (Colab) Pro. Machine learning classifiers (XGBoost, RF, KNN and ANN) were com-pared regarding their performance in classifying the four lodging classes. The balanced dataset was split into training and testing with 80% and 20%, respectively. The model performance was evaluated using a 5-fold cross-validation (CV) to calculate the classification accuracy.

The four classes of soybean lodging scores were assessed based on the number of samples that were correctly or falsely classified as either presence (True Positive, TP or False Positive, FP) or absence (True Negative, TN or False Negative, FN) using XGBoost, RF, KNN, and ANN models. A group of metrices were used for evaluation and they were calculated using Eqs. 1-5. The evaluation was based on several performance metrices, including precision, recall, F1-score, kappa, and overall accuracy (OA). The precision indicates the proportion of correctly predicted presences, recall represents the ratio of correctly predicted positive samples, and F1-score is the harmonic mean of precision and recall the F1-score is measure of model accuracy as well that balances precision and recall which ranges from 0 to 1, with 1 being the best possible score, indicating perfect precision and recall. Kappa value represents the proportion of correctly predicted sites, and OA indicates the overall accuracy of the model.

$$\text{Accuracy} = \frac{\text{No. of samples classified correctly in a test set}}{\text{Total No. of samples in a test set}} \times 100\% \quad (1)$$

$$\text{Kappa} = \frac{\text{Po} - \text{Pe}}{1 - \text{Pe}} \quad (2)$$

Where, P_0 = is the overall accuracy of the model

P_e = is the measure of the agreement between the model predictions and actual class values

$$\text{Precision} = \frac{\text{TP}}{\text{TP} + \text{FP}} \quad (3)$$

$$\text{Recall} = \frac{\text{TP}}{\text{TP} + \text{FN}} \quad (4)$$

$$\text{F1 score} = \frac{2 * (\text{Precision} * \text{Recall})}{(\text{Precision} + \text{Recall})} \quad (5)$$

2.4 Results

2.4.1 Feature selection

Twelve texture features were selected using the random forest recursive feature elimination (RF-RFE) method with two others (Entropy and Information measures of correlation I) eliminated from the all the features. The result show that the 12 features were important to obtain the highest score by performing the RFE algorithm with cross-validation. Figure 4 shows that the RFE uses a random forest algorithm to test combination of features, where the number of features was 12 with the maximum score of 0.754. These twelve features and one target and 1266 observations (plots) were used to analyze the soybean lodging using four different machine learning classifiers.

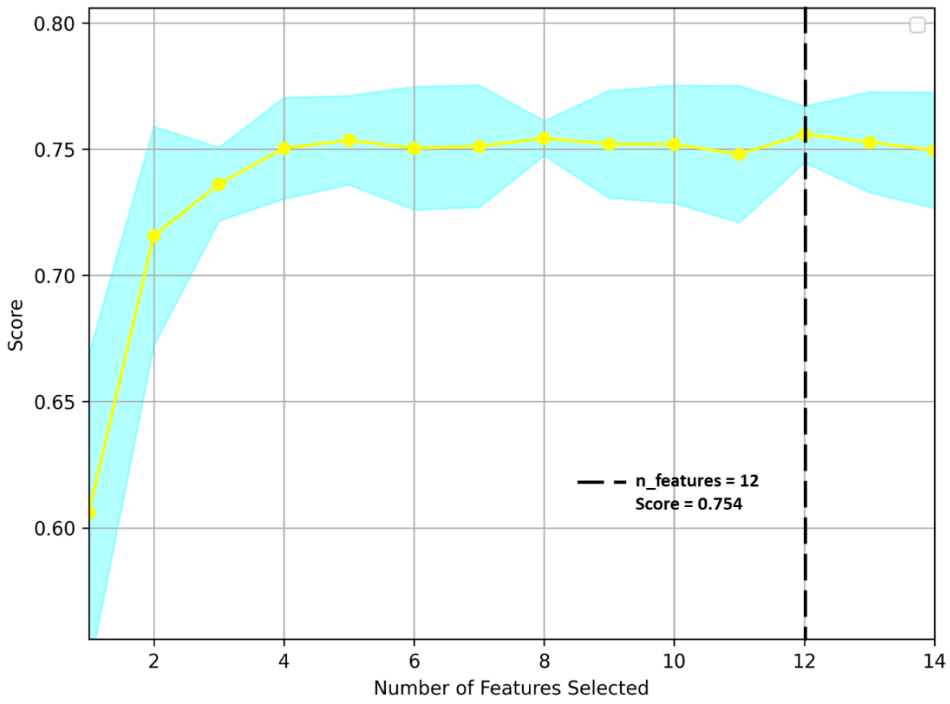

Figure 2-4. Recursive feature elimination (RFE) for feature selection.

2.4.2 Original and balanced dataset

Table 6 shows the number of data points included in each class for original dataset and for four classifiers. Each classifier includes five pre-processing methods datasets. Original dataset was highly imbalanced, where non-lodging class was 76%, medium lodging was 16%, high lodging was 6% and severe lodging was 0.08% of all datasets. To overcome the imbalance issue, five pre-processing (SMOTE-Tomek Link, SMOTE-ENN, Borderline-SMOTE, SMOTE-NC and ADASYN) methods was used to balance the dataset and the number of data points included in each pre-processing method for each class are shown in Table 6.

Table 2-6. Comparison of datasets before and after pre-processing for each classifier.

Dataset	NL	ML	HL	SL
Original	964	206	85	11
SMOTE-Tomek Link	923	964	964	964
SMOTE-ENN	224	700	784	925
Borderline-SMOTE	964	964	964	964
SMOTE-NC	964	964	964	964
ADASYN	964	976	966	962

2.4.3 Classification performance of machine learning models

2.4.3.1 Classification performance of four machine learning models using original dataset

Using the original dataset for the classification of soybean lodging, we found that XGBoost, RF, KNN, and ANN showed the overall accuracy of 0.80, 079, 0.77, and 0.73, respectively. All the machine learning classifiers only showed higher precision, recall, and F1-score for NL class. No model correctly classified other classes of ML, HL, and SL. Be-cause of there were a very few numbers of data points was associated in ML, HL, and SL classes. More precisely, 36 data points in ML, 12 data points in HL, and only 4 data points were associated in testing set for the classification using original dataset. Due to this limited number of data points, classifiers couldn't recognize any of them and resulted in very poor precision, recall, and F1-score for these classes. Confusion matrix and model performance metrices of four lodging classes using original dataset are shown Table 7. Overall accuracy, kappa value, and misclassification rate are shown in a supplementary Figure 5. Due to the poor results using original and imbalanced dataset, we used

five data balancing method (SMOTE-Tomek Links, SMOTE-ENN, Borderline-SMOTE, SMOTE-NC, and ADASYN). Following section describes the results of ML classifiers using five balancing methods.

Table 2-7. Confusion matrix and model performance metrices of four lodging classes of soybean using original dataset and four machine learning (XGBoost, RF, KNN, and ANN) classifiers.

Pre-processed Dataset	Actual samples	NL	ML	HL	SL	Precision	Recall	F1-score
SMOTE-Tomek Link	NL	201	1	0	0	0.80	1.00	0.89
	ML	35	1	0	0	0.25	0.03	0.05
	HL	10	2	0	0	0.00	0.00	0.00
	SL	4	0	0	0	0.00	0.00	0.00
Borderline-SMOTE	NL	200	2	0	0	0.80	0.99	0.88
	ML	35	1	0	0	0.25	0.03	0.05
	HL	11	1	0	0	0.00	0.00	0.00
	SL	4	0	0	0	0.00	0.00	0.00
SMOTE-NC	NL	193	8	1	0	0.80	0.96	0.87
	ML	34	2	0	0	0.18	0.06	0.09
	HL	11	1	0	0	0.00	0.00	0.00
	SL	4	0	0	0	0.00	0.00	0.00
ADASYN	NL	186	4	3	0	0.75	0.96	0.84
	ML	35	0	0	0	0.00	0.00	0.00
	HL	21	1	0	0	0.00	0.00	0.00
	SL	4	0	0	0	0.00	0.00	0.00

Where, soybean lodging classes are NL = Non-lodging, ML = Moderate lodging, HL = High lodging, and SL = Severe lodging. Data processing methods are SMOTE-Tomek Link = Synthetic Minority Over-sampling Method with Tomek Link, SMOTE-ENN= Synthetic Minority Oversampling Method with Edited Nearest Neighbor, Borderline-SMOTE = Borderline method with Synthetic Minority Oversampling, SMOTE-NC = Synthetic Minority Oversampling Method with Nominal Continuous ADASYN = Adaptive Synthetic method and OA = overall accuracy.

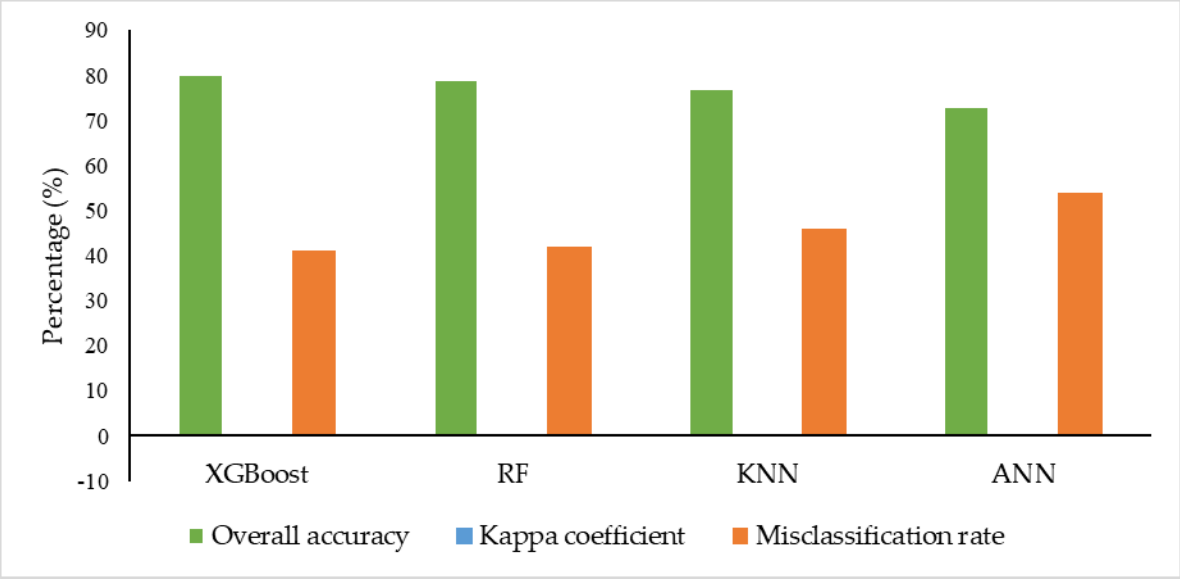

Figure 2-5. Overall accuracy, kappa coefficient and misclassification rate achieved using original imbalanced dataset and four machine learning classifiers.

2.4.3.2 Classification performance using five pre-processed datasets of XGBoost classifier using five balancing methods

Table 8 represents the results of the evaluation of XGBoost classifier using five types of balanced dataset for classifying four soybean lodging classes (NL, ML, HL and SL). The results of XGBoost model shown in the table shows higher classification accuracy of 0.94 using SMOTE-ENN dataset, whereas using other dataset the classification accuracy ranges between 0.84-0.89 (Figure 6). SMOTE-ENN dataset outperformed than other datasets. Where the precision, recall, F1-score, and kappa value. Higher precision, recall and F1-score was obtained for SL classes with the values of 0.99, 0.99 and 0.99, respectively. On the other hand, higher kappa value of 0.91 was also obtained using SMOTE-ENN dataset. Overall accuracy, kappa coefficient and misclassification rate of each class for five balanced datasets are showed in figure 5. Lower misclassification rate of 12% was obtained using SMOTE-ENN dataset among all other datasets. A comprehensive comparison showed that using SMOTE-ENN was the most ideal dataset, with higher area under the receiver

operating curve (AUC) from ROC curve and the average precision (AP) values from the precision-recall curve (Figure 7 and 8).

Table 2-8. Confusion matrix and model performance metrices of four lodging classes of soybean using XGBoost classifier.

Pre-processed Dataset	Actual samples	NL	ML	HL	SL	Precision	Recall	F1-score
SMOTE-Tomek Link	NL	123	30	20	14	0.77	0.66	0.71
	ML	21	166	10	4	0.82	0.83	0.82
	HL	13	5	181	1	0.85	0.91	0.88
	SL	2	1	1	171	0.90	0.98	0.94
SMOTE-ENN	NL	27	9	5	1	0.93	0.64	0.76
	ML	1	127	4	0	0.87	0.96	0.91
	HL	1	9	153	0	0.94	0.94	0.94
	SL	0	1	1	188	0.99	0.99	0.99
Borderline-SMOTE	NL	135	20	15	6	0.77	0.77	0.77
	ML	29	183	3	2	0.88	0.84	0.86
	HL	8	4	179	0	0.91	0.94	0.92
	SL	3	2	0	183	0.96	0.97	0.97
SMOTE-NC	NL	135	27	12	1	0.82	0.77	0.80
	ML	22	184	4	1	0.86	0.87	0.86
	HL	7	4	179	0	0.92	0.94	0.93
	SL	0	0	0	196	0.99	1.00	0.99
ADASYN	NL	122	30	23	6	0.80	0.67	0.73
	ML	20	160	11	4	0.80	0.82	0.81
	HL	11	9	179	1	0.84	0.90	0.86
	SL	0	0	1	179	0.95	0.99	0.97

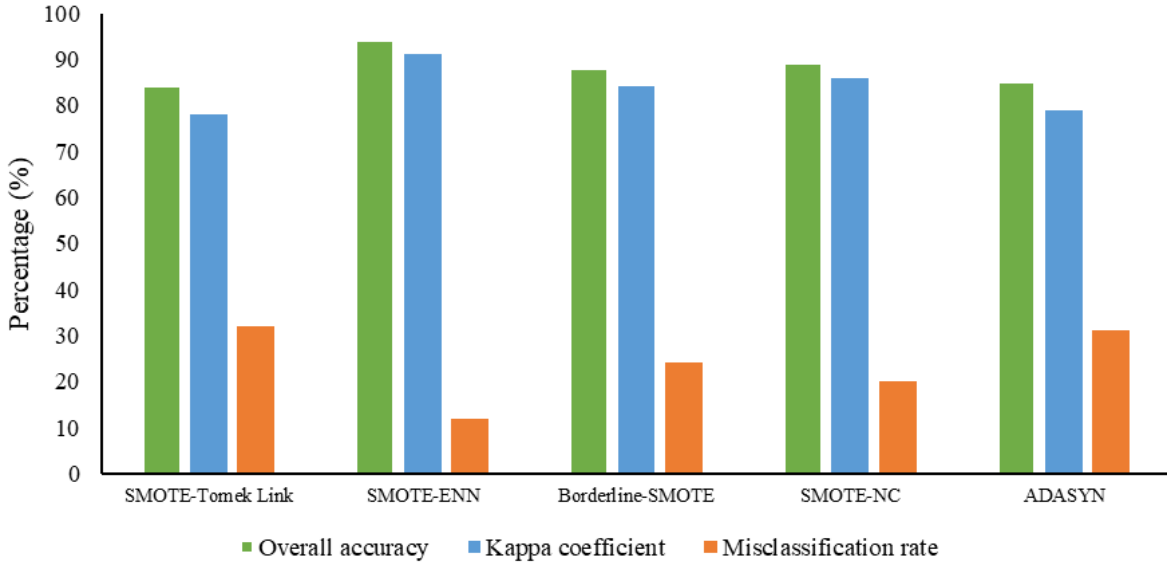

Figure 2-6. Overall accuracy, kappa coefficient and misclassification rate achieved using five balanced dataset and XGBoost classifier.

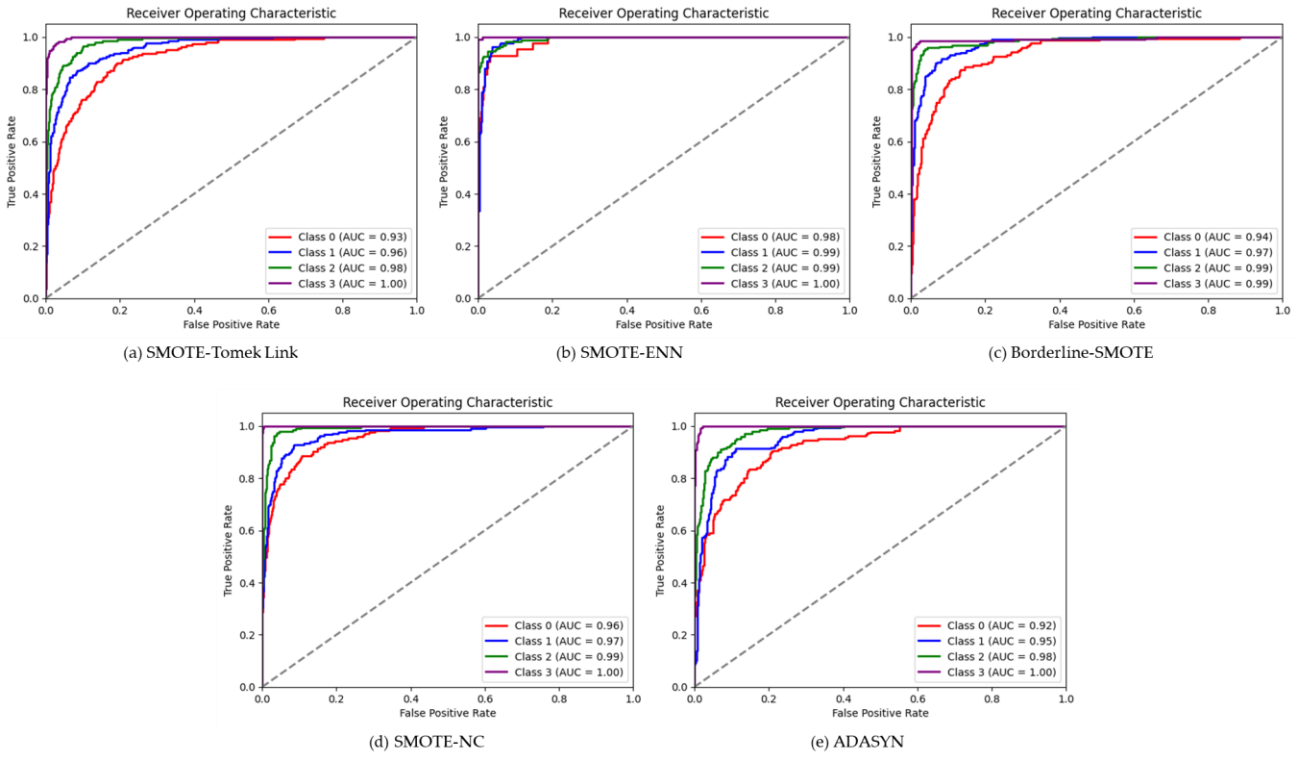

Figure 2-7. The ROC curve using five balanced datasets and XGBoost classifier.

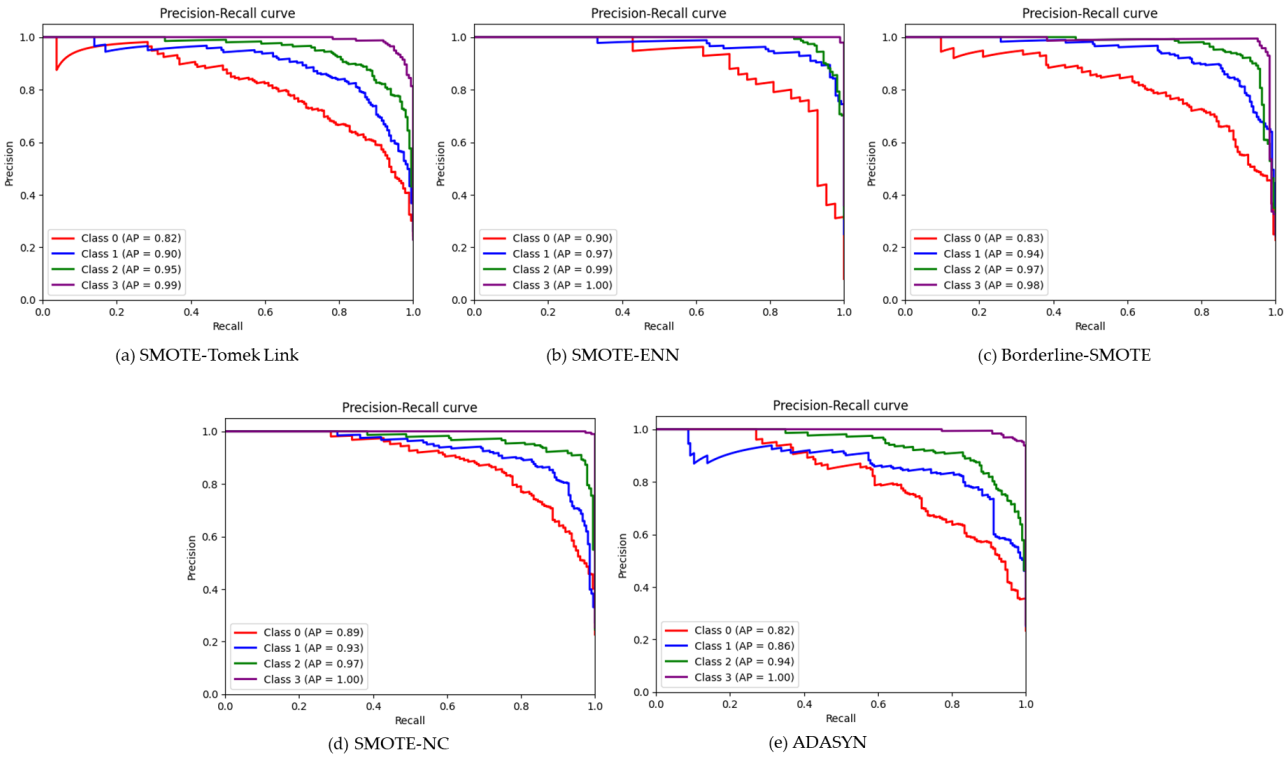

Figure 2-8. The Precision-Recall curve using five balanced datasets and XGBoost classifier.

2.4.3.3 Classification performance using five pre-processed datasets of RF classifier using five balancing methods

Table 9 represents the results of RF classifier to classify soybean lodging using five balanced datasets. RF classifier resulted in higher overall classification accuracy of 0.93 was obtained using SMOTE-ENN dataset whereas 0.85, 0.88, 0.86 and 0.85 was obtained from SMOTE-Tomek Link, Borderline-SMOTE, SMOTE-NC and ADASYN, respectively. SMOTE-ENN outperformed all other methods with higher precision, recall, F1-score, kappa value. The misclassification rate was also minimum for SMOTE-ENN dataset with the value of 13%. Overall accuracy, kappa coefficient and misclassification rate of each balanced dataset are shown in Figure 9. As using SMOTE-ENN dataset showed better results than other datasets, it resulted best AUC from ROC curve AP values from the precision-recall curve (Figure 10 and 11).

Table 2-9. Confusion matrix and model performance metrices of four lodging classes of soybean using RF classifier.

Pre-processed Dataset	Actual samples	NL	ML	HL	SL	Precision	Recall	F1-score
SMOTE-Tomek Link	NL	121	34	19	13	0.81	0.65	0.72
	ML	16	174	6	5	0.82	0.87	0.84
	HL	9	4	184	3	0.87	0.92	0.90
	SL	4	0	2	169	0.89	0.97	0.93
SMOTE-ENN	NL	25	12	4	1	0.89	0.60	0.71
	ML	3	123	4	2	0.87	0.93	0.90
	HL	0	6	156	1	0.94	0.96	0.95
	SL	0	0	2	188	0.98	0.99	0.98
Borderline-SMOTE	NL	134	22	16	4	0.78	0.76	0.77
	ML	25	187	5	0	0.88	0.86	0.87
	HL	10	4	177	0	0.89	0.93	0.91
	SL	3	0	0	185	0.98	0.98	0.98
SMOTE-NC	NL	125	26	18	6	0.80	0.71	0.76
	ML	22	179	7	3	0.85	0.85	0.85
	HL	7	6	172	5	0.87	0.91	0.89
	SL	2	0	1	193	0.93	0.98	0.96
ADASYN	NL	118	34	22	7	0.80	0.65	0.72
	ML	19	161	12	3	0.79	0.83	0.80
	HL	9	9	181	1	0.84	0.91	0.87
	SL	2	1	0	195	0.95	0.98	0.97

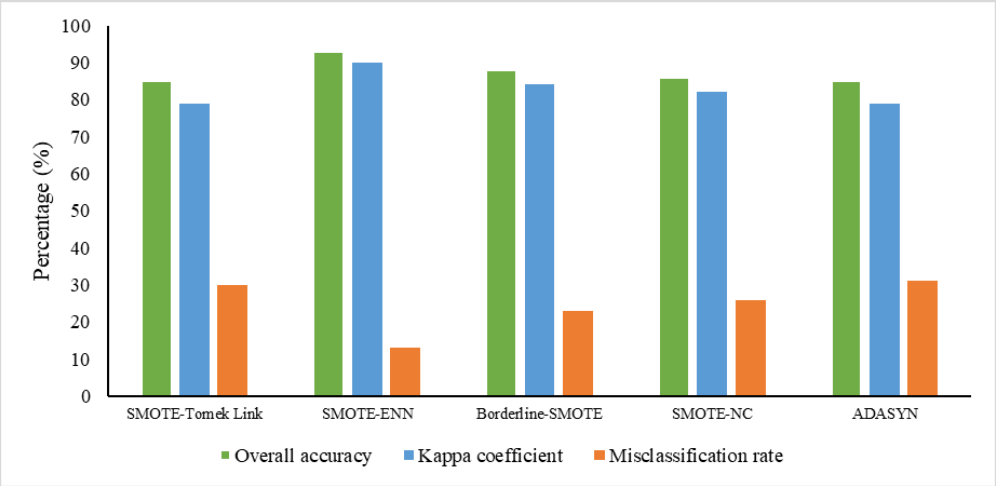

Figure 2-9. Overall accuracy, kappa coefficient and misclassification rate achieved using different balanced dataset and RF classifier.

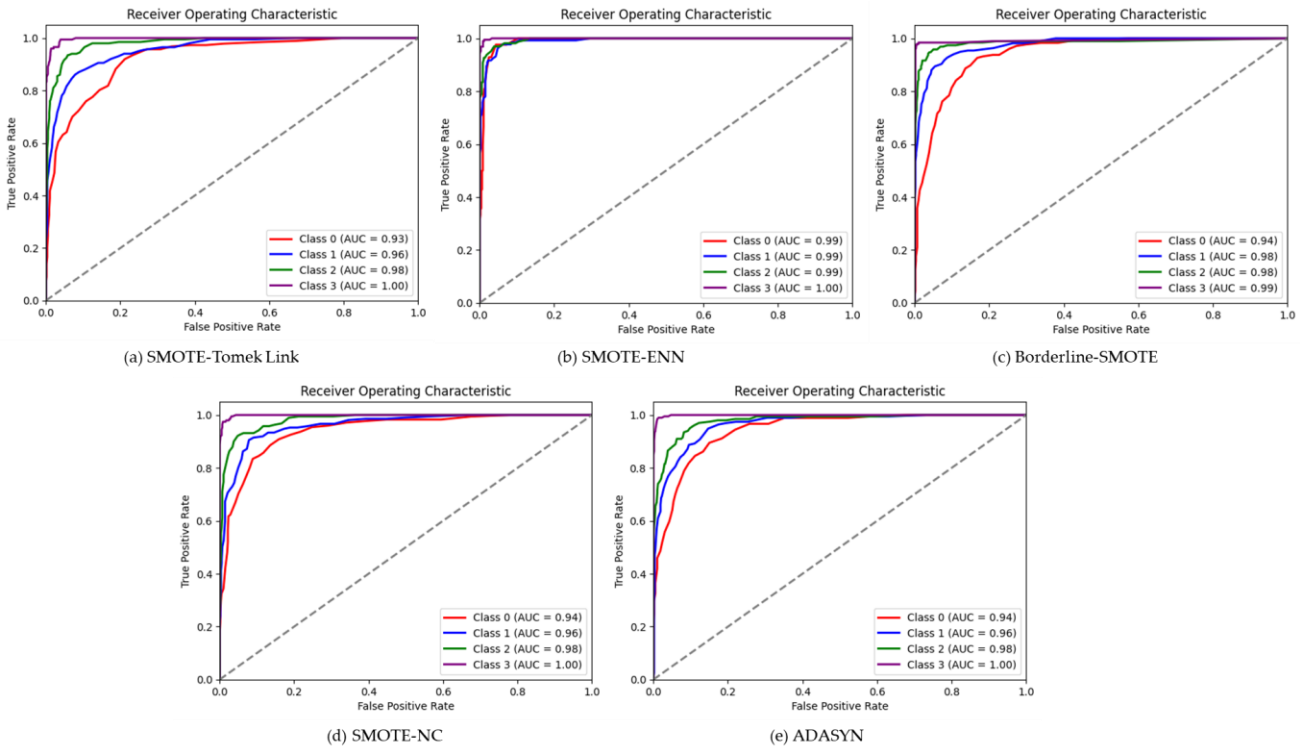

Figure 2-10. The ROC curve using five balanced datasets and RF classifier.

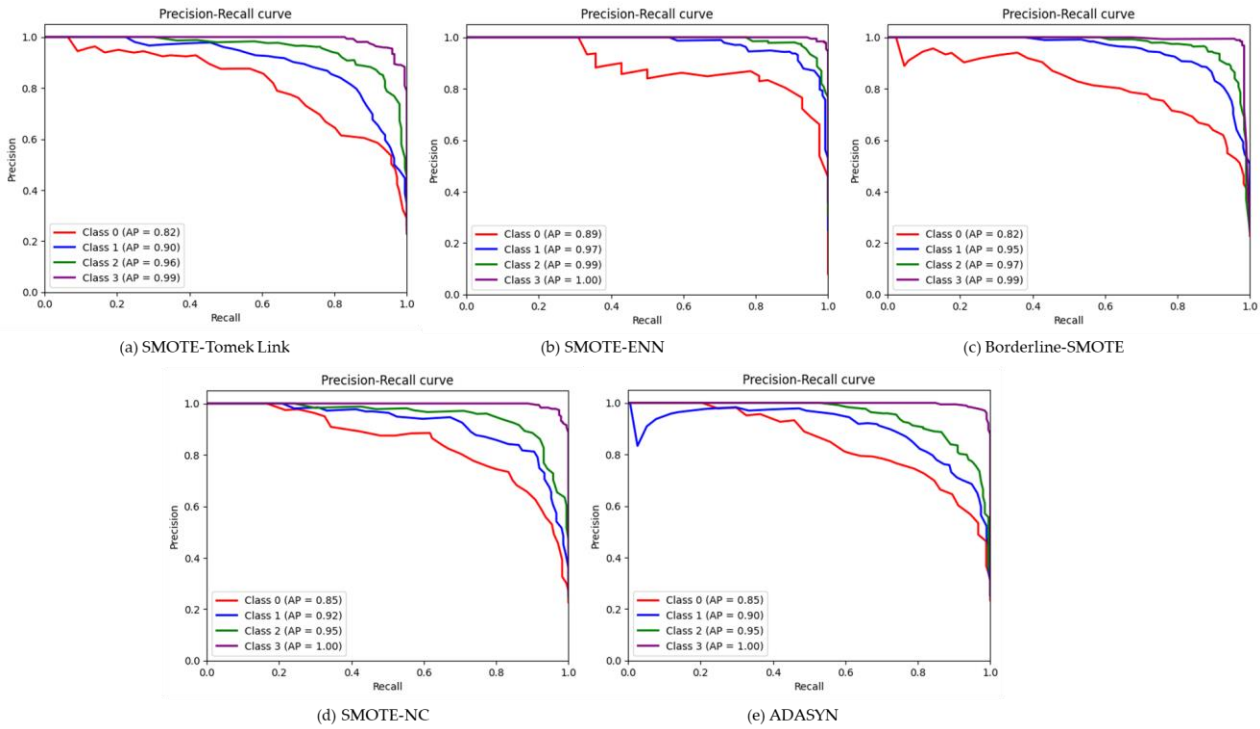

Figure 2-11. The Precision-Recall curve using five balanced datasets and RF classifier.

2.4.3.4 Classification performance using five pre-processed datasets of KNN classifier using five balancing methods

Soybean lodging classification results of KNN classifier using five types of balanced dataset are presented in Table 10. Unlike other classifiers XGBoost and RF, KNN showed the similar trend in classifying the soybean lodging. Higher overall classification accuracy was obtained using the SMOTE-ENN dataset with the value of 0.91 (Figure 12), where NL class showed lower recall and f1-score of 0.55 and 0.69, respectively. Other classes ML, HL and SL showed consistency with the value greater than 0.75 in all respect. Higher kappa value of 0.87 and lower misclassification rate was also obtained from SMOTE-ENN with the value of 17% (Figure 12). Other results using balanced dataset doesn't show as better as SMOTE-ENN. The AUC values for each class were 0.96, 0.98, 1.00, and 1.00 for NL, ML, HL, and SL, respectively whereas, AP values were 0.90, 0.96, 0.99 and 1.00 (Figure 13 and 14) for SMOTE-ENN dataset.

Table 2-10. Confusion matrix and model performance metrices of four lodging classes of soybean using KNN classifier.

Pre-processed Dataset	Actual samples	NL	ML	HL	SL	Precision	Recall	F1-score
SMOTE-Tomek Link	NL	64	60	36	27	0.89	0.34	0.49
	ML	6	173	15	7	0.72	0.86	0.78
	HL	1	7	189	3	0.78	0.94	0.86
	SL	1	1	2	171	0.82	0.98	0.89
SMOTE-ENN	NL	23	17	1	1	0.92	0.55	0.69
	ML	1	115	12	4	0.82	0.87	0.84
	HL	1	9	153	0	0.92	0.94	0.93
	SL	0	0	0	190	0.97	1.00	0.99
Borderline-SMOTE	NL	91	48	28	9	0.79	0.52	0.63
	ML	18	191	5	3	0.77	0.88	0.82
	HL	5	9	177	0	0.84	0.93	0.88
	SL	1	1	1	185	0.94	0.98	0.96
SMOTE-NC	NL	84	55	24	12	0.74	0.48	0.58
	ML	18	172	17	4	0.72	0.82	0.76
	HL	10	12	164	4	0.77	0.86	0.81
	SL	2	1	9	184	0.90	0.94	0.92
ADASYN	NL	61	51	49	20	0.80	0.34	0.47
	ML	9	170	15	1	0.72	0.87	0.79
	HL	6	12	181	1	0.73	0.91	0.81
	SL	0	2	2	194	0.90	0.98	0.98

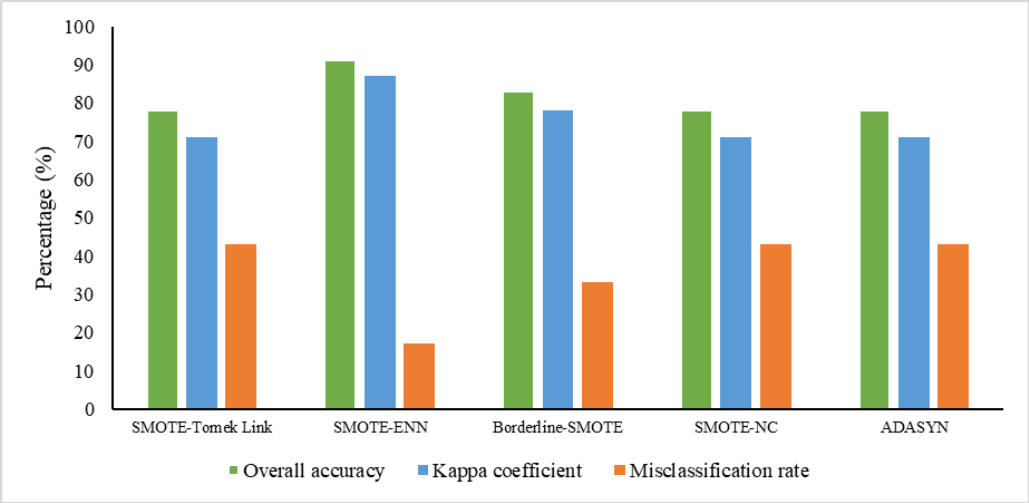

Figure 2-12. Overall accuracy, kappa coefficient and misclassification rate achieved using different balanced dataset and KNN classifier.

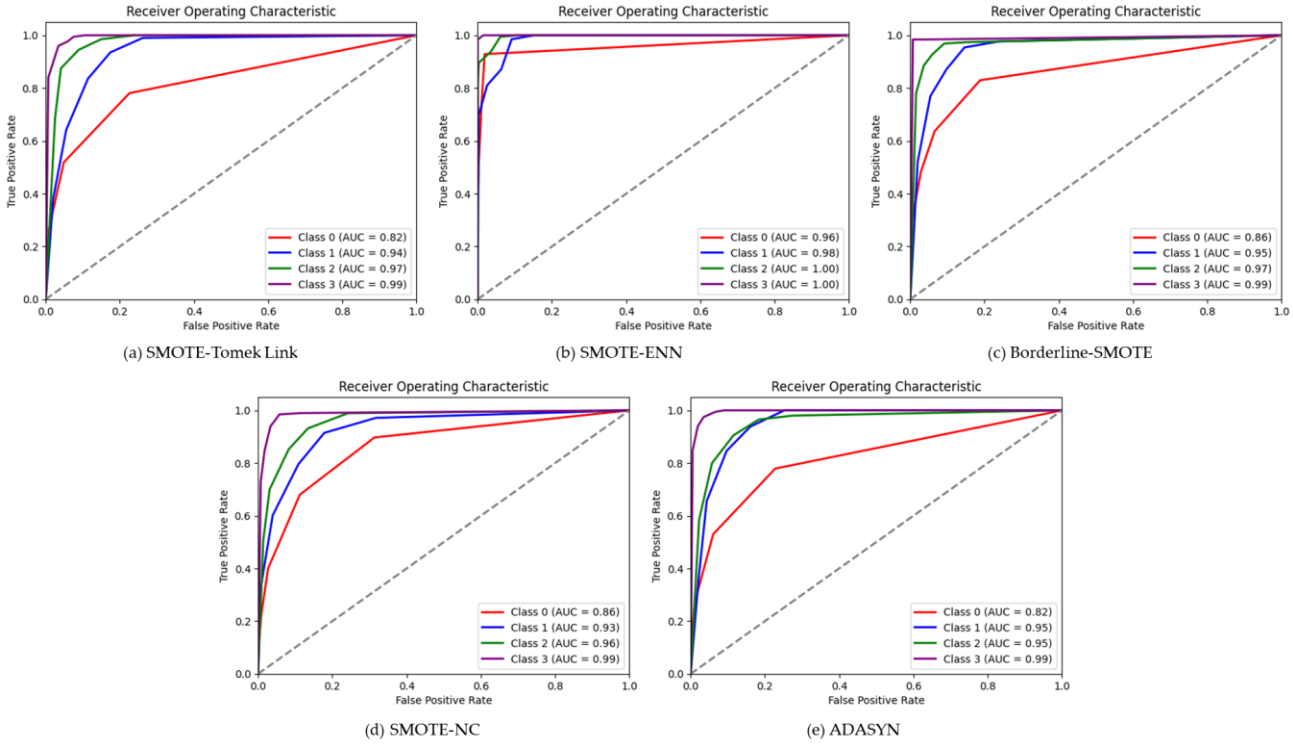

Figure 2-13. The ROC curve using five balanced datasets and KNN classifier.

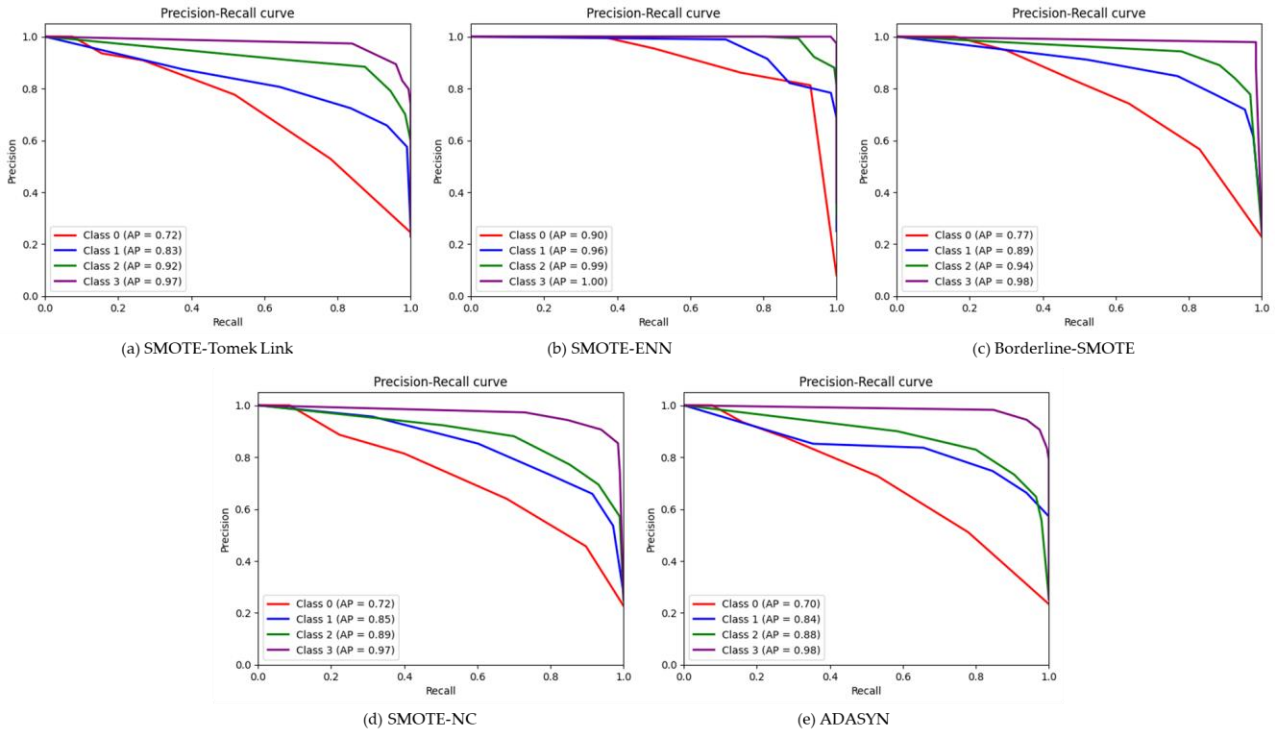

Figure 2-14. The Precision-Recall curve using five balanced datasets and KNN classifier.

2.4.3.5 Classification performance using five pre-processed datasets of ANN classifier using five balancing methods

Table 11 shows the lodging classification results using five balanced dataset and ANN classifier. As previous results, SMOTE-ENN showed the higher classification accuracy of 0.96 (Figure 15) with higher precision, recall and f1-score for ML, HL and SL except the class NL (Table 6). Very minimum misclassification rate of 7% was obtained using the SMOTE-ENN dataset, whereas other datasets resulted in 32%, 25%, 25% and 36% misclassification rate (Figure 15). Other results using SMOTE-Tomek Link, Borderline-SMOTE, SMOTE-NC and ADASYN dataset showed classification accuracy higher than 0.8 but SMOTE-ENN outperformed in every case. On the other hand, higher AUC and AP values was obtained from the SMOTE-ENN dataset for each class (Figure 16 and 17).

Table 2-11. Confusion matrix and model performance metrices of four lodging classes of soybean using ANN classifier.

Pre-processed Dataset	Actual samples	NL	ML	HL	SL	Precision	Recall	F1-score
SMOTE-Tomek Link	NL	105	58	24	5	0.55	0.87	0.67
	ML	14	162	8	4	0.86	0.72	0.78
	HL	2	6	193	1	0.95	0.86	0.90
	SL	0	0	0	181	1.00	0.95	0.97
SMOTE-ENN	NL	22	15	3	1	0.53	0.92	0.67
	ML	1	147	0	0	0.99	0.91	0.95
	HL	1	0	158	0	0.99	0.98	0.98
	SL	0	0	0	179	1.00	0.99	0.99
Borderline-SMOTE	NL	133	56	21	0	0.63	0.90	0.74
	ML	7	171	2	0	0.95	0.74	0.83
	HL	6	3	191	0	0.95	0.89	0.92
	SL	1	1	0	180	0.98	1.00	0.99
SMOTE-NC	NL	166	27	15	2	0.79	0.82	0.81
	ML	21	149	10	0	0.83	0.81	0.82
	HL	14	8	177	1	0.88	0.87	0.88
	SL	0	0	0	182	1.00	0.98	0.99
ADASYN	NL	94	59	40	5	0.48	0.85	0.61
	ML	12	166	9	1	0.88	0.72	0.79
	HL	4	4	184	5	0.93	0.78	0.85
	SL	0	0	0	191	1.00	0.94	0.97

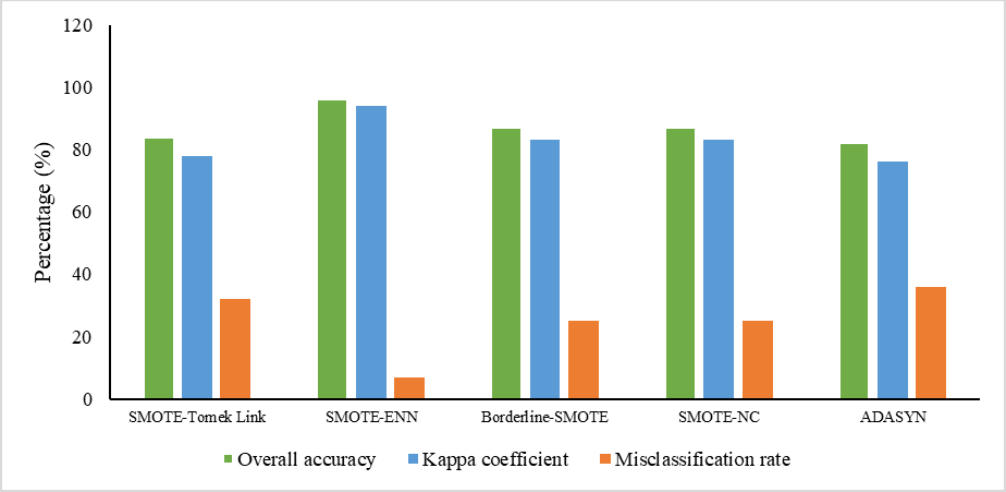

Figure 2-15. Overall accuracy, kappa coefficient and misclassification rate achieved using different balanced dataset and ANN classifier.

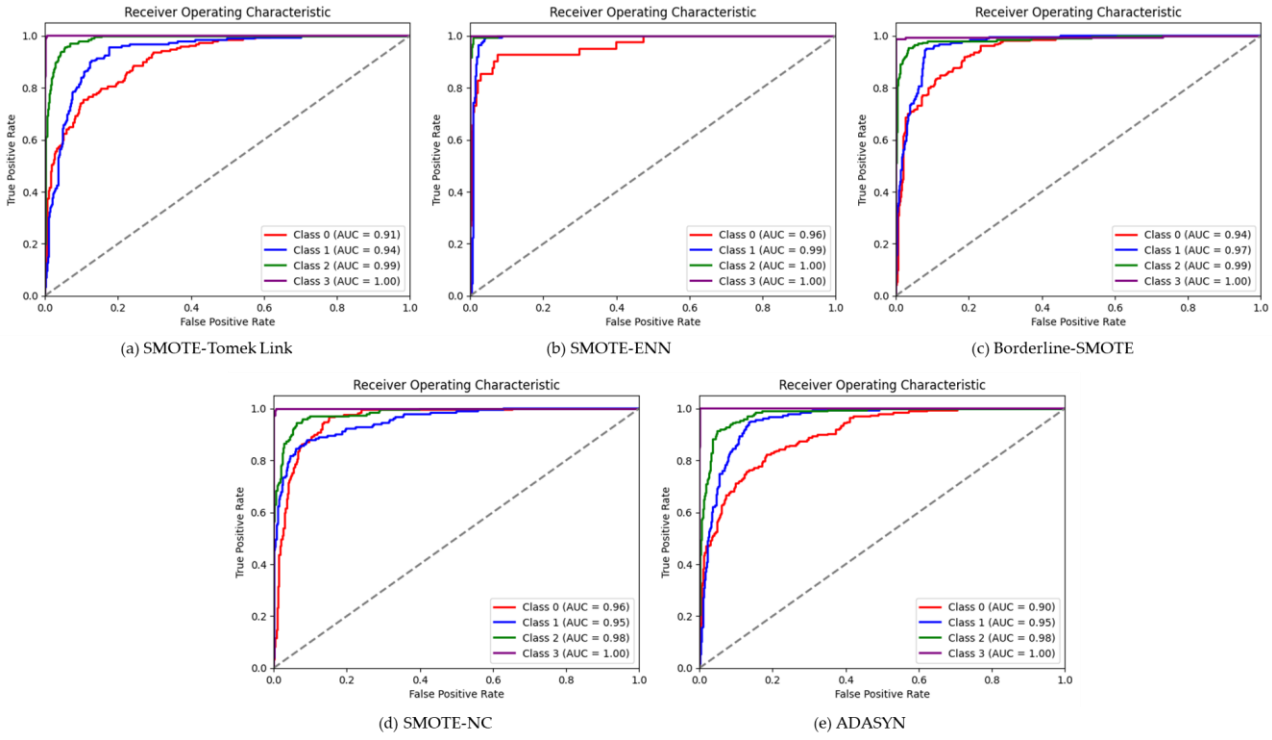

Figure 2-16. The ROC curve using five balanced datasets and ANN classifier.

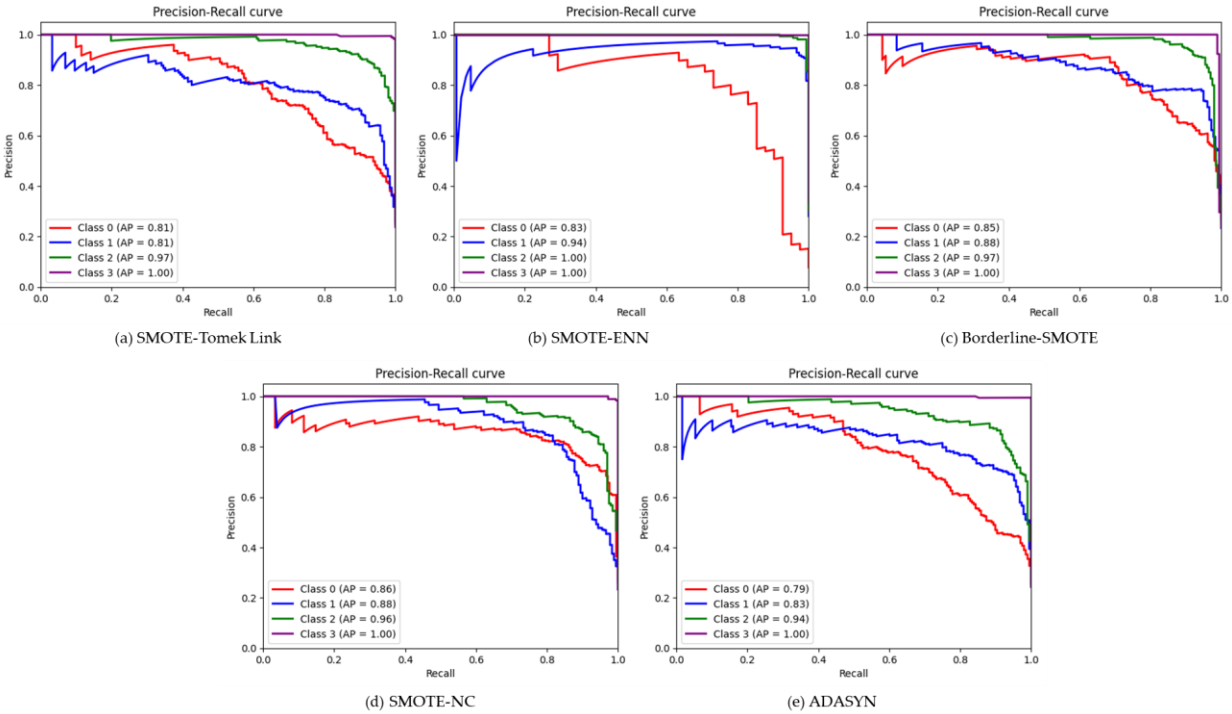

Figure 2-17. The Precision-Recall curve using five balanced datasets and ANN classifier.

2.5 Discussion

Lodging is one of the major factors of reduced crop yields (Wu et al., 2022). Accurate classification of crop lodging is highly economical for decision-making regarding breeding purposes. Some researchers already used UAV RGB imagery to classify lodging of different crops with the increasing development of UAV technology. But in our knowledge, there is no research conducted to classify soybean lodging for breeding purposes. One of the reasons might be complexity of analysis using imbalanced dataset and focuses on mostly known phenotypic traits leads to put less focus on soybean lodging classification using UAV-based imagery. Though there was big challenge associated with the data pre-processing as the lodging classes were highly imbalanced, we came to a point to justify our results with other researcher's findings. We used original dataset and five data balancing methods (SMOTE-Tomek Link, SMOTE-ENN, Borderline-SMOTE, SMOTE-NC and ADASYN) to balance the dataset and were analyzed each

of these balanced datasets using XGBOOST, RF, KNN and ANN classifiers. From the above-described results, SMOTE-ENN performed the best among all balancing techniques for all the machine learning classifiers, achieving the highest overall accuracy, lowest misclassification rate and highest Kappa coefficient in all the cases. Based on the SMOTE-ENN dataset results of four classifiers, the comparison was described in this following section.

RGB image features for maize lodging severity with the accuracy of 94.5% with the XGBoost classifier after using SMOTE-ENN pre-processing (Han et al., 2022). The researchers used be-fore and after balancing the dataset method for maize lodging classification, where the non-lodging and lodging data distribution was 713 and 87 before balancing, respectively. After balancing using SMOTE-ENN method, the non-lodging and lodging dataset be-comes 546 and 671, respectively. Which reduces the non-lodging dataset and increases the lodging dataset for balancing the dataset [81]. Undersampling and SMOTE method was used for wheat yield estimation by (Chemchem et al., 2019), where the researcher finds out that the SMOTE data balancing method significantly increases training score and AUC ROC values using well known machine learning methods. Random forest classifier showed the training score and AUC ROC values of 99.40% and 0.72 (without sampling), 99.78% and 0.73 (undersampling), and 99.92% and 0.90 (SMOTE sampling), respectively. Hyperspectral imagery data available from the public domain with 16 classes were classified using tree based ensembled classifiers by Datta (Datta et al., 2022), encompassing several data balancing methods, which resulted in SMOTE, Tomek-Links and their combinations higher accuracy and best resampling strategy.

In our study we follow the same data balancing method SMOTE-ENN, where the number of NL dataset (Table 2) reduced and the number of ML, HL, SL increased, using the data balancing method. In result, our study of soybean lodging classification resulted in 94% accuracy with the

XGBoost classifier and SMOTE-ENN data balancing method. RGB image features was used for grass lodging severity and found the accuracy of 79.1% (Tan et al., 2021), whereas 86.61% accuracy was observed by (Sun et al., 2019) for maize lodging classification using maximum likelihood classification (MLC) algorithm. On the other hand, used random forest (RF) classifier was used for barley lodging mapping and found the overall accuracy of 99.7% using multispectral imagery (Vlachopoulos et al., 2021). In our study, we found overall accuracy of 93% on the testing dataset using RF classifier for soybean lodging classification. Other re-searcher's results superiority using RF may be associated with its data feature extraction and number of training and testing balanced dataset. Furthermore, KNN yield classification accuracy of 91% for soybean lodging whereas nearest neighborhood classification and support vector machine (SVM) by (Chauhan et al., 2019; Rajapaksa et al., 2018) reported wheat lodging classification 90% and 92.6%, respectively using multispectral imagery. Furthermore, Principal component analysis and ANN was used to differentiate the rice lodging with the overall accuracy of 97.8% using hyperspectral reflectance data (Liu et al., 2011), whereas our study reveals the overall accuracy of 96% using RGB image derived textural features for soybean lodging. The higher accuracy obtained by [85] might be the reason for using hyperspectral imagery technique which can identify and quantify molecular absorption. Soybean lodging which can have effects on crop yield and quality can be minimized by accurately classifying soybean lodging. Breeders can identify and address the factors associated in lodging such as genetics, environmental conditions or other agronomic factors. On the other hand, soybean lodging classification based of deep learning algorithm can automatically extract intrinsic feature from the dataset using different supervised and unsupervised learning to classify the different extent of soybean lodging. The best advantage of RGB imagery technique, which includes low cost and beneficial for smallholders to detect crop lodging.

There is still a huge lack in soybean lodging detection research for breeding. Though there are other traits such as yield, plant height, days to maturity, leaf wilting are associated to select the best genotypes for breeding purpose, lodging is one of the crucial factors considered by the breeders which somehow not in mainstream research using UAV based imagery technology. One of the biggest limitations in soybean lodging detection is imbalanced dataset of different classes which creates the challenge for researchers in analyzing and obtaining good output. To address the emerging issue four balancing method was used to balance the class difference. Further, detailed classification exploring other super-vised deep learning methods along with the machine learning methods can be explored to obtain higher accuracy for soybean lodging detection.

2.6 Conclusions

In this study, the research was aimed to classify the soybean lodging extent using UAV RGB imagery technology for breeding purposes. The RGB image derived textural features and RGB image were tested to classify the different soybean lodging extent. The im-ages were pre-processed by adjusting the grids according to each plot shape, cropping and background removing to generate the texture features for machine learning models. The experimental results indicate that the developed classification models precisely distinguished high lodged and severe lodged soybean genotypes with different genotype background with higher precision and recall using every machine learning deep learning models. The classification performance of the machine learning models using RGB image derived texture features was 94%, 93%, 91% and 96% using SMOTE-ENN XGBoost, SMOTE-ENN RF, SMOTE-ENN KNN and SMOTE-ENN ANN, respectively. In addition, image features and overall classification accuracies of different machine learning models shows the consistency and similar pattern in classifying four classes which can be more justified using different environments dataset of non-tested genotypes. Further research is highly

encouraged using multispectral imagery technology and different supervised deep learning methods to enhance the classification accuracies. But as a cost-effective choice for breeders and associated researchers UAV based RGB imagery system can be the solution for plant breeding program in identifying the superior genotypes by identifying the lodged genotypes.

References

Ai-Jun, L., Peng, Z. (2020). Research on unbalanced data processing algorithm base Tomek Links-SMOTE. In the Proceedings of the 2020 3rd International Conference on Artificial Intelligence and Pattern Recognition June 2020 Pages 13–17. 10.1145/3430199.3430222.

Akhtar, A., Nazir, M., Khan S. A. (2012). Crop Classification using feature extraction from satellite imagery. In the Proceeding of the 15th International Multitopic Conference (INMIC), Islamabad, Pakistan, 2012. 10.1109/INMIC.2012.6511479.

Al-Tamimi, N., Langan, P., Bernád, V., Walsh, J., Mangina, E., Negrão, S. (2022). Capturing crop adaptation to abiotic stress using image-based technologies. Open Biology, 12, 210353. 10.1098/rsob.210353.

Amirruddin, A. D., Muharam, F. M., Ismail, M. H., Tan, N. P., Ismail, M. F. (2022). Synthetic Minority Over-sampling Technique (SMOTE) and Logistic Model Tree (LMT)-Adaptive Boosting algorithms for classifying imbalanced datasets of nutrient and chlorophyll sufficiency levels of oil palm (Elaeis guineensis) using spectroradiometers and unmanned aerial vehicles. Computer and Electronics in Agriculture, 193, 106646. 10.1016/j.compag.2021.106646.

Bagherzadi, L. (2017). Assessing physiological mechanisms to elucidate the slow-wilting trait in soybean genotypes, PhD thesis from North Carolina State University: Raleigh, NC, USA, 2017.

Bai, H., Purcell, L. C. (2018). Aerial canopy temperature differences between fast- and slow-wilting soyabean genotypes. Journal of Agronomy and Crop Science, 204, 243-251. 10.1111/jac.12259.

Barrett, J. (2022). Corn and soybean production up in 2021, USDA Reports, Corn and soybean stocks up from year earlier, Winter Wheat Seedings up for 2022. United States Department of Agriculture, National Agricultural Statistics Service. https://www.nass.usda.gov/Newsroom/2022/01-12-2022.php#:~:text=Soybean%20production%20for%202021%20totaled,the%20second%20highest%20on%20record. (accessed on February 28, 2023).

Batista, G. E. A. P. A., Prati, R. C., Monard, M. C. (2004). A study of the behavior of several methods for balancing machine learning training data. ACM SIGKDD Explorations Newsletter. 6(1), 20-29.

Beck, M. W. (2018). Neural Net Tools: Visualization and analysis tools for neural networks. Journal of Statistical Software, 85(11), 1-20. 10.18637/jss.v085.i11.

Berry, P., Spink, J., Sylvester-Bradley, R., Pickett, A., Sterling, M., Baker, C., Cameron, N. (2002). Lodging control through variety choice and management. In the Proceedings of the 8th Home-Grown Cereals Association R & D Conference on Cereals and Oilseeds, Harrogate, UK, 9–10 January 2002, pp. 7-1.

Cao, W., Zhou, J., Yuan, Y., Ye, H., Nguyen, H. T., Chen, J., Zhou, J. (2019). Quantifying variation in soybean due to flood using a low-cost 3D imaging system. Sensors. 19, 2682. 10.3390/s19122682.

Chan, T. F., Vese, L. A. (2001). Active contours without edges. IEEE Transaction of Image Processing, 10(2), 266–277. 10.1109/83.902291.

Chauhan, S., Darvishzadeh, R., Lu, Y., Boschetti, M., Nelson, A. (2020). Understanding wheat lodging using multi-temporal Sentinel-1 and Sentinel-2 data. Remote Sensing of Environment, 243, 111804. 10.1016/j.rse.2020.111804.

Chauhan, S., Darvishzadeh, R., Lu, Y., Stroppiana, D., Boschetti, M., Pepe, M., Nelson, A. D. Wheat lodging assessment using multispectral UAV data. In the Proceedings of the ISPRS Geospatial Week Volume XLII-2/W13, 2019 ISPRS Geospatial Week 2019, 10–14 June 2019, Enschede, The Netherlands.

Chawla, N. V., Bowyer, K. W., Hall, L. O., Kegelmeyer, W. P. (2002). SMOTE: Synthetic minority oversampling technique. Journal of Artificial Intelligence Research, 16, 321–357.

Chemchem, A, Alin, F., Krajecki, M. (2019). Combining SMOTE sampling and machine learning for forecasting wheat yields in France. In the proceedings of 2019 IEEE Second International Conference on Artificial Intelligence and Knowledge Engineering (AIKE), Sardinia, Italy, 2019, pp. 9-14. 10.1109/AIKE.2019.00010.

Cisty, M., Soldanova, V. (2018). Flow prediction versus flow simulation using machine learning algorithms. In: Perner, P. (eds) Machine Learning and Data Mining in Pattern Recognition.

MLDM 2018. Lecture Notes in Computer Science, vol 10935. Springer, Cham. 10.1007/978-3-319-96133-0_28.

Datta, D, Mallick, P. K., Shafi, J, Choi, J, Ijaz, M. F. (2022). Computational intelligence for observation and monitoring: A case study of imbalanced hyperspectral image data classification. Computational Intelligence and Neuroscience, 30, 2022:8735201. 10.1155/2022/8735201.

Díaz-Varela, R. A., de la Rosa, R., León, L., Zarco-Tejada, P. J. (2015). High-resolution airborne UAV imagery to assess olive tree crown parameters using 3D photo reconstruction: Application in breeding trials. Remote Sensing, 7, 4213-4232. 10.3390/rs70404213.

Duan, L., Han, J., Guo, Z., Tu, H., Yang, P., Zhang, D., Zeng, D., Tan, J., Qiao, Y., Zhuang, D. (2018). Novel digital features discriminate between drought resistant and drought sensitive rice under controlled and field conditions. Frontiers in Plant Science, 9, 492. 10.3389/fpls.2018.00492.

Duan, T., Chapman, S. C., Guo, Y., Zhen, B. (2017). Dynamic monitoring of NDVI in wheat agronomy and breeding trials using an unmanned aerial vehicle. Field Crops Research, 210, 71-80. 10.1016/j.fcr.2017.05.025.

Fehr, W. R., Caviness, C. E., Burmood, D. T., Pennington, J. S. (1971). Stage of development descriptions for soybeans, Glycine Max (L.) Merrill1. Crop Science, 11(6), 929-931. 10.2135/cropsci1971.0011183X001100060051x.

Fernández, A., García, S., Herrera, F., Chawla, N. V. (2018). SMOTE for learning from imbalanced data: progress and challenges, marking the 15-year anniversary. Journal of Artificial Intelligence Research, 61, 863–905.

Gao, C. C., Hui, X. W. (2010). GLCM-based texture feature extraction. Computer Systems and Application, 19(6), 195-198.

Gao, Q., Jin, X., Xia, E., Wu, X., Gu, L., Yan, H., Xia, Y., Li, S. (2020). Identification of orphan genes in unbalanced datasets based on ensemble learning. Frontiers in Genetics, 2(11), 820. 10.3389/fgene.2020.00820.

Genuer, R., Poggi, J. M., Tuleau-Malot, C. (2015). VSURF: An R package for variable selection using random forests. The R Journal, 7, 1, 19-33.

Georganos, S., Grippa, T., Vanhuysse, S., Lennert, M., Shimoni, M., Wolff, E. (2018). Very high-resolution object-based land use-land cover urban classification using extreme gradient boosting. IEEE Geoscience and Remote Sensing Letters, 15(4), 607-611. 10.1109/LGRS.2018.2803259.

Hall-Beyer, M. (2017). Practical guidelines for choosing GLCM textures to use in landscape classification tasks over a range of moderate spatial scales. International Journal of Remote Sensing, 38(5), 1312–1338. 10.1080/01431161.2016.1278314.

Han, L., Yang, G., Feng, H., Zhou, C., Yang, H., Xu, B., Li, Z., Yang, X. (2018). Quantitative identification of maize lodging-causing feature factors using unmanned aerial vehicle images and a nomogram computation. Remote Sensing, 10, 1528. 10.3390/rs10101528.

Han, L., Yang, G., Yang, X., Song, X., Xu, B., Li, Z., Wu, J., Yang, H., Wu, J. (2022). An explainable XGBoost model improved by SMOTE-ENN technique for maize lodging detection based on multi-source unmanned aerial vehicle images. Computer and Electronics in Agriculture, 194, 106804. 10.1016/j.compag.2022.106804.

Haralick, M. R. (1973). Textural features for image classification. IEEE Transactions on Systems, Man, and Cybernetics, SMC-3(6), 610–621. 10.1109/TSMC.1973.4309314.

He, H., Bai, Y., Garcia, E. A., Li, S. (2008). ADASYN: Adaptive synthetic sampling approach for imbalanced learning. In the proceedings of the IEEE International Joint Conference on Neural Networks (IEEE World Congress on Computational Intelligence) 2008, Hong Kong, China: IEEE Press, 1322-1328.

He, H., Garcia, E. A. (2009). Learning from imbalanced data. IEEE Transaction Knowledge and Data Engineering, 21(9), 1263-1284.

Iqbal, N., Mumtaz, R., Shafi, U., Zaidi, S. M. (2021). Gray level co-occurrence matrix (GLCM) texture-based crop classification using low altitude remote sensing platforms. PeerJ Computer Science, 7, e536. 10.7717/peerj-cs.536.

Kato, S., Cober, E., O'Donoghue, L., Morrison, M. J., Rajcan, I. (2020). Phenotyped the materials, performed GWAS and complementary data analysis, and wrote the manuscript. Canadian Journal of Plant Science, 100(6), 1243-1252.

Kitabatake, T., Yamaguchi, N., Sayama, T., Taguchi-Shiobara, F., Suzuki, H., Ishimoto, M., Yoshihira, T. (2019). Morpho-logical traits associated with the quantitative trait locus for

lodging tolerance in soybean. Crop Science, 59(2), 504-516. 10.2135/cropsci2018.08.0496.

Kwak, G. H., Park, N. W. (2019). Impact of texture information on crop classification with machine learning and UAV images. Applied Science, 9(4), 643. 10.3390/app9040643.

Liu, H. Y., Yang, G. J., Zhu, H. C. (2014). The extraction of wheat lodging area in UAV's image used spectral and texture features. Applied Mechanics and Materials, 651-653, 2390-2393. 10.4028/www.scientific.net/AMM.651-653.2390.

Liu, L., Wang, J., Song, X., Li, C., Huang, W., Zhao, C. (2005). The canopy spectral features and remote sensing of wheat lodging. Journal of Remote Sensing, 9, 323-327. (in Chinese with English abstract).

Liu, Z., Li, C., Wang, Y., Huang, W., Ding, X., Zhou, B., Wu, H., Wang, D., Shi, J. (2011). Comparison of spectral indices and principal component analysis for differentiating lodged rice crop from normal ones. In the proceedings of computer and computing technologies in agriculture V. CCTA 2011. IFIP Advances in Information and Communication Technology, vol 369. Springer, Berlin, Heidelberg. 10.1007/978-3-642-27278-3_10.

Lodging of soybean. (2021, September 1) Retrieved from https://www.dekalbasgrowdeltapine.com/en-us/agronomy/soybean-lodging.html. Accessed on 06/19/2023.

Lu, D., Hetrick, S., Moran, E. Land cover classification in a complex urban-rural landscape with Quickbird im-agery. Photogramm. Eng. Remote Sensing. 2010. 76(10), 1159–1168.

Mardanisamani, S., Maleki, F., Kassani, S. H., Rajapaksa, S., Duddu, H., Wang, M., Shirtliffe, S., Ryu, S., Josuttes, A., Zhang, T., Vail, S., Pozniak, C., Parkin, I., Stavness, I., Eramian, M. (2019). Crop lodging prediction from UAV-acquired images of wheat and canola using a dcnn augmented with handcrafted texture features. Remote Sensing, 11, 2657-2664. 10.3390/rs11222657.

Mausda, R., Nomura, K., Iida, M., Suguri, M. (2012). Detection of rice plant lodging using camera and laser range finder. In the proceeding of the Information Technology Automation and Precision Farming. International Conference of Agricultural Engineering - CIGR-AgEng 2012: Agriculture and Engineering for a Healthier Life, Valencia, Spain, 8-12 July 2012, pp.C-1888 ref.6

Mekhalfa, F., Yacef, F. (2021). Supervised learning for crop/weed classification based on color and texture features. Cornell University, 2021. arXiv:2106.10581.

Moumni, A., Lahrouni, A. (2021). Machine learning-based classification for crop-type mapping using the fusion of high-resolution satellite imagery in a semiarid area. Scientifica, 2021. 10.1155/2021/8810279.

Murthy, C., Raju, P., Badrinath, K. (2003). Classification of wheat crop with multi-temporal images: Performance of maximum likelihood and artificial neural networks. International Journal of Remote Sensing, 24, 4871–4890. 10.1080/0143116031000070490.

Park, B., Chen, Y. R. (2001). Co-occurrence matrix texture features of multi-spectral images on poultry carcasses. Journal of Agricultural Engineering Research, 78(2), 127-139. 10.1006/jaer.2000.065.

Pinto, L. S., Ray, A., Reddy, M. U., Perumal, P., Aishwarya, P. (2016). Crop disease classification using texture analysis. In the proceeding of 2016 IEEE International Conference on Recent Trends in Electronics, Information & Communication Technology (RTEICT), Bangalore, India, 2016, pp. 825-828. 10.1109/RTEICT.2016.7807942.

Rajapaksa, S., Eramian, M., Duddu, H., Wang, M., Shirtliffe, S., Ryu, S., Josuttes, A., Zhang, T., Vail, S., Pozniak, C., Parkin, I. (2018). Classification of crop lodging with gray level co-occurrence matrix. IEEE, 251-258. 10.1109/CCECE.2018.8447704.

Rashu, R. I., Haq, N., Rahman, R. M. (2014). Data mining approaches to predict final grade by overcoming class imbalance problem. In the Proceedings of the 2014 17th International Conference on Computer and Information Technology (ICCIT), Dhaka, Bangladesh, 22–23 December 2014, IEEE: Piscataway, NJ, USA, 2014, pp. 14–19.

Rubel, F., Brugger, K., Haslinger, K., Auer, I. (2017). The climate of the European alps: shift of very high resolution Köppen-Geiger climate zones1800–2100. Meteorologische Zeitschrift, 26(2), 115–125. 10.1127/metz/2016/0816. 10.1127/metz/2016/0816.

Saito, K., Nishimura, K., Kitahara, T. (2012). Effect on lodging on seed yield of field-grown soybean-artificial lodging and lodging preventing treatments. Japan Journal of Crop Science, 81(1), 27-32. 10.1626/jcs.81.27.

Shearer, S. A., Holmes R. G. (1990). Plant identification using color co-occurrence matrices. Transaction of the ASAE. 33(6), 1237-1244. 10.13031/2013.31574.

Shi, X, Tingyu, Q., Gijs, V. P., Marjan, V. D. A., Bart, D. M. (2022). A resampling method to improve the prognostic model of end-stage kidney disease: A better strategy for imbalanced data. Frontiers in Medicine, 9, 730748. 10.3389/fmed.2022.730748.

Singh, S., Srivastava, D., Agarwal, S. (2017). GLCM and its application in pattern recognition. In the Proceedings of the 5th International Symposium on Computational and Business Intelligence (ISCBI), Bangkok, Thailand, 20–25 November 2017, IEEE.

Skryjomski, P., Krawczyk, B. (2017). Influence of minority class instance types on SMOTE imbalanced data over-sampling. Proceedings of Machine Learning Research, 74,7–21.

Soares, J. V., Rennó, C. D., Formaggio, A. R., Yanasse, C. C. F., Frery, A. C. (1997). An investigation of the selection of texture features for crop discrimination using SAR imagery. Remote Sensing of Environment, 59(2), 234-247. 10.1016/S0034-4257(96)00156-3.

Sun, Q., Sun, L., Shu, M., Gu, X., Yang, G., Zhou, L. (2019). Monitoring maize lodging grades via unmanned aerial vehicle multispectral image. Plant Phenomics, 2019, 5704154. 10.1155/2019/5704154.

Taghizadeh-Mehrjardi, R, Schmidt, K, Eftekhari, K. (2020). Synthetic resampling strategies and machine learning for digital soil mapping in Iran. European Journal of Soil Science, 71(3), 352– 368. 10.1111/ejss.12893.

Tan, S., Mortensen, A. K., Ma, X., Boelt, B., Gislum, R. (2021). Assessment of grass lodging using texture and canopy height distribution features derived from UAV visual-band images.

Agricultural and Forest Meteorology, 308-309, 108541. 10.1016/j.agrformet.2021.108541.

Teodoro, P. E., Teodoro, L. P. R., Baio, F. H. R., da Silva Junior, C. A., dos Santos, R. G., Ramos, A. P. M., Pinheiro, M. M. F., Osco, L. P., Gonçalves, W. N., Carneiro, A. M., Junior, J. M., Pistori, H., Shiratsuchi, L. S. (2021). Predicting days to maturity, plant height, and grain yield in soybean: a machine and deep learning approach using multispectral data. Remote Sensing, 13, 4632. 10.3390/rs13224632.

Tian, M., Ban, S., Yuan, T., Ji, Y., Ma, C., Li, L. (2021). Assessing rice lodging using UAV visible and multispectral image. International Journal of Remote Sensing, 42, 8840-8857. 10.1080/01431161.2021.1942575.

Uddin, S., Haque, I., Lu, H., Moni, M. A., Gide, E. (2022). Comparative performance analysis of K-nearest neighbor (KNN) algorithm and its different variants for disease prediction. Scientific Reports, 12(1), 6256. 10.1038/s41598-022-10358-x.

Vann, R., Reisig, D., Thiessen, L. (2018). Soybean Considerations Following Hurricane Florence. Retrieved from https://soybeans.ces.ncsu.edu/2018/09/soybean-considerations-following-hurricane-florence/. Accessed on 6/19/2023.

Veas, R. E. A., Ergo, V. V., Vega, C. R. C., Lascano, R. H., Rondanini, D. P., Carrera C. S. (2021). Soybean seed growth dynamics exposed to heat and water stress during the filling period under field conditions. Journal of Agronomy and Crop Science. 208(4), 1–14. 10.1111/jac.12523.

Vieira, C.C., Sarkar, S., Tian, F., Zhou, J., Jarquin, D., Nguyen, H.T., Zhou, J., Chen, P. (2022). Differentiate soybean response to off target dicamba damage based on UAV imagery and machine learning. Remote Sensing, 14(7), 1618. 10.3390/rs14071618.

Vlachopoulos, O., Leblon, B., Wang, J., Haddadi, A., LaRocque, A., Patterson, G. (2021). Mapping barley lodging with UAS multispectral imagery and machine learning. The International Archives of the Photogrammetry, Remote Sensing and Spatial Information Sciences, XLIII-B1-2021, 553–560. 10.5194/isprs-archives-XLIII-B1-2021-553-2021.

Wang, H., Zhang, J., Xiang, K., Liu, Y. (2009). Classification of remote sensing agricultural image by using artificial neu-ral network. In the Proceedings of the 2009 International Workshop on Intelligent Systems and Applications, Wuhan, China, 23–24 May 2009.

Whitaker, R. T. (1998). A level-Set approach to 3D reconstruction from range data. International Journal of Computer Vision, 29, 203–231.

Woods, S. J., Swearingin, M. L. (1977). Influence of simulated early lodging upon soybean seed yield and its components. Agronomy Journal, 69, 239-242. 10.2134/agronj1977.00021962006900020011x.

Wu, W., Ma, B. L. (2016). A new method for assessing plant lodging and the impact of management options on lodging in canola crop production. Scientific Reports, 6, 31890. 10.1038/srep31890.

Wu, W., Shah, F., Ma, B. L. (2022). Understanding of crop lodging and agronomic strategies to improve the resilience of rapeseed production to climate change. Crop and Environment, 1(2), 133-144. 10.1016/j.crope.2022.05.005.

Yang, D. J., Zhao, J., Lan, Y. B., Wen, Y. T., Pan, F. J., Cao, D. L., Hu, C. X., Guo, J. K. (2021). Research on farmland crop classification based on UAV multispectral remote sensing images. International Journal of Precision Agriculture Aviation, 4(1), 29–35.

Yang, G., Liu, J., Zhao, C., Li, Z., Huang, Y., Yu, H., Zhu, X., Singh, R. P. (2017). Unmanned aerial vehicle remote sensing for field-based crop phenotyping: current status and perspectives. Frontiers in Plant Science, 8, 1111. 10.3389/fpls.2017.01111.

Yang, M., Huang, K., Kuo, Y., Tsai, H. P., Lin, L. (2017). Spatial and spectral hybrid image classification for rice lodging assessment through UAV imagery. Remote Sensing, 9, 583. 10.3390/rs9060583.

Zeng, M., Zou, B., Wei, F., Liu, X., Wang, L. (2016). Effective prediction of three common diseases by combining SMOTE with Tomek links technique for imbalanced medical data. In the Proceedings of the 2016 IEEE International Conference of Online Analysis and Computing Science (ICOACS), Chongqing, China, 28–29 May 2016.

Zhang, C., Walters, D., Kovacs, J. M. (2014). Applications of low altitude remote sensing in agriculture upon farmers' requests: a case study in Northeastern Ontario, Canada. PLOS ONE, 9(11), e112894. 10.1371/journal.pone.0112894.

Zhang, Z., Flores, P., Igathinathane, C., Naik, L. D., Kiran, R., Ransom, J. K. (2020). Wheat lodging detection from UAS imagery using machine learning algorithms. Remote Sensing, 12(11), 1838. 10.3390/rs12111838.

Zhou, C, Gong, Y, Fang, S, Yang, K, Peng, Y, Wu, X, Zhu, R. (2022). Combining spectral and wavelet texture features for unmanned aerial vehicles remote estimation of rice leaf area index. Frontiers in Plant Science, 4(13), 957870. 10.3389/fpls.2022.957870.

Zhou, J., Chen, H., Zhou, J., Fu, X., Ye, H., Nguyen, H. T. (2018). Development of an automated phenotyping platform for quantifying soybean dynamic responses to salinity stress in greenhouse environment. Computer and Electronics in Agriculture, 151, 319–330. 10.1016/j.compag.

Zhou, J., Yungbluth, D., Vong, C. N., Scaboo, A., Zhou, J. J. R. (2019). Estimation of the maturity date of soybean breeding lines using UAV-based multispectral imagery. Remote Sensing, 11, 2075. 10.3390/rs11182075.

Zhou, J., Zhou, J., Ye, H., Ali, M.L., Nguyen, H. T., Chen, P. (2020). Classification of soybean leaf wilting due to drought stress using UAV-based imagery. Computer and Electronics in Agriculture, 175, 105576. 10.1016/j.compag.2020.105576.

Zhou, Y., Luo, J., Feng, L., Yang, Y., Chen, Y., Wu, W. (2019). Long-Short-Term-Memory-based crop classification using high-resolution optical images and multi-temporal SAR data. GIScience Remote Sensing, 56(8), 1170-1191. 10.1080/15481603.2019.1628412.

Zhu, N., Zhu, C., Zhou, L., Zhu, Y., Zhang, X. (2022). Optimization of the random forest hyperparameters for power industrial control systems intrusion detection using an improved grid search algorithm. Applied Science, 12(20), 10456. 10.3390/app122010456.

CHAPTER THREE

ASSESSMENT OF SOYBEAN PUBESCENCE COLOR USING UAV-BASED IMAGERY AND DEEP LEARNING METHODS

3.1 Abstract

Soybean pubescence color is an essential phenotype, the information required for cultivar registration and decision-making in the breeding program. In a conventional breeding program, pubescence color is classified by the breeders through visual observation and scoring, which is time-consuming, laborious, and subject to human error. Hence, the goal of the study was to use UAV-based imagery as a potential alternative in identifying the soybean pubescence color for an accurate and time-efficient breeding program. The UAV was equipped with an RGB sensor, and the imagery was collected from the breeding field in 2019. The field consists of a total of 1266 breeding four-row plots. UAV images were stitched to build orthomosaic, and soybean plots were segmented using a grid method. Three classes of pubescence color (gray, tawny, and segregation) were classified using UAV-based imagery and seven pre-trained deep learning models, namely, ResNet50, InceptionResNet-V2, Inception-V3, EfficientNet, DenseNet121, DenseNet169, and DenseNet201. The images were pre-processed, resized, and augmented for the input of the deep learning models, and the pre-trained deep learning models were fine-tuned for the expected output. The result depicts that the ResNet50 and DenseNet121 show higher overall accuracy of 88% with higher precision, recall, and F1-score for three classes. The results indicate that the UAV-based imagery can be used to correctly classify the soybean crucial phenotypes and justify the potentiality of UAV-based imagery and deep learning methods.

3.2 Introduction

Soybean (Glycine max L.) is one of the most valuable crops worldwide, enabling its use in feed, oilseed crops, and as a nutritional source (Food and Agriculture Organization of the United Nations, 2012). At present, Argentina, Brazil, and the USA are the top soybean producer countries in the world at the global scale comprising 16, 32, and 33%, respectively (USDA NASS, 2017). The global projected soybean production was expected to reach 311.1 million metric tons in 2020, whereas it increased to 371.3 million metric tons by 2030. The growth rate of soybean production from 2020 to 2030 is 1.8%, 2.9% from 2005 to 2007, and 2.5% from 2007 to 2010 (Siamabele, 2021). Increasing the soybean production to achieve the goal, advanced genotypes are a prime concern for soybean breeders with different phenotypes. Soybean pubescence color is one of the phenotypes that breeders look for and are used in cultivar registration and to determine cultivar purity (Bruce et al., 2021).

Soybean pubescence colour is a trichome colour that all soybean plants grow “hair” on the stem and leaves, which is visually assessed. The trait is mainly scored in the maturity stage of the soybean by an experienced breeder for each soybean plot. Soybean pubescence color are mainly three types: tawny, light tawny (near-gray) and gray. Tawny and gray pubescence colors are visually distinguishable, while the light tawny colours are often misclassified due to the colour similarities with other colour classes. The soybean plant breeding program enables different types of phenotypic traits encompassing a large scale of field data to decide on cultivar advancement. Soybean pubescence colours are controlled by two genes T and Td (Palmer et al., 2004). The T gene plays a significant role and affects pubescence colour. Dominant T and recessive t alleles produce tawny and gray pubescence colours, respectively. On the other hand, T gene maintains the seed coat coloration and hypocotyl (Palmer and Payne, 1979; Palmer et al., 2004; Murai et al.,

2016). Furthermore, Bernard (1975) investigated that a different gene Td affects pubescence color in the presence of the dominant T allele. Dominant and recessive alleles of the Td locus produce tawny and light tawny pubescence colour in the soybean (Bernard, 1975).

In a conventional soybean breeding program, thousands of soybean rows from progeny trial (PT), preliminary yield trail (PYT) and advanced yield trail (AYT) with different traits and phenotypes are identified based on the visual observation by experienced breeders. The visual observation and scoring of the soybean pubescence colour are very laborious and subjective to human bias, which may affect the preciseness of breeding purposes (Jiménez et al., 2017). Therefore, there is an essentiality of improving and developing and efficient and effective tool to classify the soybean pubescence color using emerging technologies. With the improvement of remote sensing technologies in agriculture, several soybean traits and phenotypes are successfully assessed using unmanned aerial vehicles (UAV) and imaging systems along with different machine learning (ML) and deep learning (DL) methods. With the availability of a range of imaging platforms and increasing availability of analytical methods to use the data for plant and associated researchers were able to make more frequent and effective decisions for their research. Several research on quantifying crop growth traits such as plant height (Feng et al., 2019), canopy area (An et al., 2016), leaf temperature (Sagan et al., 2019), yield estimation (Maimaitijinag et al., 2020), determining maturity stages (Zhou et al., 2019), and identifying plant stresses (Moghimi et al., 2018; Zhou et al., 2020) have been done using UAV based imaging technology. Furthermore, image-derived features have been used by numerous researchers to quantify different crop responses such as biotic and abiotic stress (Tamimi et al., 2022), drought stress (Duan et al., 2018), salt stress (Zhou et al., 2018), and flooding stress (Cao et al., 2019). Furthermore, several research have been conducted to identify the lodging of different crops using UAV-based imagery, such as

rice (Tian et al., 2021), maize (Bagherzadi et al., 2017), oats (Zhang et al., 2014), and barley (Vlachopoulos et al., 2021).

Conventional approaches to classify different crop traits or phenotypes using UAV-based imagery have relied on classical machine learning algorithms, which include support vector machine (SVM), random forest (RF), K-nearest neighbor (KNN), decision tree, K-means clustering, naive bayes and so on. These techniques are based on extracting image features using different image feature extraction methods, such as Local Binary Pattern (LBP), Histogram of Oriented Gradients (HOG), and Scale Invariant Feature Transform (SIFT). The problem with ML methods is time-consuming and inefficient regarding complex data (Bouguettaya et al., 2022). Hence, the combination of UAV imagery and deep learning methods plays an important role in identifying crops and phenotypes. Numerous research is spotted on from last few years using UAV imagery and deep learning methods such as cotton and rice yield estimation (Ashapure et al., 2020; Yang et al., 2019), water stress monitoring (Gao et al., 2020), crop monitoring (Theau et al., 2020; Wu et al., 2021), pesticide and fertilizer spraying (Hasan et al., 2019), and wheat lodging (Zhang et al., 2020). Though several research have been conducted using UAV imaging and deep learning methods, to our knowledge there is only one research is available only on soybean pubescence color using UAV-based multispectral imagery and ML methods to classify the pubescence color. Insufficient attention has been paid to classifying soybean pubescence colour using deep learning methods. The goal of this study was to investigate the potential use of UAV-based imagery in quantifying pubescence color of soybean breeding lines using UAV-based imagery and deep learning methods. The objective of this work was to use pre-trained deep-learning models to classify three classes of soybean pubescence colour and evaluate the results with performance matrices.

3.3 Materials and methods

3.3.1 Field experiment

A field experiment was conducted in 2019 at the Bay Farm Research Facility (38°54'08.3"N, 92°12'29.8"W) in Columbia, Missouri, United States. The research field is described as humid subtropical climate region (Köppen climate classification code: Cfa) (Rubel et al., 2017). A total of 1773 soybean plots were planted on June 3, 2019, without replicates, in a four-row plots. Each row length was 3.6 m with a spacing of 0.8 m. The experiment was managed according to standard operation protocol by the farm management team. Soybean pubescence color in this experiment was evaluated and scored by the experienced plant breeders at the full maturity stage of R8. Pubescence color was rated with character letter as T for tawny, g for gray and S for segregating color. In this study there was no light tawny class, instead of there was a color class named as segregating which cannot be classified as tawny or gray or light tawny class. Hence, the class was named as segregating by the breeders. A total of 1773 plots were processed, and 1266 plots were used for the final images to be used for the deep learning models. Rest of the plots were filler and were discarded from the pre-processing and analysis. Pubescence color classes T, G, and S based on their scoring are shown in Figure 1.

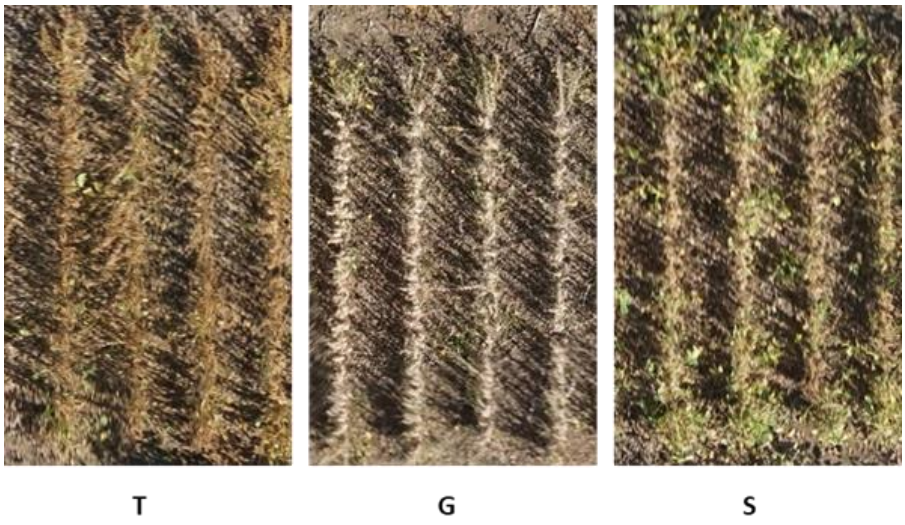

Figure 3-1. Ground-based classification scale of filed plots of soybean pubescence color with three phenotypic classes which includes tawny (T), gray (G), and segregation (S).

3.3.2 UAV Imagery data collection

The aerial images were collected at the maturity stage of R8 on 29th August 2019 us-ing an UAV platform (DJI Matrice 600 Pro, DJI, Shenzhen, China) equipped with a Sony A6300 (Sony Corporation, Tokyo, Japan) RGB (red-green-blue) camera. The digital camera was used to acquire images at 0.5 frames per second (fps) along with the resolution (number of pixels) of 6000×4000 pixels at a flight height of 30 m above the ground level with an overlap of 80% for both sides of image. During the image acquisition, the camera configuration was set to shutter 1/1000 s, ISO 100-200, F-stop auto and daylight mode. The Real-Time Kinematic (RTK) GNSS positioning system (Reach RS+, Emlid, St. Petersburg, Russia) was used to obtain the GNSS coordinates of the GCPs. To ensure sufficient satellite reception for each data collection, the base station was mounted on a tribrach that was fixed in an open area in the fields. The base position was obtained in the initial setting by accumulating its GNSS coordinates for 5 minutes, with an averaged single accuracy of ap-proximately 2.5 meters. The base station was placed in the same location over a

growing season during every flight. The rover receiver was placed vertically in the holes on a monopod after the GCPs were pulled out, and the GNSS coordinate of each GCP was recorded after accumulating for 10 seconds using a manufacturer-developed App. ReachView. The geo-referencing information of each image was recorded in a separate .csv file. Images were stitched using Agisoft PhotoScan Pro (v1.3.4, St. Petersburg, Russia) for further processing.

3.3.3 Image processing

First, in the data processing step, an orthomosaic image was generated using Agisoft PhotoScan Pro (v1.3.4, St. Petersburg, Russia) from the acquired images on 1st September 2019. The procedures were described by (Zhou et al., 2018). Orthomosaic image was generated and exported as .tif images. The images were processed using the Image Processing Toolbox and Computer Vision System Toolbox (ver. 2021b, The MathWorks, Natick, MA, USA). Individual soybean plots were separated from each orthomosaic image by manually cropping a rectangle region of interest (ROI) around each plot. Size of each plot varied hence the size of ROI also varied to cover each soybean plot according to its width and length. The image size of each plot was resized with the size of 224 × 224 pixels as the requirement of every deep learning model by using the function "resize" from the package TensorFlow (ver. 2.8.0). Furthermore, the method of interpolation was set to be "nearest", so each pixel value becomes rounded by following (Fengkai et al., 2023). The background of each image such as soil, shadow, and plant residue were not removed from the images as the soil color and the plant color was almost same which makes impossible to remove the background from the images.

3.3.4 Image augmentation

In this study, image enhancement was done to increase the number of images for the input of pre-trained deep learning models. As, original dataset consist of 1266 images of three classes which is very low number of images to for the deep learning models. We used image rotation (two rotation angels: 0◦ (i.e., the original image), and 90◦) and scaling (two scaling factors: 1.2, and 1.8) to enhance the soybean pubescence color image dataset collected from the breeding field. By using the image rotation and scaling factor techniques, we were able to obtain soybean pubescence color images with different resolution and angles. This image transformation added varying diversity to our dataset and reduces the chance of model overfitting issues due to the limited number of samples. In this study we used Python scikit-learn and Numpy libraries to extract, rotate and scale the soybean images.

Table 3-1. Division of each soybean class images in training and testing set.

Class	Training Dataset	Testing Dataset
T	473	203
G	410	177
S	2	1
Total	885	381
Enhancement	3544	1520

3.3.5 Deep learning methods for soybean pubescence color classification

Seven pre-trained convolutional neural network (CNN) deep learning models were tested to classify the soybean cultivars into three pre-defined pubescence color classes (tawny, gray, and segregating). The Residual Network (ResNet) brings a novel concept to tackle complex tasks and improve the detection accuracy. Furthermore, ResNet minimize the problems such as saturation and degradation of training process of deep CNN (Mukti and Biswas, 2019). In this study, we used

ResNet50 architecture which have 50 layers of residual networks. ResNet50 has been used by several researchers as well to assess the soybean leaf defoliation, plant disease detection and corn emergence (Silva et al., 2019; Mukti and Biswas, 2019; and Vong et al., 2022).

Inception-V3 network is a transfer learning algorithm, which has been implemented in this study for the classification of pubescence color. The neural networks are mostly dependent on the depth of the network by increasing the number of convolutional layers. But the inception architecture has changed the method and uses Inception Neural Network with different sizes of filters and different maximum pooling to reduce the dimension of the data which leads to obtain improved features and fewer computational parameters (Lambat et al., 2022). Furthermore, Inception-V3 uses a batch normalization layer in between the classifier and the fully connected layers, following a batch gradient approach also used in the batch normalization to fasten the deep neural network training and model convergence process (Igried et al., 2023). The Inception-v3 network architecture has been used for the precise agricultural modeling (Igried et al., 2023), crop diseases classification and detection (Patel et al., 2022; Lambat et al., 2022).

Inception-ResNet-V2 was also used in this study for the classification of soybean pubescence color which is composed of inception modules with different functions. The algorithm extracts the features more precisely from the input image by adopting a stronger connection structure in the inception module. The dense connection block in the architecture increases the rate of feature using and the network learn the data more intensively (Zhang et al., 2019). The depth wise convolution is being used and the number of feature maps also become halves to improve the calculation efficiency which reduced due the increasing number of dense blocks. InceptionResNet-v2 have been used by different researchers, such as for crop pest identification (Liu et al., 2022), plant lead disease classification (Naveenkumar et al., 2021), and weed recognition (Hasan et al., 2022).

EfficientNet was used in this study for the classification of soybean pubescence color. EfficientNet is one of the state-of-the-art models, achieves 84.4% accuracy with 66M parameters in the ImageNet classification problem. The algorithm uniformly scales down the depth, width, and resolution during the scaling down the model. Furthermore, the algorithm consists of total 8 models in between B0 and B7. Though the model grows but the calculated parameters doesn't increase much but increase the accuracy. Numerous researchers have used the model in the agricultural crops, such as plant leaf disease classification (Atila et al., 2021; Hanh et al., 2022), crop insect identification (Monis et al., 2022), and maize disease detection (Liu et al., 2020).

Another deep convolutional architecture DenseNet which draws on the idea of ResNet and propose the explicit connection from all previous layers to all subsequent layers (He et al., 2016). In the DenseNet architecture, a transition layer is introduced between the adjacent dense blocks. Transition layer consists of 1×1 convolution and 2×2 average pooling layers. Pooling is used to adjust the size of the output feature map. 1×1 convolution is mainly used in the DenseNet to decrease the number of input feature maps which not only reduce the dimension amount but also consolidate the features of each channel (Zhang et al., 2019). For an example, in the DenseNet201, there is a dense block which have 48 convolution operations which includes 1×1 and 3×3 filters. In summary, the DenseNet architecture adequately decrease the computational complexity but maintains the flow of the information by effectively implying 1×1 convolutions before the 3×3 convolutions in the dense block (Feng et al., 2022). In this study, DenseNet-121, DenseNet-169, and DenseNet-201 was used to classify the soybean pubescence color.

For all the above mentioned pre-trained deep learning models, in the last layer Softmax was chosen as the activation function and categorical cross entropy was used as loss function. Adam optimizer

was used to improve the accuracy and reduce the testing loss while training, and the learning rate was 0.001.

3.3.6 Experimental setup

All models used in this study were runed with GPU support and all the experimental models were conducted in Jupyter Lab on a 64-bit Windows 11 Enterprise operating system running on Intel® Core™ i9-10900X CPU @ 3.70GHz and 128 GB RAM with NVIDIA GeForce RTX 3090 Ti having 64GB RAM. All codes were written in python with Keras and TensorFlow framework. The augmented dataset of soybean pubescence color was randomly divided into training and testing set by 80% and 20%, respectively. Table-1 represents the full dataset have been used in the study.

3.3.7 Performance metrices

The three classes of soybean pubescence color were assessed based on the number of samples that were correctly or falsely classified as either presence (True Positive, TP or False Positive, FP) or absence (True Negative, TN or False Negative, FN) using seven different pre-trained deep learning algorithms. A group of metrices were used for evaluation and they were calculated using equations 1-4. The evaluation was based on several performance metrices, including precision, recall, F1-score, and overall accuracy (OA). The precision indicates the proportion of correctly predicted presences, recall represents the ratio of correctly predicted positive samples, and F1-score is the harmonic mean of precision and recall the F1 score is measure of model accuracy as well that balances precision and recall which ranges from 0 to 1, with 1 being the best possible score, indicating perfect precision and recall. Kappa value represents the proportion of correctly predicted sites, and OA indicates the overall accuracy of the model.

$$\text{Accuracy} = \frac{\text{No. of samples classified correctly in a test set}}{\text{Total No. of samples in a test set}} \times 100\% \qquad (1)$$

$$\text{Precision} = \frac{\text{TP}}{\text{TP} + \text{FP}} \quad (2)$$

$$\text{Recall} = \frac{\text{TP}}{\text{TP} + \text{FN}} \quad (3)$$

$$\text{F1 score} = \frac{2 * (\text{Precision} * \text{Recall})}{(\text{Precision} + \text{Recall})} \quad (4)$$

3.4 Results

3.4.1 Classification performance of pre-trained ResNet50 deep learning model

Table 2 represents the results of seven pre-trained deep learning models for the classification of soybean pubescence color. The deep learning models were selected based on user friendly and most popular in recent times for the classification practices. The classification accuracy using pre-trained deep learning model ResNet50 was 0.88 with the precision, recall, and F1-score higher than 0.86 for all classes. The misclassification rate of the model was 25% and the kappa value was 0.75. Precision, recall, and F1-score was found 1.00 for segregation color as the segregation class correctly classified all four samples. Figure 2 shows the loss versus epochs and model accuracy versus epochs graphic for the ResNet50 model. The training step of 10 epochs and learning rate of 0.0001 was set to obtain the accuracy level. The loss curve of training and testing dataset was not far from each other. On the other hand, figure 3 shows the receiver operating characteristic curve (ROC) and precision-recall (PR) curve of the model using ResNet50 classifier. Area under the curve (AUC) and average precision (AP) are commonly used metrices for evaluating the performance of classification models and indicates that the classifier performs better in classifying the soybean pubescence color with the value of 0.93, 0.93, and 1.00 for gray, tawny, and segregation class. Whereas 0.92, 0.92, and 1.00 AP values was obtained for three classes, respectively.

Table 3-2. Confusion matrix and model performance metrices of three pubescence classes of soybean using seven pre-trained deep learning model.

Classifier	Actual samples	G	T	S	Precision	Recall	F1-score	OA
ResNet50	G	605	103	0	0.87	0.85	0.86	0.88
	T	85	723	0	0.87	0.89	0.88	
	S	0	0	4	1.00	1.00	1.00	
InceptionResNetV2	G	642	66	0	0.83	0.90	0.87	0.87
	T	129	679	0	0.91	0.84	0.87	
	S	0	0	4	1.00	1.00	1.00	
InceptionV3	G	625	83	0	0.84	0.88	0.86	0.86
	T	120	688	0	0.89	0.85	0.87	
	S	0	0	4	1.00	1.00	1.00	
EfficientNet	G	527	181	0	0.91	0.74	0.82	0.84
	T	48	760	0	0.80	0.94	0.86	
	S	0	0	4	1.00	1.00	1.00	
DenseNet169	G	425	283	0	0.89	0.60	0.72	0.78
	T	49	759	0	0.72	0.93	0.82	
	S	0	0	4	1.00	1.00	1.00	
DenseNet121	G	586	122	0	0.89	0.82	0.86	0.88
	T	66	742	0	0.85	0.91	0.88	
	S	0	0	4	1.00	1.00	1.00	
DenseNet201	G	594	114	0	0.87	0.83	0.85	0.86
	T	87	721	0	0.86	0.89	0.87	
	S	0	0	4	1.00	1.00	1.00	

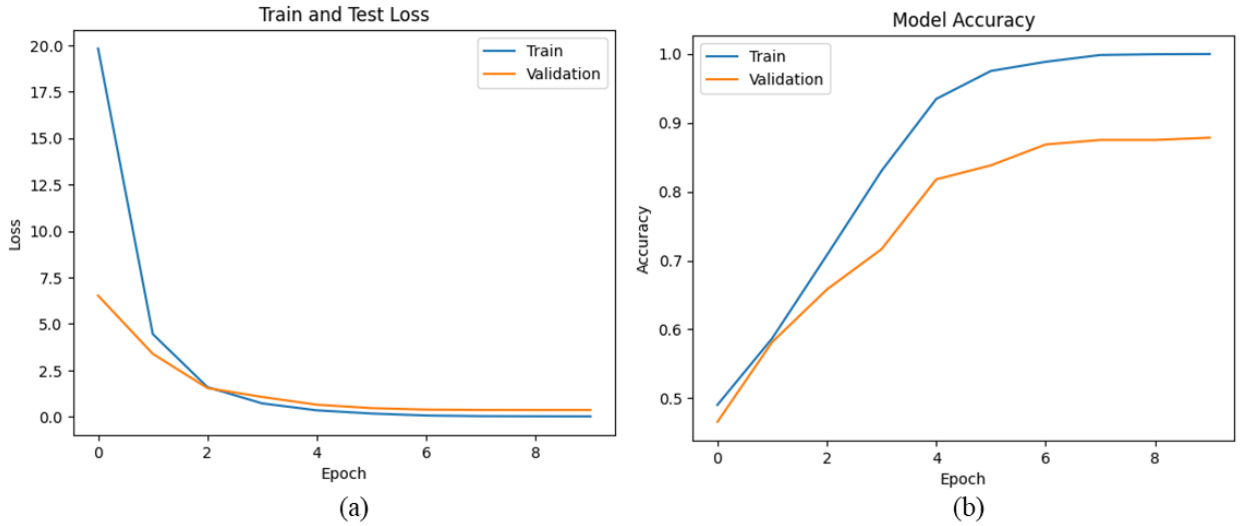

Figure 3-2. Accuracy and loss curves using training and testing datasets for ResNet50 model. (a) best-fit model loss versus epochs, and (b) best-fit model accuracy versus epochs.

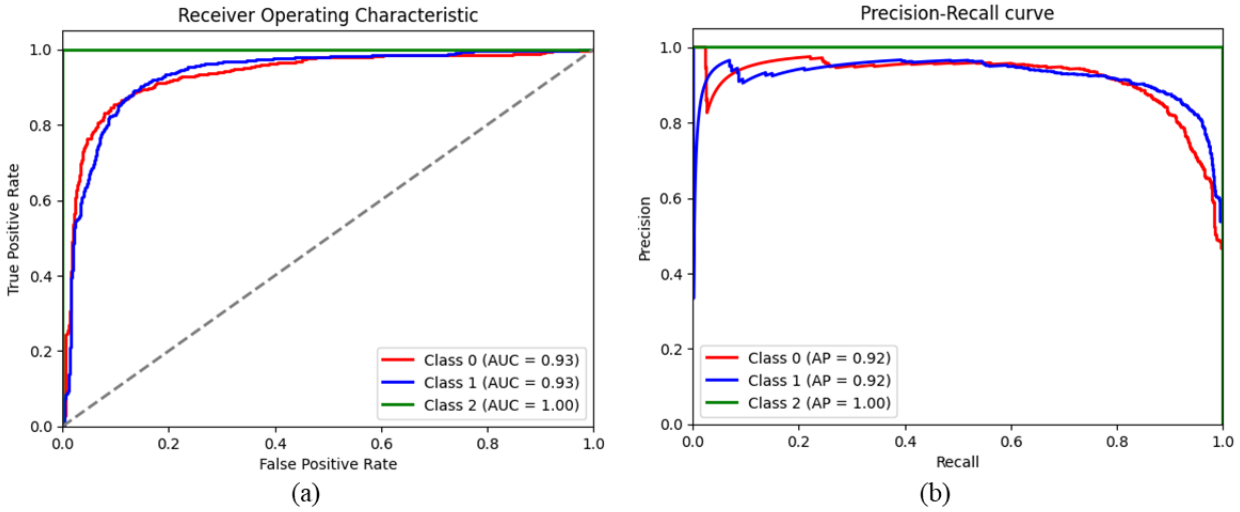

Figure 3-3. The ROC and precision-recall curves using testing datasets for ResNet50 model. (a) true positive rate versus false positive rate versus, and (b) precision versus recall.

3.4.2 Classification performance of pre-trained InceptionResNet-V2 deep learning model

Another pre-trained classifier InceptionResNet-V2 resulted in the overall accuracy of 0.87 along with the higher recall value of 0.90 for gray and lower recall of 0.84 for tawny color because the number of correctly classified sample was higher for gray and lower for tawny color, respectively. Higher precision, recall, and F1-score also obtained for segregation as there was no misclassification. The kappa value was 0.74 and the misclassification rate of the model was 26%. The training and testing loss and model accuracy curve (Figure 4) shows that the testing loss is far apart from the training loss and testing accuracy is very low than the training accuracy, which suggests that the model is overfitting. The training step of 12 epochs and learning rate of 0.0001 was set to obtain the accuracy level. The AUC and AP values from the ROC and PR curve (Figure 5) shows that the values range from 0.95-1.00 for three classes.

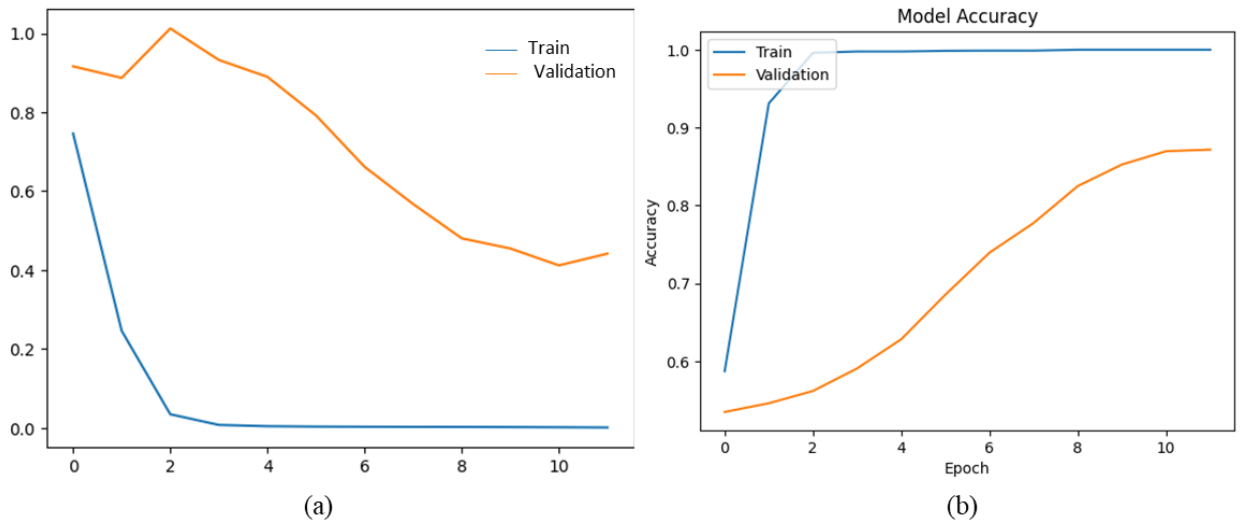

Figure 3-4. Accuracy and loss curves using training and testing datasets for InceptionResNet-V2 model. (a) best-fit model loss versus epochs, and (b) best-fit model accuracy versus epochs.

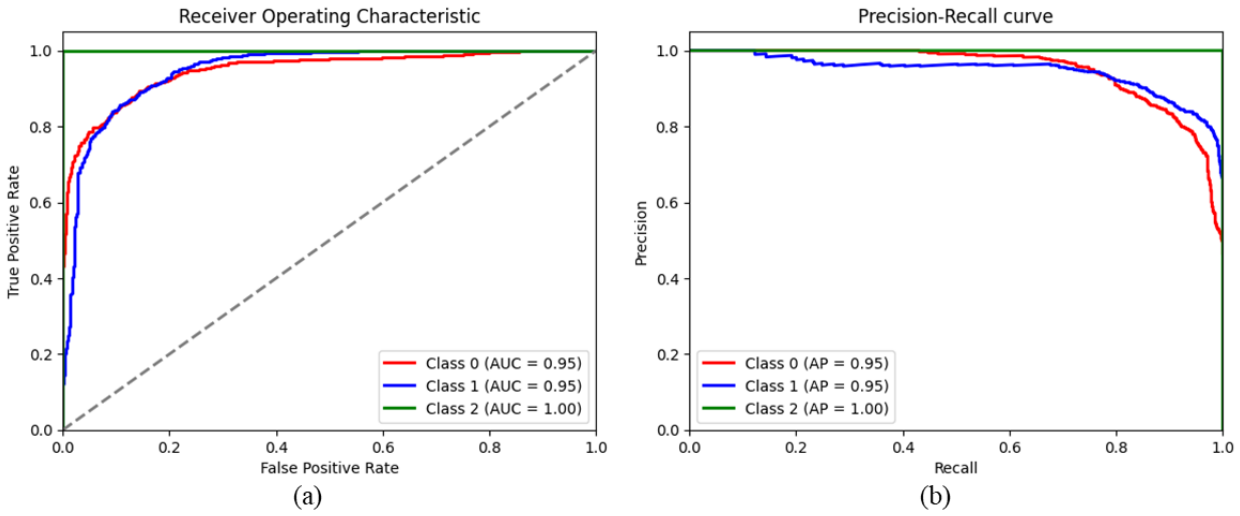

Figure 3-5. The ROC and precision-recall curves using testing datasets for InceptionResNet-V2 model. (a) true positive rate versus false positive rate versus, and (b) precision versus recall.

3.4.3 Classification performance of pre-trained Inception-V3 deep learning model

Inception-V3 was also used to classify the three classes of soybean pubescence color which resulted in overall accuracy of 0.86, precision, recall, and F1-score was 0.84, 0.88, and 0.86 for gray class and 0.89, 085, 0.87 was for tawny class, respectively. The kappa value was 0.74 and the misclassification rate of the model was 27%. Figure 6 depicts the training and testing losses with training step of 100 epochs and learning rate of 0.0001. The AUC and AP values from ROC and PR curve (Figure 7) was 0.92, 092, 1.00 and 0.89, 090, 1.00 for gray, tawny, and segregation classes, respectively.

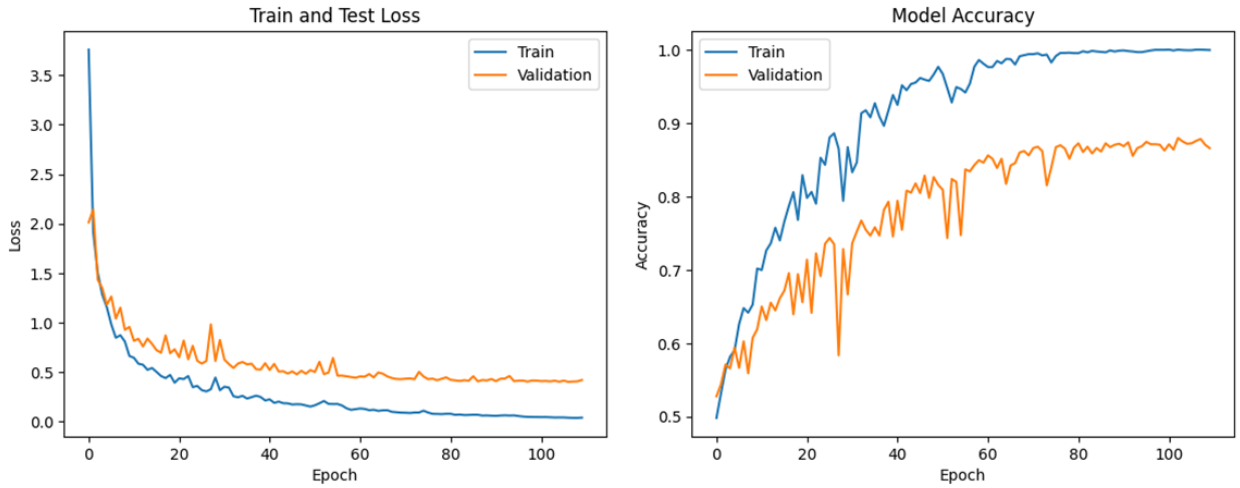

Figure 3-6. Accuracy and loss curves using training and testing datasets for Inception-V3 model. (a) best-fit model loss versus epochs, and (b) best-fit model accuracy versus epochs.

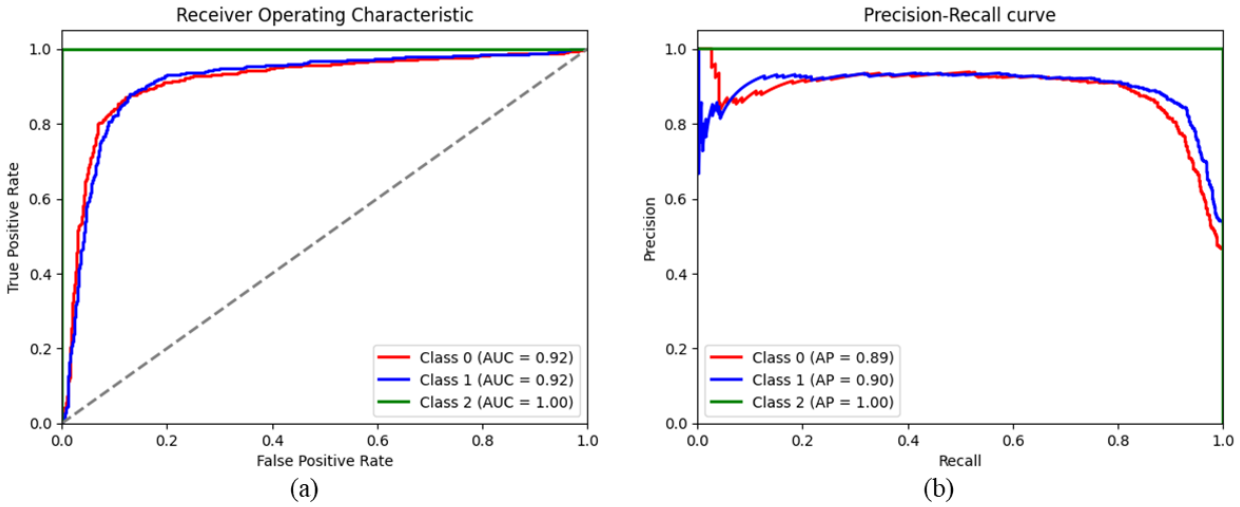

Figure 3-7. The ROC and precision-recall curves using testing datasets for Inception-V3 model. (a) true positive rate versus false positive rate versus, and (b) precision versus recall.

3.4.4 Classification performance of pre-trained EfficientNet deep learning model

EfficientNet resulted in lower recall of 0.74 for gray class as the classifier misclassified a significant number of samples but correctly classified the greatest number of tawny classes, which

resulted in higher recall of 0.94. The total misclassification rate of the model was 30% with the kappa value of 0.69. The overall classification accuracy of the model was 0.84 with a training set of 70 epochs and learning rate of 0.0001. Figure 8 shows the training and testing loss curve and model accuracy performance. The AUC and AP values were 0.94, 0.94, 1.00 and 0.92, 0.94, 1.00 for gray, tawny, and segregation class of soybean pubescence color (Figure 9).

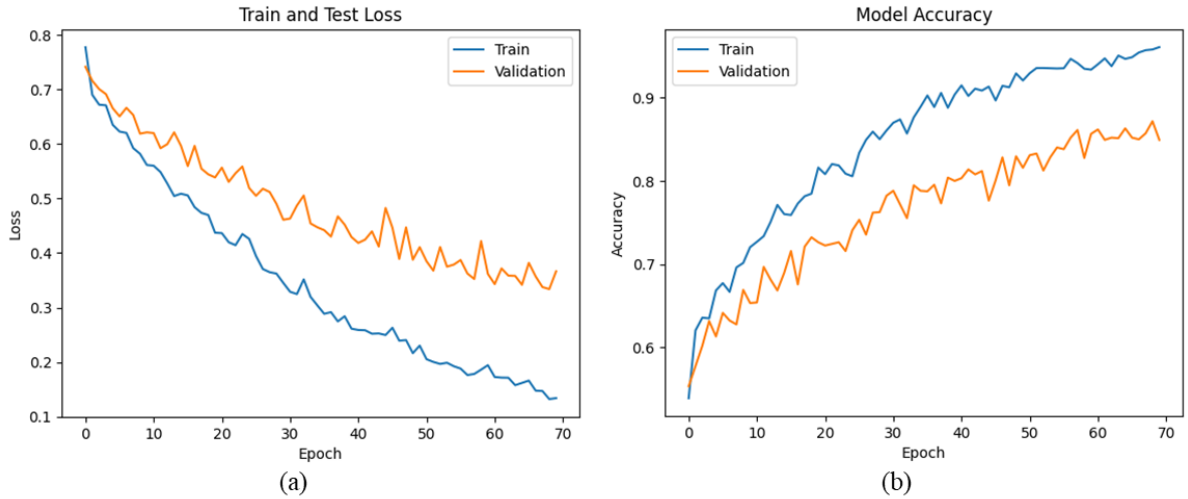

Figure 3-8. Accuracy and loss curves using training and testing datasets for EfficeintNet model. (a) best-fit model loss versus epochs, and (b) best-fit model accuracy versus epochs.

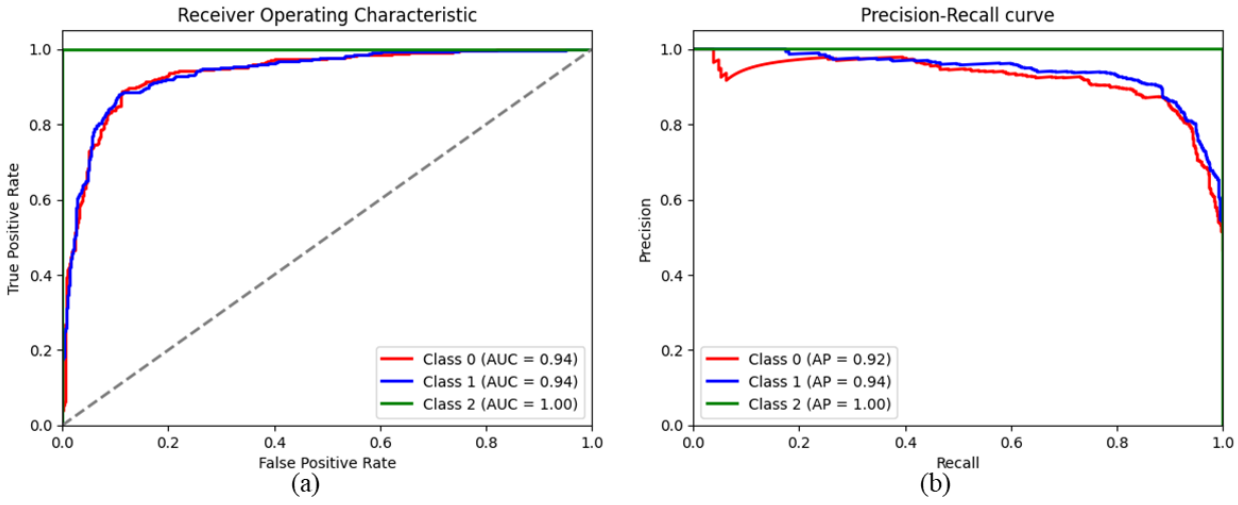

Figure 3-9. The ROC and precision-recall curves using testing datasets for EfficientNet model. (a) true positive rate versus false positive rate versus, and (b) precision versus recall.

3.4.5 Classification performance of pre-trained DenseNet169 deep learning model

DenseNet169 was tested to classify three classes of soybean pubescence color, which resulted poor overall classification accuracy of 0.78 among all the pre-trained deep learning models. Where gray class has the highest number of misclassifications which resulted in lower recall of 0.60. But the tawny class was classification rate was comparatively high which resulted in higher recall of 0.93. The model produces a total of 44% misclassification rate with a kappa value of 0.55. Figure 10 depicts the training and testing losses with training step of 120 epochs and learning rate of 0.0001. The AUC and AP values from ROC and PR curve (Figure 11) was 0.90, 0.90, 1.00 and 0.88, 0.89, 1.00 for gray, tawny, and segregation classes, respectively.

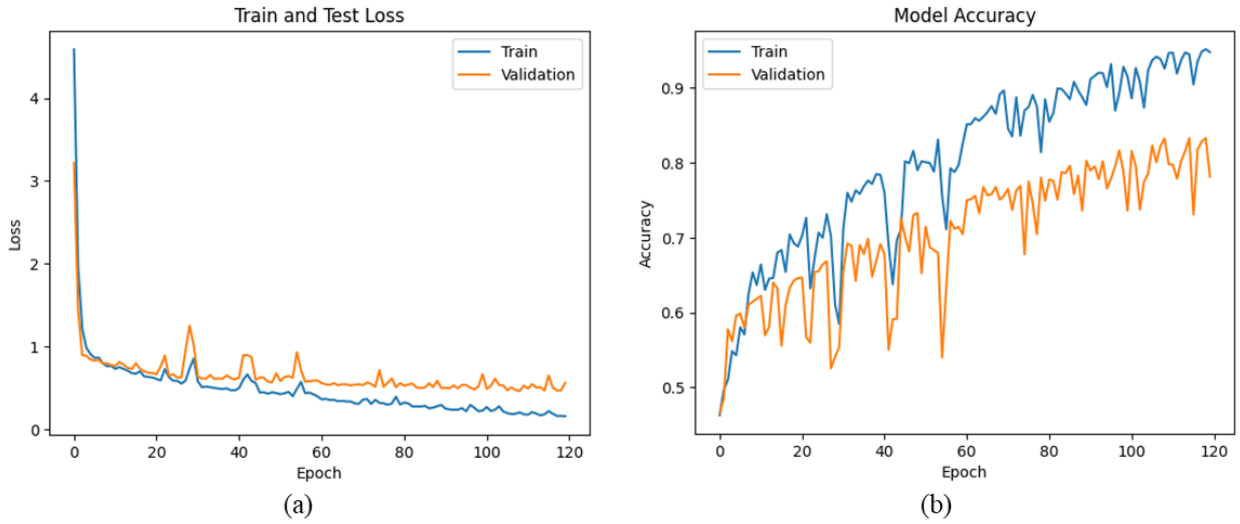

Figure 3-10. Accuracy and loss curves using training and testing datasets for DenseNet169 model. (a) best-fit model loss versus epochs, and (b) best-fit model accuracy versus epochs.

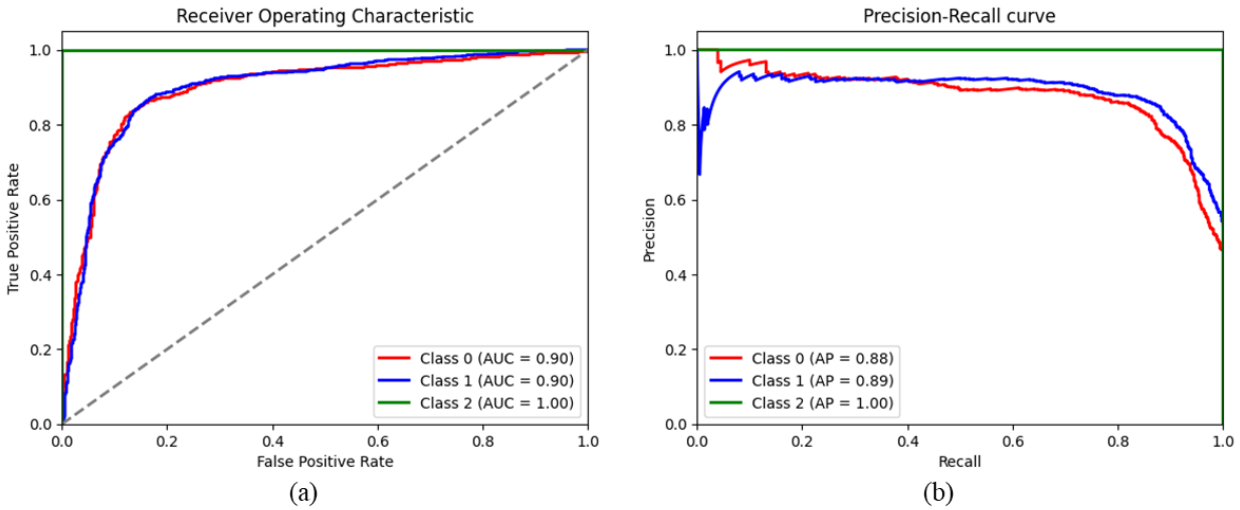

Figure 3-11. The ROC and precision-recall curves using testing datasets for DenseNet169 model. (a) true positive rate versus false positive rate versus, and (b) precision versus recall.

3.4.6 Classification performance of pre-trained DenseNet121 deep learning model

DenseNet121 was tested as well and which resulted in overall accuracy of 0.88 with comparatively better results in classifying both the gray and tawny class with precision and recall of 0.89, 0.82 and 0.85, 0.91, respectively. The misclassification rate of the model was 25% with the kappa value of 0.75. The training and testing loss and accuracy curve is displayed in Figure 12. The accuracy was obtained with a training step of 80 epochs with the learning rate of 0.0001. Figure 13 indicates the AUC and AP values from the ROC and PR curve with the values of 0.93, 0.93, 1.00 and 0.88, 0.93, 1.00 for gray, tawny, and segregation class, respectively.

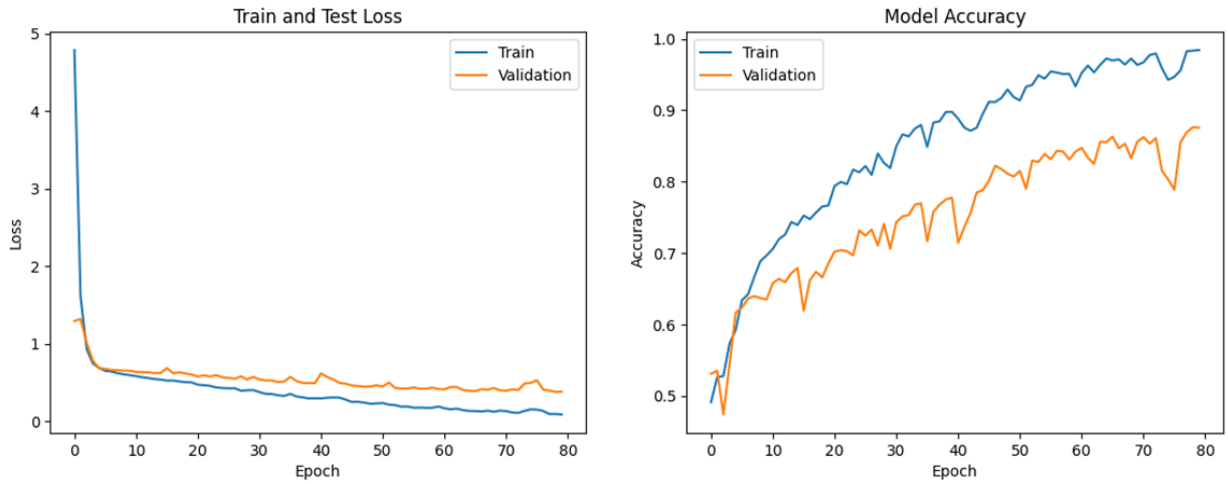

Figure 3-12. Accuracy and loss curves using training and testing datasets for DenseNet121 model. (a) best-fit model loss versus epochs, and (b) best-fit model accuracy versus epochs.

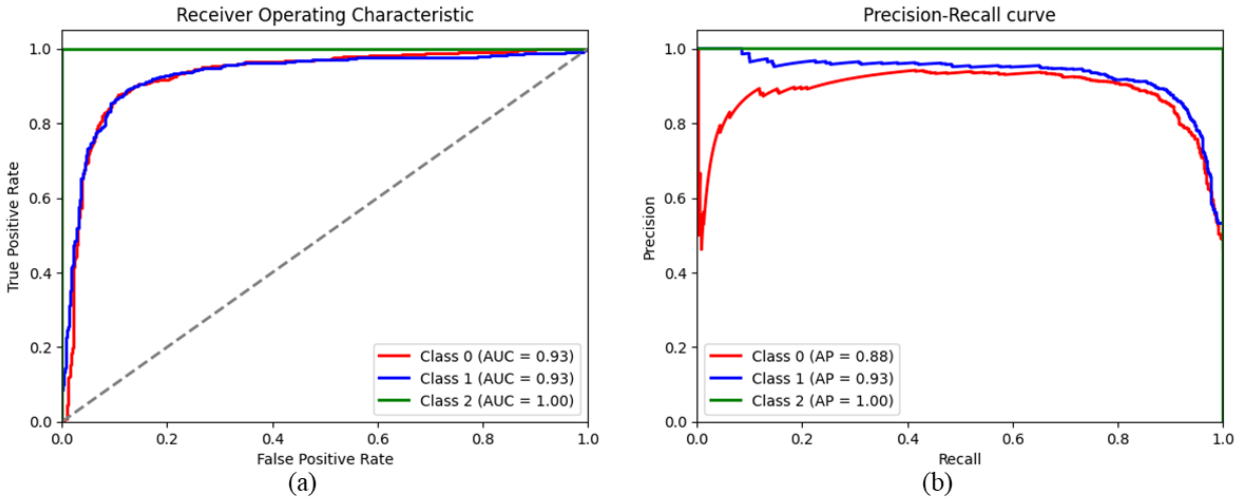

Figure 3-13. The ROC and precision-recall curves using testing datasets for DenseNet121 model. (a) true positive rate versus false positive rate versus, and (b) precision versus recall.

3.4.7 Classification performance of pre-trained DenseNet201 deep learning model

The last classifier was tested using DenseNet201 algorithm which resulted in the overall accuracy of 0.86 with the precision, recall for gray and tawny classes are 0.87, 0.83 and 0.86, 0.89. The

misclassification rate of the model was 26% with a kappa value of 0.73. The accuracy was obtained with the training set of 70 epochs and learning rate of 0.0001. Figure 14 depicts the training and testing loss curve along with the accuracy curve. Which resulted in similar loss factor of DenseNet121 and ResNet50. Figure 14 shows the AUC and AP values from the ROC and PR curve for the three classes of soybean pubescence color with the values of 0.91, 0.91, 1.00 and 0.89, 0.91, 1.00, respectively.

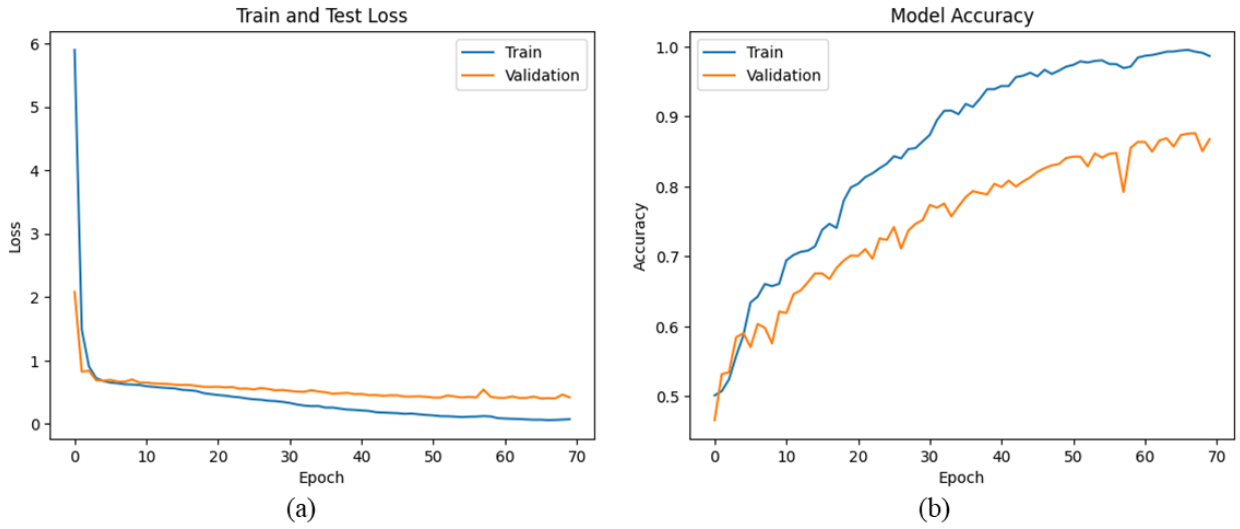

Figure 3-14. Accuracy and loss curves using training and testing datasets for DenseNet201 model. (a) best-fit model loss versus epochs, and (b) best-fit model accuracy versus epochs.

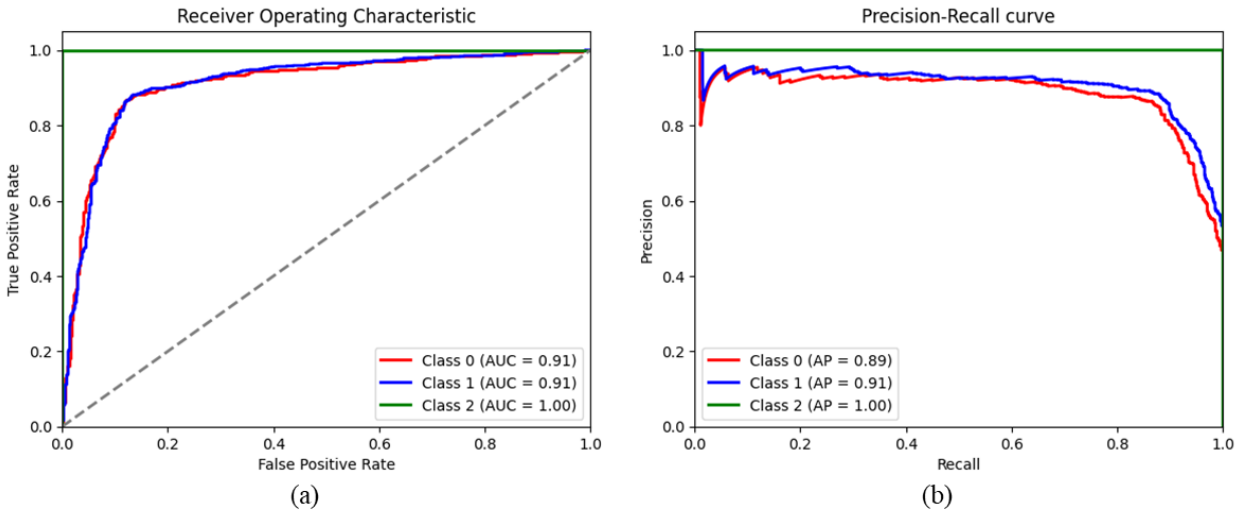

Figure 3-15. The ROC and precision-recall curves using testing datasets for DenseNet201 model. (a) true positive rate versus false positive rate versus, and (b) precision versus recall.

3.5 Comparison of deep learning model results and discussion

Pubescence color is one of the phenotypes that breeders look after during the maturity stage of soybean. The potentiality of using UAV based imaging technology and related tools would be valuable to the soybean researchers to quickly discriminate the pubescence color. In our knowledge, there is only one research has been conducted on soybean pubescence color classification using UAV based imagery technology. Bruce et al., (2021) used support vector machine to classify the pubescence color and 83.1% accuracy was obtained to distinguish gray and tawny class. One of the reasons might be that pubescence color is not known as focused phenotype and complexity of analyzing imbalanced dataset. Soybean pubescence color mostly three types, i.e., gray, tawny, and light tawny but in this study, there was no light tawny class. Instead, light tawny there was segregation color which are mainly cannot be identified as mentioned types. The objective was to use pre-trained deep learning models for the classification of three classes namely, gray, tawny, and segregation. As of there is no pubescence color study using deep learning

methods, this section will compare the results of other researchers using same deep learning models for different crop classification. Figure 16 shows the overall accuracy was obtained with the training set of epochs was used and Figure 17 depicts the misclassification rate and kappa value for each deep learning models. From the above-described results, ResNet50 and DenseNet121 performed the best among all other classifiers, achieving the higher overall accuracy, precision, recall, F1-score, kappa value and lowest misclassification rate. The overall accuracy of 88% was obtained from ResNet50 and DenseNet121 but the required epochs was 10 and 80 with the kappa value of 75 and 25% misclassification rate. Atila et al., (2021) used ResNet50 for the plant leaf disease classification and resulted in 99.88% average accuracy using the augmented dataset where the researcher had the big data of more than sixty thousand with 38 classes which resulted in higher classification accuracy. On the other hand, ResNet50 was used by Lu et al., (2022) along with other classifiers for the crop classification which resulted in 84.1% overall accuracy with the 0.848 kappa value using RGB and NDVI satellite imagery. Nandhini and Ashokkumar (2022) used DenseNet121 to classify the plant leaf disease with 14 classes with the accuracy of 98.7%. Also, a big dataset of 54,000 images containing 38 classes with 26 diseases and 14 species of crops was used by Andrew et al., (2022) using DenseNet121 which resulted in a classification accuracy of 99.81%.

On the other hand, similar result of overall accuracy of 87% obtained from InceptionResNet-V2 with 12 epochs with the kappa value of 74 and misclassification rate of 26%. But the training and testing loss curve and accuracy curve (Figure 4) shows that the model is overfitting by depicting the curves are far from each other. Furthermore, 86% overall accuracy was obtained from both the Inception-V3 and DenseNet201 with the training set of 110 and 70 epochs, respectively. The models also resulted in the kappa value of 74 and 73 with the misclassification rate of 27% and

26%, respectively. Hasan et al., (2023) used InceptionResNet-V2 and InceptionV3 fine-tuned model to classify different types of weeds with 20 classes in which 89.39% and 86.08% testing accuracy was obtained to classify DeepWeeds and 77.14% and 98.10% testing accuracy was obtained to classify the cotton tomato weed. On the other hand, cotton weed, and soybean weed was classified with a test accuracy of 99.33%, 99.59% and 98.42%, 99.71% using InceptionResNet50 and InceptionV3 classifier, respectively (Hasan et al., 2023). DenseNet201 was used for tomato classification system with an overall accuracy of 96.16% and 100% by Lu et al., (2021). EfficeintNet produced the overall accuracy of 84% with the epochs of 70 and kappa value was 69 with the misclassification rate of 30%. DenseNet169 depicted very poor classification accuracy of 78% with the epochs 70 and the misclassification rate of the model was 44%. EfficientNet was used for corn leaf disease detection by Fathimathul et al., (2023) with an overall accuracy of 98.99%. An overall accuracy of 83.5% was obtained for corn leaf disease detection with augmented dataset by Wahyuningrum et al., (2021) using DenseNet169.

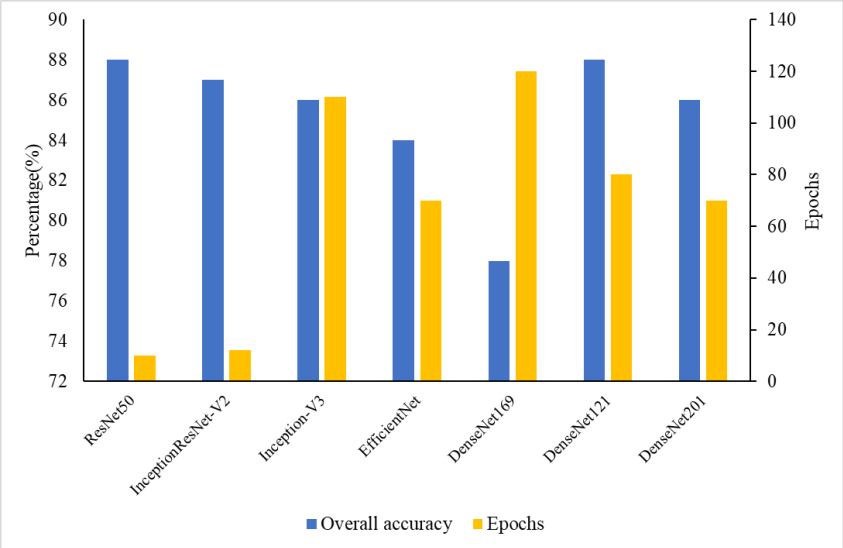

Figure 3-16. The overall accuracy and number of epochs of different deep learning models.

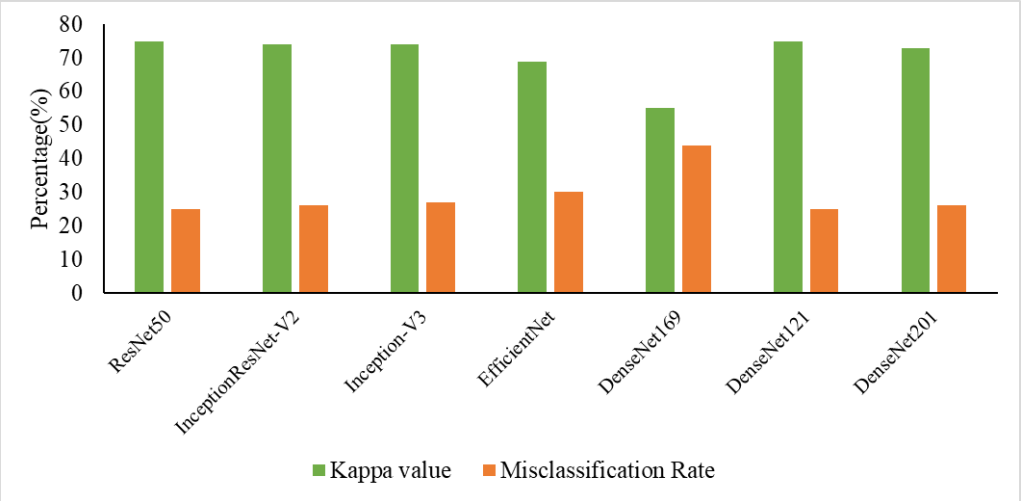

Figure 3-17. The kappa value and misclassification rate of different deep learning models.

3.6 Conclusion

In this study, the research was aimed to classify the soybean pubescence color using UAV-based imagery and pre-trained deep learning methods for breeding purposes. The RGB image was used after few pre-processing steps which includes grid generation, adjusting the grids according to the size and shape of each plot and cropping the plots. The images were resized to 224×224 pixels for the input of the deep learning models and the models were fine tuned for the expected output. The classification performance was 88%, 87%, 86%, 84%, 78%, 88%, and 86% using ResNet50, InceptionResNet-V2, Inception-V3, EfficientNet, DenseNet169, DenseNet121, and DenseNet201, respectively. In comparison, ResNet50 and DenseNet121 comparatively showed better performance in classifying three classes of pubescence color along with other evaluation metrices. There is still limitation in research such as earlier stages of data can be used to classify the pubescence color with different environment of datasets and non-tested genotypes. Another problem is the imbalance dataset can be considered in the future research to address the balancing treatments for the improved results with increasing number of samples. Furthermore, revised

research is encouraged using color based limited augmentation in the RGB imagery and separately using multispectral imagery with improved and deep learning algorithms. But as a cost-effective tool for the breeders and associated researchers UAV-based RGB imagery technology can be used in identifying the genotypes by reducing the human labor and time.

References

Al-Tamimi, N., Langan, P., Bernád, V., Walsh, J., Mangina, E., Negrão, S. (2022). Capturing crop adaptation to abiotic stress using image-based technologies. Open Biology, 12, 210353. 10.1098/rsob.210353.

An, N., Palmer, C. M., Baker, R. L., Markelz, R. J. C., Ta, J., Covington, M. F. et al. (2016). Plant high-throughput phenotyping using photogrammetry and imaging techniques to measure leaf length and rosette area. Computers and Electronics in Agriculture, 127, 376–394. 10.1016/j.compag.2016.04.002.

Andrew, J., Eunice, j., Popescu, D. E., Chowdary, M. K., Hemanth, J. (2022). Deep learning-based leaf disease detection in crops using images for agricultural applications. Agronomy, 12(10), 2395. 10.3390/agronomy12102395.

Ashapure, A., Jung, J., Chang, A. et al. (2020). Developing a machine learning based cotton yield estimation framework using multi-temporal UAS data. ISPRS Journal of Photogrammetry Remote Sensing, 169, 180–194. 10.1016/j.isprsjprs.2020.09.015.

Bagherzadi, L. (2017). Assessing physiological mechanisms to elucidate the slow-wilting trait in soybean genotypes. PhD thesis from North Carolina State University: Raleigh, NC, USA.

Bernard, R. L. (1975). The inheritance of near-gray pubescence color. Soybean Genetics Newsletter, 2, 31–35.

Bouguettaya, A., Zarzour, H., Kechida, A. et al. (2022). Deep learning techniques to classify agricultural crops through UAV imagery: a review. Neural Computing and Applications, 34, 9511–9536. 10.1007/s00521-022-07104-9.

Bruce, R. W., Rajcan, I., Sulik, J. (2021). Classification of soybean pubescence from multispectral aerial imagery. Plant Phenomics, 2021, 9806201. 10.34133/2021/9806201. PMID: 34409302; PMCID: PMC8363756.

Cao, W., Zhou, J., Yuan, Y., Ye, H., Nguyen, H. T., Chen, J., Zhou, J. (2019). Quantifying variation in soybean due to flood using a low-cost 3d imaging system. Sensors, 19, 2682. 10.3390/s19122682.

da Silva, L. A., Bressan, P. O., Goncalves, D. N., Freitas, D. M., Machado, B. B., Goncalves, W. N. (2019). Estimating soybean leaf defoliation using convolutional neural networks and synthetic images. Computer and Electronics in Agriculture, 156, 360–368.

Duan, L., Han, J., Guo, Z., Tu, H., Yang, P., Zhang, D., Zeng, D., Tan, J., Qiao, Y., Zhuang, D. (2018). Novel digital features discriminate between drought resistant and drought sensitive rice under controlled and field conditions. Frontiers in Plant Science, 9, 492. 10.3389/fpls.2018.00492.

Feng, A., Zhang, M. Sudduth, K. A., Vories, E. D., Zhou, J. (2019). Cotton yield estimation from UAV-based plant height. Transactions of the ASABE, 62(2), 393–404. 10.13031/trans.13067.

Feng, S., Yang, Z., Huang, M., Wu, Y. (2022). Classification of crop disasters based on DenseNet. In the Proceedings of the 2022 5th International Conference on Pattern Recognition and Artificial Intelligence (PRAI), Chengdu, China, 2022, pp. 252-256. 10.1109/PRAI55851.2022.9904230.

Food and Agriculture Organization of the United Nations (2012). FAOSTAT Database. Rome: Food and Agriculture Organization of the United Nations.

Gao, Z., Luo, Z., Zhang, W. et al. (2020). Deep learning application in plant stress imaging: A review. Agri Engineering, 2(3),430–446. 10.3390/agriengineering2030029.

Hanh, B. T., Van Manh, H., Nguyen, N. V. (2022). Enhancing the performance of transferred EfficientNet models in leaf image-based plant disease classification. Journal of Plant Disease Protection, 129, 623–634. 10.1007/s41348-022-00601-y.

Hasan A. S. M. M., Sohel, F., Diepeveen, D. et al. (2023). Weed recognition using deep learning techniques on class-imbalanced imagery. Crop & Pasture Science, 74(6), 628–644. 10.1071/CP21626.

Hasan, M., Tanawala, B., Patel, K. J. (2019). Deep learning precision farming: Tomato leaf disease detection by transfer learning. In the Proceedings of 2nd international conference on advanced computing and software engineering (ICACSE). 10.2139/ssrn.3349597.

He, K., Zhang, X., Ren, S. Sun, J. (2016). Deep Residual Learning for Image Recognition. In the Proceedings of the IEEE Conference on Computer Vision and Pattern Recognition (CVPR), 770-778.

Igried, B., AlZubi, S., Aqel, D., Mughaid, A., Ghaith, I., Abualigah, L. (2023). An intelligent and precise agriculture model in sustainable cities based on visualized symptoms. Agriculture, 13, 889. 10.3390/agriculture13040889.

Jiménez, J. d. l. C., Cardoso, J. A., Leiva, L. F., Gil, J., Forero, M. G., Worthington, M. L., Miles, J. W., Rao, I. M. (2017). Non-destructive phenotyping to identify brachiaria hybrids tolerant to waterlogging stress under field conditions. Frontiers in Plant Science, 8, 167. 10.3389/fpls.2017.00167.

Lambat, M., Kothari, R., Kabi, M., Mane, T. (2022). Plant disease detection using InceptionV3. International Research Journal of Engineering and Technology (IRJET), 9(6), 2295-2300.

Liu, Y., Zhang, X., Gao, Y., Qu, T., Shi, Y. (2022). Improved CNN method for crop pest identification based on transfer learning. Computational Intelligence and Neuroscience, 2022. 10.1155/2022/9709648.

Liua, J., Wang, M., Bao, L., Li, X. (2020). EfficientNet based recognition of maize diseases by leaf image classification. Journal of Physics: Conference Series, 1693, 012148. 10.1088/1742-6596/1693/1/012148.

Lu, T., Han, B., Chen, L., Yu, F., Xue, C. (2021). A generic intelligent tomato classification system for practical applications using DenseNet-201 with transfer learning. Scientific Reports, 11(1), 15824. 10.1038/s41598-021-95218-w.

Lu, T., Wan, L. Wang, L. (2022). Fine crop classification in high resolution remote sensing based on deep learning. Frontiers in Environmental Science, 10, 991173. 10.3389/fenvs.2022.991173.

Maimaitijiang, M., Sagan, V., Sidike, P., Hartling, S., Esposito, F., Fritschi, F. B. (2020). Soybean yield prediction from UAV using multimodal data fusion and deep learning. Remote Sensing of Environment, 237, 111599. 10.1016/j.rse.2019.111599.

Moghimi, A., Yang, C., Miller, M. E., Kianian, S. F., Marchetto, P. M. (2018). A novel approach to assess salt stress tolerance in wheat using hyperspectral imaging. Frontiers in Plant Science, 9, 1182. 10.3389/fpls.2018.01182.

Monis, J. B., Sarkar, R., Nagavarun, S., Bhadra, J. (2022). Efficient Net: Identification of crop insects using convolutional neural networks. In the Proceedings of the 2022 International Conference on Advances in Computing, Communication and Applied Informatics (ACCAI), Chennai, India, 2022, pp. 1-7. 10.1109/ACCAI53970.2022.9752514.

Mukti, I. Z., Biswas, D. (2019). Transfer learning-based plant diseases detection using resnet50. In the Proceedings of the 4th International Conference on Electrical Information and Communication Technology (EICT). IEEE. Date of Conference: 20-22 December 2019. Date Added to IEEE Xplore: 16 April 2020. 10.1109/EICT48899.2019.9068805.

Murai, Y., Yan, F., Iwashina, T., Takahashi R. (2016). Analysis of anthocyanin pigments in soybean hypocotyl. Canadian Journal of Plant Science, 96, 935–938. 10.1139/cjps-2016-0055.

Nandhini, S., Ashokkumar, K. (2022). An automatic plant leaf disease identification using DenseNet-121 architecture with a mutation-based henry gas solubility optimization algorithm. Neural Computing and Applications 34, 5513–5534. 10.1007/s00521-021-06714-z.

Naveenkumar, M., Srithar, S., Kumar, B. R., Alagumuthukrishnan, S., Baskaran, P. (2021). InceptionResNetV2 for plant leaf disease classification. In the proceedings of the 2021 Fifth International Conference on I-SMAC (IoT in Social, Mobile, Analytics and Cloud) (I-SMAC), Palladam, India, 2021, pp. 1161-1167. 10.1109/I-SMAC52330.2021.9641025.

Palmer, R. G., Payne, R. C. (1979). Genetic control of hypocotyl pigmentation among white-flowered soybeans grown in continuous light. Crop Science, 19, 124–126. 10.2135/cropsci1979.0011183X001900010033x.

Palmer, R. G., Pfeiffer, T. W., Buss, G. R., Kilen, T. C. (2004). Qualitative genetics," in Soybeans: Improvement, Production, and Uses, 3rd edition Eds. Boerma H. R., Specht. J. E. (Madison, WI: American Society of Agronomy)

Patel, D., Rawat, A., Katiyar, S. (2022). A novel approach to classify types of crop and associated disease by using InceptionV3. In the Proceedings of the 2022 2nd International Conference on Advance Computing and Innovative Technologies in Engineering (ICACITE), Greater Noida, India, 2022, pp. 1033-1037. 10.1109/ICACITE53722.2022.9823796.

Rubel, F., Brugger, K., Haslinger, K., Auer, I. (2017). The climate of the european alps: shift of very high resolution Köppen-Geiger Climate Zones 1800–2100. Meteorologische Zeitschrift, 26, 115–125. 10.1127/metz/2016/0816.

Sagan, V., Maimaitijiang, M., Sidike, P., Eblimit, K., Peterson, K. T., Hartling, Esposito, F. et al. (2019). UAV-based high resolution thermal imaging for vegetation monitoring, and plant phenotyping using ICI 8640 P, FLIR Vue Pro R 640, and thermos map cameras. Remote Sensing, 11(3), 330. 10.3390/rs11030330.

Siamabele, B. (2021). The significance of soybean production in the face of changing climates in Africa. Cogent Food and Agriculture, 7(1),1933745. 10.1080/23311932.2021. 1933745.

Théau, J., Gavelle, E., Ménard, P. (2020). Crop scouting using UAV imagery: A case study for potatoes. Journal of Unmanned Vehicle Systems, 8(2), 99–118. 10.1139/juvs-2019-0009.

Tian, F., Vieira, C. C., Zhou, J., Zhou, J., Chen, P. (2023). Estimation of off-target dicamba damage on soybean using UAV imagery and deep learning. Sensors, 23(6), 3241. 10.3390/s23063241.

Tian, M., Ban, S., Yuan, T., Ji, Y., Ma, C., Li, L. (2021). Assessing rice lodging using UAV visible and multispectral image. International Journal of Remote Sensing, 42, 8840-8857. 10.1080/01431161.2021.1942575.

Ümit, A., Uçar, M., Akyol, K., Uçar, E. (2021). Plant leaf disease classification using EfficientNet deep learning model. Ecological Informatics, 61, 101182. 10.1016/j.ecoinf.2020.101182.

Ümit, A., Uçar, M., Akyol, K., Uçar, E. (2021). Plant leaf disease classification using EfficientNet deep learning model. Ecological Informatics, 61, 101182. 10.1016/j.ecoinf.2020.101182.

USDA NASS. United States and all state data–crops. 2017. Avaiable on: http://www.nass.usda.gov/QuickStats/

Vlachopoulos, O., Leblon, B., Wang, J., Haddadi, A., LaRocque, A., Patterson, G. (2021). Mapping barley lodging with uas multispectral imagery and machine learning. ISPRS International Archives Photogrammetry Remote Sensing Spatial Information Science, XLIII-B1-2021, 553–560. 10.5194/isprs-archives-XLIII-B1-2021-553-2021.

Vong, C. N., Conway, L. S., Feng, A., Zhou, J., Kitchen, N. R., Sudduth, K. A. (2022). Corn emergence uniformity estimation and mapping using UAV imagery and deep learning. Computer and Electronics in Agriculture, 198, 107008.

Wahyuningrum, R. T., Kusumaningsih, A., Rajeb, W. P., Purnama, I. K. E. (2021). Classification of corn leaf disease using the optimized DenseNet-169 model. In the Proceedings of the 2021 The 9th International Conference on Information Technology: IoT and Smart City (ICIT2021), December2225, 2021, Guangzhou, China. ACM, NewYork, NY, USA, 7 pages. 10.1145/3512576.3512588.

Wu, S., Wang, J., Yan, Z. et al (2021) Monitoring tree-crown scale autumn leaf phenology in a temperate forest with an integration of planet scope and drone remote sensing observations. ISPRS Journal of Photogrammetry Remote Sensing, 171, 36–48. 10.1016/j.isprsjprs.2020.10.017.

Yang, Q., Shi, L., Han, J. et al. (2019). Deep convolutional neural networks for rice grain yield estimation at the ripening stage using UAV-based remotely sensed images. Field Crops Research, 235, 142–153.

Zhang, C., Walters, D., Kovacs, J. M. (2014). Applications of low altitude remote sensing in agriculture upon farmers' requests: A case study in northeastern Ontario, Canada. PLOS ONE, 9(11), e112894. 10.1371/journal.pone.0112894.

Zhang, K., Guo, Y., Wang, X., Yuan, J., Ding, Q. (2019). Multiple feature reweight DenseNet for image classification. IEEE Access, 07, 9872-9880. 10.1109/ACCESS.2018.2890127.

Zhang, Z. Q., Liu, H., Meng, Z. J., Jingping, C. (2019). Deep learning-based automatic recognition network of agricultural machinery images. Computers and Electronics in Agriculture, 166(1), 1–11.

Zhang, Z., Flores, P., Igathinathane, C., Naik, D. L., Kiran, R., Ransom, J. K. (2020). Wheat lodging detection from UAS imagery using machine learning algorithms. Remote Sensing, 12(11), 1838. 10.3390/rs12111838.

Zhou, J., Chen, H., Zhou, J., Fu, X., Ye, H., Nguyen, H. T. (2018). Development of an automated phenotyping platform for quantifying soybean dynamic responses to salinity stress in

greenhouse environment. Computer and Electronics in Agriculture, 151, 319–330. 10.1016/j.compag.

Zhou, J., Chen, H., Zhou, J., Fu, X., Ye, H., Nguyen, H. T. (2018). Development of an Automated Phenotyping Platform for Quantifying Soybean Dynamic Responses to Salinity Stress in Greenhouse Environment. Computer and Electronics in Agriculture, 151, 319–330. 10.1016/j.compag.

Zhou, J., Yungbluth, D., Vong, C. N., Scaboo, A., Zhou, J. (2019). Estimation of the maturity date of soybean breeding lines using UAV-based multispectral imagery. Remote Sensing, 11(18), 2075. 10.3390/rs11182075.

Zhou, J., Zhou, J., Ye, H., Ali, M. L., Nguyen, H. T., Chen, P. (2020). Classification of soybean leaf wilting due to drought stress using UAV-based imagery. Computers and Electronics in Agriculture, 175, 105576. 10.1016/j.compag.2020.105576.

CHAPTER FOUR

CONCLUSIONS AND FUTURE WORK

4.1 Conclusions

With the advancement of the UAV technique, it is becoming easier, more efficient, and user-friendly to screen high-throughput phenotypic data. In this study, a HTP based UAV equipped with a digital camera was used to develop an image-based crop trait quantification for soybean breeding program. A digital camera was equipped with a UAV to obtain high-resolution images, along with the GNSS units to provide accurate geo-referencing to stitch the images and processing. Soybean crucial morphological (lodging and pubescence colour) traits were classified from UAV-based RGB-derived image features and images directly. The goal was to exploit the potentiality of using UAV-acquired phenotypic information on evaluating these morphological traits for soybean breeding program.

For soybean lodging classification, RGB image-derived texture features were used after a few pre-processing steps. A total of fourteen texture features were derived. Random forest-recursive feature elimination method was used to eliminate the least important image features, and finally, 12 features were obtained for the analysis. One of the biggest challenges was to analyze the imbalanced dataset of soybean lodging classes. There were four classes of soybean lodging, namely, non-lodging, medium lodging, high lodging, and severe lodging. The original dataset was highly imbalanced, where the non-lodging class was 76%, medium lodging was 16%, high lodging was 6%, and severe lodging was 0.08% of the total dataset. To overcome the imbalance problem, five different (SMOTE-Tomek Links, SMOTE-ENN, Borderline-SMOTE, SMOTE-NC, and ADASYN) balancing methods were used to treat and balance the dataset. The SMOTE-ENN method proved to be the best balancing method for soybean lodging dataset as we achieved best

results from different machine learning (XGBoost, RF, KNN, and ANN) methods. The classification performance of the machine learning models using RGB image-derived texture features was 94%, 93%, 91% and 96% using SMOTE-ENN XGBoost, SMOTE-ENN RF, SMOTE-ENN KNN and SMOTE-ENN ANN, respectively. In addition, image features and overall classification accuracies of different machine learning models show consistency and a similar pattern in classifying four classes which can be more justified using different environments datasets of non-tested genotypes. The proposed method showed a new technique to deal with the highly imbalanced dataset and to classify a crucial soybean phenotype for the breeding program. In which the breeders would benefit identifying the lodged and non-lodged genotypes within a short period of time and with higher efficiency.

Seven pre-trained deep learning models were used for the classification of soybean pubescence colour, which is identified as a secondary trait by the breeders and mainly used for registering the genotypes and making decisions on the genotype advancement. From an orthomosaic image, each plot of the breeding field was cropped, which involves grid generation and manual adjustment of grids according to the size and shape of the plot. Then the images were resized to 224×224 pixels for the input of the pre-trained DL models. There were three pubescence color classes and a total of 1266 images (plots) were obtained; hence the four-image augmentation method was applied to enhance the number of images and to prevent the overfitting of the models. Among seven pre-trained models, ResNet50 and DenseNet121 showed a higher overall accuracy of 88% in classifying three soybean pubescence colour classes. Whereas other methods also showed a similar trend in classification and results, which could be more justified by using several days of datasets and by using different environments datasets. Therefore, the method could help the breeders in

selecting and identifying different colour classes of soybean pubescence, which will improve the soybean breeding efficiency by advancing the genotype selection intensity and accuracy.

4.2 Future work

There is still a huge lack of soybean lodging and pubescence colour detection research for breeding programs. Though there are other traits such as yield, plant height, days to maturity, and leaf wilting are associated with genotype selection for breeding purposes, lodging and pubescence colour are crucial factors considered by the breeders which somehow not in mainstream research using UAV-based imagery and advanced ML technology. One of the biggest limitations was an imbalanced dataset of different classes, which created a challenge for researchers in analyzing and obtaining good output. Further, detailed classification using different environments and different stages of datasets exploring other advanced machine learning methods can be explored to obtain higher accuracy for these trait detections and identification.

VITA

Shagor Sarkar was born in February 1994 in Rajshahi, Bangladesh. He obtained his Bachelor of Science in Agricultural Engineering from Hajee Mohammad Danesh Science Technology University in 2016. After obtaining his BSc in Engineering, he worked as a research assistant at the same university for one and a half years on a project on farm fatalities associated with agricultural machinery. He joined for his master's degree at Gyeongsang National University, South Korea, majoring in Biosystems Engineering. He worked in non-destructive fruit quality evaluation during his master's degree in South Korea. Shagor joined Mizzou for a graduate program in 2021 and pursued his master's degree in Food and Hospitality Systems (Agricultural Systems Technology). He has been involved in several projects using unmanned aerial vehicle (UAV/UAS) based remote sensing technology for quantifying crucial phenotypes of soybean. His research focused on remote sensing, image processing, machine learning, and precision agriculture. Furthermore, he is committed to continually developing and enhancing these methodologies to contribute to sustainable solutions and agricultural practice improvements.